

Spring 2023

Sustainable Approaches to Photo-, Thermo-, and Electro-Chemical Reactions of Amines

James David Sitter

Follow this and additional works at: <https://scholarcommons.sc.edu/etd>

 Part of the [Chemistry Commons](#)

Recommended Citation

Sitter, J. D.(2023). *Sustainable Approaches to Photo-, Thermo-, and Electro-Chemical Reactions of Amines*. (Doctoral dissertation). Retrieved from <https://scholarcommons.sc.edu/etd/7310>

This Open Access Dissertation is brought to you by Scholar Commons. It has been accepted for inclusion in Theses and Dissertations by an authorized administrator of Scholar Commons. For more information, please contact digres@mailbox.sc.edu.

SUSTAINABLE APPROACHES TO PHOTO-, THERMO-, AND
ELECTRO-CHEMICAL REACTIONS OF AMINES

by

James David Sitter

Bachelor of Science
University of South Carolina, 2019

Submitted in Partial Fulfillment of the Requirements

for the Degree of Doctor of Philosophy in

Chemistry

College of Arts and Sciences

University of South Carolina

2023

Accepted By:

Aaron K. Vannucci, Major Professor

Natalia B. Shustova, Committee Member

Brian C. Benicewicz, Committee Member

John R. Regalbuto, Committee Member

Cheryl L. Addy, Interim Vice Provost and Dean of the Graduate School

© Copyright by James David Sitter, 2023
All Rights Reserved

DEDICATION

To my wife, Kimberly, who motivated me to pursue this path and supported me along the way and to my children, the greatest blessings I could've ever asked for. To my grandparents, thank you for the love and support and guidance you have given me through life. Grandma and Grandpa, I miss you both. Grandmama and Papa, I am so fortunate to have you in my corner. I love you all.

ACKNOWLEDGEMENTS

The work on this dissertation could not have been completed on my own. First, I would like to thank PBI Performance Products Incorporated for funding my schooling and research for the last four years. This funding made everything possible and the lessons I learned from you all during our meeting were invaluable. I would also like to thank the National Defense Science and Engineering Graduate (NDSEG) Fellowship for assisting in funding for the last three years. The mentorship I received, namely from Michael Peretich, throughout my graduate school was immensely impactful and greatly appreciated. I would like to thank everyone who has helped me along the way on this journey starting with my advisor, Dr. Aaron K. Vannucci. You convinced me that science was in fact cool and took me in as an undergraduate biochemist to make me a chemist. The patience you have shown me along this journey has been nothing short of a miracle at times and the knowledge you have shared has been just as impressive. I would also like to thank Dr. Natalia B. Shustova for her endless support and knowledge when guiding me throughout classes and my doctoral requirements. Your group has felt like a second home to me while I have been pursuing this degree which speaks volumes to the type of group culture you cultivate. To my other committee members, Dr. Regalbuto and Dr. Benicewicz, you have both taught me so much, whether in class and undergraduate research, or in life by being the advisors and people you are. You all give me a lot to live up to as researchers and as people.

Working in the VRG has been an immense privilege and, more often than not, an immense amount of fun. To those who taught me the ropes when I was first joining and have since kept in touch, Dr. Nick Delucia, Dr. Mevan Dissanayake and Dr. Pooja Araye, your relationships have meant the world to me and your guidance has been nothing short of spectacular. Thank you all for taking me in with such kindness and teaching me how to be a graduate student. To my fellow classmate, Jacob Tillou, you have been a solid support system throughout our times of navigating this new experience. You and Caroline will always be welcome to be our neighbors. To the other graduate students of my year and our group as well as a few others, thanks for always brightening my day with a smile and being willing to sit down to discuss life and science. It truly has been, and hopefully will continue being, my honor.

To my wife and my family. Kimberly, you have been amazing throughout this and never cease to amaze me. You completed your doctorate all while being a mother and a wife. Superwoman is the only way to describe you. Liam, you are a rockstar. You have so much potential and two parents who love you incredibly. You have no idea the effect that your morning hugs have had on me. The curiosity that you show daily is something that I hope I have the ability to nourish so that you may never cease being curious. To Emily, it's crazy that this whole journey ends how it began, with another addition to our family. I barely know you at the moment, but you mean just as much to me as the rest of our family. You are a miracle and the world is yours if you want it. Dad loves you all so much and can't thank you all enough for being a part of his life. And to the last acknowledgement,

God. Thank you for the abilities you have given me and the support system you have instilled for me. Help me to never take any of it for granted.

ABSTRACT

In recent years, sustainable routes for chemical synthesis have garnered renewed interest. As the world continues to fight pollution and rising costs, it is imperative that new routes of synthesis that continuously fight the issues of pollution and waste are discovered, defined and explored. While traditional synthesis routes that require energy input typically require the burning of fossil fuels to produce heat, the amount of resources that go into the production of these fossil fuels and the sequestration of its waste to minimize its impact on the carbon footprint is enormous. Furthermore, sustainable chemistry research aims to decrease and minimize waste produced by traditional synthesis methods by increasing selectivity, removing the utilization of halogenated and/or volatile solvents and decreasing waste produced by harmful and/or expensive byproducts of these reactions.

The second chapter of this dissertation details the photochemical oxidation of aniline derivatives for the synthesis of azobenzene molecules. This research has provided a route for azobenzene synthesis that obtains unprecedented selectivity while utilizing light as a renewable energy source. Furthermore, this reaction scheme replaces traditional sacrificial electron acceptors with oxygen showing that the only waste produced is hydrogen peroxide. Throughout this chapter, the mechanism is explored to show the unique radical coupling mechanism and that oxygen is not involved in the oxidation of the aniline products.

Carbon-nitrogen bonds are utilized for many pharmaceutical and material purposes. The third chapter in this dissertation explores the relationship between nitrogen heterocycle's pK_a and how the electrochemical generation of their anions provide unique reactivity and selectivity for the purpose of synthesizing new carbon-nitrogen bonds. It is also explained throughout this chapter the relationship between the electrolyte and anion reactivity as well as the electronic properties of the electrophile and their effect on the success of the nucleophilic substitution.

The last project discussed herein is the development of an understanding in the benzidine rearrangement method. This method of synthesizing aromatic carbon-carbon bonds has been of interest in the past due to its unique ability to form bonds without the utilization of expensive transition metal catalysts. The mechanism by which this rearrangement occurs is hypothesized to be via an intramolecular mechanism. The electronic effects and functionality of a wide range of substituents is explored seeking to understand how these factors affect the overall success of benzidine rearrangement.

TABLE OF CONTENTS

DEDICATION.....	iii
ACKNOWLEDGEMENTS.....	iv
ABSTRACT.....	vii
LIST OF TABLES.....	xii
LIST OF FIGURES.....	xiii
CHAPTER 1: INTRODUCTION.....	1
1.1 Catalysis for sustainable synthesis.....	2
1.2 The photocatalytic oxidation of amines.....	4
1.3 Traditional synthesis of azobenzene compounds.....	4
1.4 Challenges facing traditional azobenzene synthesis.....	6
1.5 Photochemistry background.....	10
1.6 Elucidating reactivity trends for the anion pool synthesis method.....	11
1.7 Traditional methods for C-N bond synthesis.....	13
1.8 Challenges facing traditional C-N bond synthesis.....	14
1.9 Electrochemistry background.....	15
1.10 Anion pool and its potential.....	16
1.11 The determination of benzidine reactivity based on electronics and functionality.....	17
1.12 Traditional synthesis methods of C-C bonds.....	17

1.13 Benzidine rearrangement.....	19
CHAPTER 2: PHOTOCATALYTIC OXIDATIVE COUPLING OF	
ARYLAMINES FOR THE SYNTHESIS OF AZOAROMATICS	
AND THE ROLE OF O ₂ IN THE MECHANISM.....	
21	21
2.1 Abstract.....	22
2.2 Introduction.....	22
2.3 Results and Discussion.....	24
2.4 Conclusions.....	32
2.5 Experimental.....	33
CHAPTER 3: INSIGHTS INTO REACTIVITY TRENDS FOR	
ELECTROCHEMICALLY GENERATED ANIONIC	
NITROGEN NUCLEOPHILES.....	
37	37
3.1 Abstract.....	38
3.2 Introduction.....	38
3.3 Results and Discussion.....	41
3.4 Conclusions.....	49
3.5 Experimental.....	50
CHAPTER 4: INVESTIGATION INTO THE BENZIDINE	
REARRANGEMENT REACTION.....	
54	54

4.1 Abstract.....	55
4.2 Introduction.....	56
4.3 Results and Discussion.....	59
4.4 Conclusion.....	62
4.5 Experimental.....	63
CHAPTER 5: CONCLUSION AND FUTURE OUTLOOKS.....	65
5.1 Conclusions.....	66
5.2 Future Works.....	67
REFERENCES.....	70
APPENDIX A: Supporting Information for Chapter 2.....	89
APPENDIX B: Supporting Information for Chapter 3.....	119
APPENDIX C: Supporting Information for Chapter 4.....	138

LIST OF TABLES

Table 2.1 Optimization of reaction conditions for the oxidative coupling of azobenzene compounds.....	25
Table 3.1 Optimization of electrolyte for the anion pool synthesis reaction involving nitrogen heterocycles.....	43
Table 3.2 Anion pool C-N bond forming reaction yields versus pK_a values of parent heterocycle.....	44
Table 3.3 Summary of % yields in the reactions of carbazole anion nucleophile with various benzylic halide electrophiles.....	47
Table 4.1 Summary of the scope of products synthesized prior to use for benzidine rearrangement.....	60
Table 4.2 Yields of benzidine rearrangement as estimated via LC-MS of 2,3 and 4 substituted rearrangement products.....	61

LIST OF FIGURES

Figure 1.1 The selective photo-oxidative coupling of azobenzene (a). The anion pool synthesis of carbon-nitrogen bonds (b). The classical benzidine rearrangement (c).....	3
Figure 1.2 The three traditional methods of azobenzene synthesis: (a) diazotization (b) reductive coupling of nitrobenzenes (c) oxidative coupling of anilines.....	5
Figure 1.3 Yields obtained utilizing an OMS-2 catalyst and high temperatures as reported by Wang et al.....	7
Figure 1.4 Reported procedure for the reductive coupling of nitrobenzenes for the purpose of azobenzene synthesis.....	8
Figure 1.5 Many stability issues remain with diazonium salts, thus leading to a need to replace them with more stable alternatives.....	9
Figure 1.6 The anion pool approach has shown unique selectivity to the N ₁ site justifying a deeper understanding of its potential uses. Reprinted from reference.....	12
Figure 1.7 General reaction scheme of the anion pool two-step synthesis method.....	16
Figure 1.8 Traditional benzidine rearrangement discovered by August von Hoffman.....	20
Figure 2.1 Comparison of routes for azoaromatic synthesis.....	23
Figure 2.2 Photocatalytic oxidative coupling of arylamines. Yields are reported for reactions performed under an O ₂ atmosphere for 4 hours. Yields in parentheses are 24 hour reactions open to ambient air.....	27
Figure 2.3 The proposed reductive quenching pathway with amine acting to quench the photocatalyst.....	29
Figure 2.4 Fluorescence quenching data and Stern-Volmer plot for the quenching of Ir with <i>p</i> -anisidine.....	30
Figure 2.5 Proposed mechanism for the photocatalytic oxidative coupling of amines for the synthesis of azoaromatics.....	32

Figure 3.1 Schematic of the anion pool synthesis method showing the electrochemical formation of anionic nitrogen-containing nucleophiles.....	40
Figure 3.2 Plot of pK_a of parent heterocycle versus % yield of anion pool reaction with benzyl bromide. Red point is pyrrole reaction run at 0 °C.....	46
Figure 4.1 The traditional catalytic cycle when conducting Suzuki-Miyaura coupling with a palladium(II) catalyst.....	56
Figure 4.2 Competition between coordinating substituents of a palladium square planar catalyst.....	57
Figure 4.3 Traditional benzidine rearrangement as discovered by August von Hofmann starting from the coupling of aniline to azobenzene followed by the reduction to hydrazobenzene and the subsequent rearrangement.....	58
Figure A.1 Control reactions involving nitrosobenzene or nitrobenzene.....	90
Figure A.2 Picture of the hydrogen peroxide test strips showing peroxide formation during coupling of azobenzenes.....	91
Figure A.3 Fluorescence quenching data and Stern-Volmer plot for the quenching of Ir with aniline.....	92
Figure A.4 Fluorescence quenching data and Stern-Volmer plot for the quenching of Ir with 4-fluoroaniline.....	93
Figure A.5 Fluorescence quenching data and Stern-Volmer plot for the quenching of Ir with <i>p</i> -anisidine with 2.5×10^{-4} M K_3PO_4 base added.....	94
Figure A.6 Fluorescence quenching data and Stern-Volmer plot for the quenching of Ir with aniline with 2.5×10^{-4} M K_3PO_4 base added.....	95
Figure A.7 Fluorescence quenching data and Stern-Volmer plot for the quenching of Ir with 4-fluoroaniline with 2.5×10^{-4} M K_3PO_4 base added.....	96
Figure A.8 Room temperature X-band (9.38 GHz) spectrum of reaction solution containing <i>p</i> -anisidine, DMPO, K_3PO_4 and Ir in dichloromethane after 35 minutes of irradiation with blue light with the proposed reaction leading to the EPR signal.....	97
Figure A.9 1H NMR spectra of product 2.1 in $(CD_3)_2CO$	98
Figure A.10 ^{13}C NMR spectra of product 2.1 in $(CD_3)_2CO$	99
Figure A.11 1H NMR spectra of product 2.2 in $CDCl_3$	100
Figure A.12 ^{13}C NMR spectra of product 2.2 in $CDCl_3$	101

Figure A.13 ^1H NMR spectra of product 2.3 in CDCl_3	102
Figure A.14 ^{13}C NMR spectra of product 2.3 in CDCl_3	103
Figure A.15 ^1H NMR spectra of product 2.4 in CDCl_3	104
Figure A.16 ^{13}C NMR spectra of product 2.4 in CDCl_3	105
Figure A.17 ^1H NMR spectra of product 2.5 in CDCl_3	106
Figure A.18 ^{13}C NMR spectra of product 2.5 in CDCl_3	107
Figure A.19 ^1H NMR spectra of product 2.6 in CDCl_3	108
Figure A.20 ^{13}C NMR spectra of product 2.6 in CDCl_3	109
Figure A.21 ^1H NMR spectra of product 2.7 in CDCl_3	110
Figure A.22 ^{13}C NMR spectra of product 2.7 in CDCl_3	111
Figure A.23 ^1H NMR spectra of product 2.8 in CDCl_3	112
Figure A.24 ^{13}C NMR spectra of product 2.8 in CDCl_3	113
Figure A.25 ^1H NMR spectra of product 2.9 in CDCl_3	114
Figure A.26 ^{13}C NMR spectra of product 2.9 in CDCl_3	115
Figure A.27 ^1H NMR spectra of product 2.10 in CDCl_3	116
Figure A.28 ^{13}C NMR spectra of product 2.10 in CDCl_3	117
Figure A.29 Plot of determined oxidation potential (V) as compared to product % yield after 4 hours under optimized reaction conditions	118
Figure B.1 ^1H NMR spectra of product 3.1 in $(\text{CD}_3)_2\text{SO}$	120
Figure B.2 ^{13}C NMR spectra of product 3.1 in $(\text{CD}_3)_2\text{SO}$	121
Figure B.3 ^1H NMR spectra of product 3.2 in $(\text{CD}_3)_2\text{SO}$	122
Figure B.4 ^{13}C NMR spectra of product 3.2 in $(\text{CD}_3)_2\text{SO}$	123
Figure B.5 ^1H NMR spectra of product 3.3 in $(\text{CD}_3)_2\text{SO}$	124
Figure B.6 ^{13}C NMR spectra of product 3.3 in $(\text{CD}_3)_2\text{SO}$	125
Figure B.7 ^1H NMR spectra of product 3.4 in $(\text{CD}_3)_2\text{SO}$	126
Figure B.8 ^{13}C NMR spectra of product 3.4 in $(\text{CD}_3)_2\text{SO}$	127
Figure B.9 ^1H NMR spectra of product 3.5 in $(\text{CD}_3)_2\text{SO}$	128
Figure B.10 ^{13}C NMR spectra of product 3.5 in $(\text{CD}_3)_2\text{SO}$	129
Figure B.11 ^1H NMR spectra of product 3.6 in $(\text{CD}_3)_2\text{SO}$	130
Figure B.12 ^{13}C NMR spectra of product 3.6 in $(\text{CD}_3)_2\text{SO}$	131

Figure B.13 ^{19}F NMR spectra of product 3.6 in $(\text{CD}_3)_2\text{SO}$	132
Figure B.14 ^1H NMR spectra of product 3.7 in $(\text{CD}_3)_2\text{SO}$	133
Figure B.15 ^{13}C NMR spectra of product 3.7 in $(\text{CD}_3)_2\text{SO}$	134
Figure B.16 ^1H NMR spectra of product 3.8 in $(\text{CD}_3)_2\text{SO}$	135
Figure B.17 ^{13}C NMR spectra of product 3.8 in $(\text{CD}_3)_2\text{SO}$	136
Figure B.18 Illustration of anion pool method in an H-cell performed with a 0.1 M solution of tetrabutylammonium hexafluorophosphate (Bu_4NPF_6) containing 0.375 mmol of carbazole in acetonitrile in the cathode side and 0.75 mmol of ferrocene on anode side. Benzyl bromide (excess) was added after 1.625 hrs and current was reduced to 0.5 mA. Reticulate Vitreous Carbon electrodes were employed as cathode and anode.....	137
Figure C.1 LC-MS showing retention times of 2,2'-dichlorobenzidine rearrangement.....	139
Figure C.2 Mass Spectra of peak B of Figure C.1 showing mass fragmentation of 2,2'-dichlorobenzidine product.....	140
Figure C.3 LC-MS showing retention times of 4,4'-diamino-[1,1'-biphenyl]-3,3'-dicarboxylic acid rearrangement.....	141
Figure C.4 Mass Spectra of peak F of Figure C.3 showing mass fragmentation of 4,4'-diamino-[1,1'-biphenyl]-3,3'-dicarboxylic acid product.....	142
Figure C.5 LC-MS showing retention times of 2,2'-dimethyl-3H,3'H-5,5'-bibenzo[d]imidazole rearrangement.....	143
Figure C.6 Mass Spectra of peak C of Figure C.5 showing mass fragmentation of 2,2'-dimethyl-3H,3'H-5,5'-bibenzo[d]imidazole product.....	144
Figure C.7 LC-MS showing retention times of benzidine rearrangement.....	145
Figure C.8 Mass Spectra of peak A of Figure C.7 showing mass fragmentation of benzidine product.....	146

CHAPTER 1: INTRODUCTION

1.1 Catalysis for sustainable synthesis

Traditional methods of chemical synthesis for the purpose of nitrogen-nitrogen, carbon-nitrogen and carbon-carbon aromatic bonds for applications in the pharmaceutical, materials and agricultural industries typically focus on the utilization of Transition Metal I catalysts and harsh conditions such as high temperatures, strong acids/bases and halogenated/carcinogenic solvents. While these synthesis methods are widely used due to the depth of understanding and ease of industrial application that has been obtained over years of research, there is a renewed focus on sustainability during the production of these molecules as well as during the disposal of the waste.

The movement towards a greener synthesis process requires the development and expansion of new synthesis routes that limit these hazardous byproducts and the extreme temperatures that are required via traditional synthesis methods. This improvement on traditional synthesis methods can occur in several aspects of the reaction design. Therefore, it is imperative to gain insights into new reactivity and applications for green synthesis routes. The focus of this dissertation is to explore green synthesis route applications and their advantages for new synthetic applications and to add understanding to the previously reported benzidine rearrangement. The routes being explored are the photocatalytic oxidation of aryl amines to form azobenzene molecules (Figure 1.1a), the electrochemical activation of nitrogen containing heterocycles for the purpose of synthesizing new carbon-nitrogen bonds (Figure 1.1b) and the exploration of the benzidine rearrangement (Figure 1.1c) and its ability to form new carbon-carbon bonds based on its electronic and steric properties.

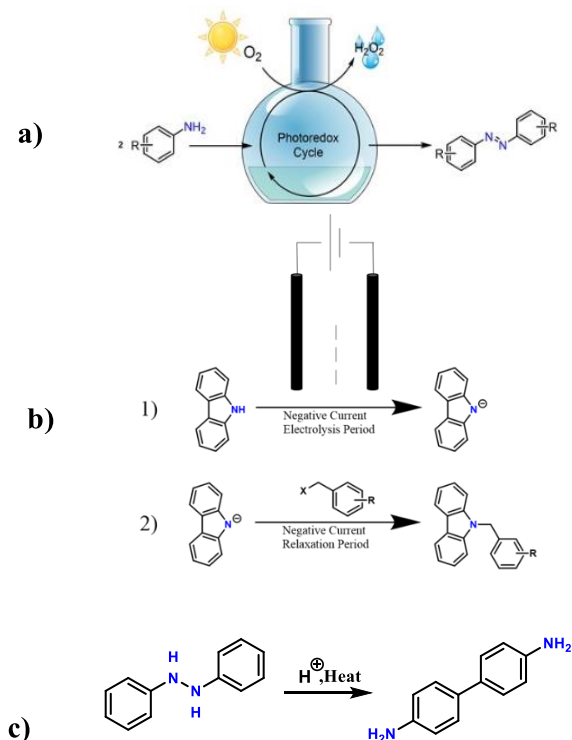


Figure 1.1: The selective photo-oxidative coupling of azobenzene (a). The anion pool synthesis of carbon-nitrogen bonds (b). The classical benzidine rearrangement (c).

There are three different projects that will be discussed in this dissertation. The first project discussed will show how we used light as a sustainable energy source in order to be the first report to our knowledge of oxidatively coupling amines with complete selectivity. The second project will show reactivity trends that have been determined for the anion pool synthesis method that allows for the rational design of green electrochemical synthesis routes of carbon-nitrogen bonds. The last project will explore the reactivity of the benzidine rearrangement based on electronics and functionality of substituents in order to synthesize difficult to access benzidines with desirable substituents.

1.2 The photocatalytic oxidation of amines

The first project in my dissertation attacks the waste and fossil fuel consumption issues that plague traditional chemical synthesis compounds. To the best of my knowledge, this project is the first report of the photocatalytic oxidative coupling of aryl amines into the highly desirable azobenzene compound with almost complete selectivity and focuses on understanding the mechanism by which this process occurs. The synthesis of azobenzene compounds has experienced progress in the photocatalytic and electrochemical synthesis of azobenzene compounds. Many issues still plague these methods, however, such as low selectivity between nitrosobenzene and azobenzene products, the requirement of sacrificial electron donors, and the requirement for inert atmospheres to allow reduction to occur. As such, this project has focused on the oxidative coupling of arylamines to eliminate the need for inert atmospheric conditions as well as the need for sacrificial electron donors. This study explores a readily available iridium photocatalyst, $\text{Ir}(\text{dF-CF}_3\text{-ppy})_2(\text{dtpby})^+$, where $\text{dF-CF}_3\text{-ppy}$ was 2-(2,4-difluorophenyl)-5-(trifluoromethyl)pyridine and dtpby was 4,4'-tert-butyl-2,2'-bipyridine, and its ability to oxidatively couple a wide substrate scope of arylamines while obtaining a high degree of selectivity. This synthesis method successfully circumvents the need for extreme temperature control and provides needed insight into the tunability of a photocatalyst for specific system requirements, thus offering exciting possibilities for industrial applications while keeping the green chemistry principles in mind.

1.3 Traditional synthesis of azobenzene compounds

Azobenzene compounds are aromatic compounds that are connected via a nitrogen-nitrogen double bond. This unique compound is of great importance due to the unique

photo-chemical and photo-optical properties it possesses. The formation of azobenzene compounds is one of the most important reactions in the pharmaceutical industry today as approximately 70% of molecules utilized in the pharmaceutical industry contain at least one azo bond.¹ Additionally, compounds utilizing the azobenzene bond have found heightened interest in pharmaceutical research due to possible applications in photo-switchable drugs.² These compounds are also of great interest in the materials industry due to their vibrant color and great stability when exposed to large quantities of light which is allowed by their ability to tautomerize.³ Furthermore, these compounds are used in optical storage due to their unique cis to trans conformation switching properties.⁴

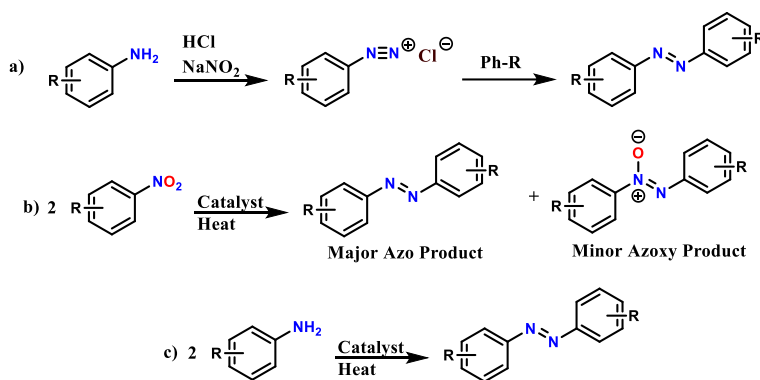


Figure 1.2: The three traditional methods of azobenzene synthesis: a) diazotization b) reductive coupling of nitrobenzenes c) oxidative coupling of anilines.

Traditional synthesis of azobenzene compounds occurs in one of three ways. These three manners are the utilization of diazonium salts (Figure 1.2a), reductive coupling of nitrobenzene (Figure 1.2b), or the oxidative coupling of aniline derivatives (Figure 1.2c). During the oxidative coupling of amines and the reductive coupling of nitrobenzenes, a transition metal catalyst is typically utilized along with heat to catalyze the reaction.

Furthermore, both the oxidative coupling and reductive coupling methods require either a sacrificial electron acceptor or a sacrificial electron donor respectively.

When utilizing the diazonium salt method, the diazonium salt is synthesized first by treating the starting aromatic amine with a strong acid, namely nitrous acid. This nitrous acid is typically developed *in situ* and at low temperatures by mixing sodium nitrate and excess acids such as hydrochloric acid or sulfuric acid. This formed diazonium salt acts as a weak electrophile that reacts with electron rich nucleophiles and generally offers acceptable yields of the desired azobenzene product. This method is typically preferred in industrial applications due to the ease of application and relatively high yields that may be obtained.

1.4 Challenges facing traditional azobenzene synthesis

While azobenzene compounds are widely used in industrial applications, there are still issues when it comes to sustainability and trying to conduct their synthesis while keeping green chemistry principles in mind. The first issue that must be addressed is the applicability of any synthesis method in industrial applications. Beginning with the oxidative coupling of amines to azobenzenes, this method allows for a broad substrate scope to be achieved. As recently reported, utilizing an octahedral molecular sieve of manganese oxide (OMS-2), high yields have been obtained (Figure 1.3).⁵ Recently it has been reported that the synthesis of a broad substrate scope of symmetrical azobenzenes oxidatively utilizing potassium persulfate and polyethylene glycol 200 as catalysts with the addition of a base.⁶ However, to achieve such yields, high heats had to be utilized along with long reaction times and halogenated solvents. Other research has recently focused on the ability to oxidatively couple aniline derivatives at milder temperatures but typically

involve the utilization of a metal catalyst like gold nanoparticles and lower yields at low concentrations.⁷ While the oxidative coupling synthesis method typically shows promising yields with a broader substrate scope, it also involves the synthesis of exotic transition metal catalysts, high temperatures and long reaction times with halogenated solvents and harsh base, thus limiting applications to renewable chemistry.

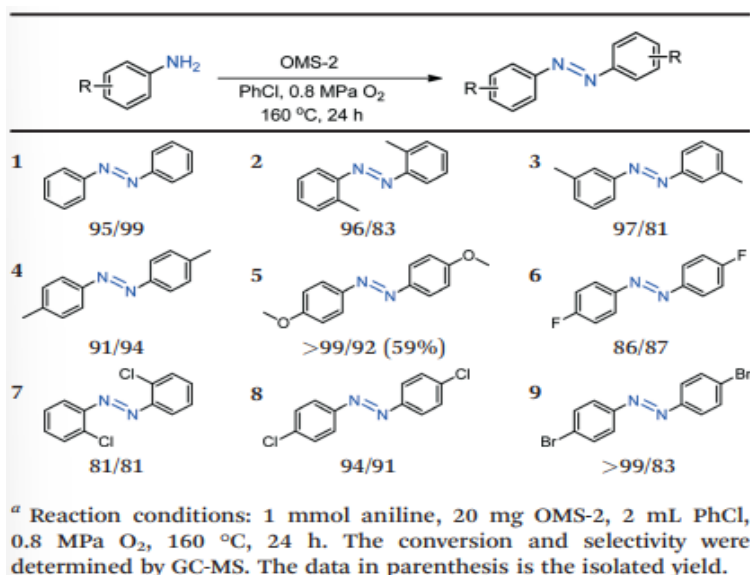


Figure 1.3: Yields obtained utilizing an OMS-2 catalyst and high temperatures as reported.⁴

With the reductive coupling synthesis method, substrate scope is typically limited to electron deficient substituents and is generally limited when attempting to activate electron neutral or electron rich substituents. Nevertheless, a lot of research has gone into the improvement of the substrate scopes available to each synthesis method and impressive strides have been made. When speaking of reductive coupling of nitroaniline compounds, recent reports have shown that a broad substrate scope can be achieved in acceptable yields

(Figure 1.4).⁸ However, this method generally is two steps and lacks the desired selectivity as azoxybenzene is an additional product.

Therefore, when looking at how to decrease waste in the synthesis of these compounds, many issues still persist. For the intent of increasing applicability of these synthesis methods, many different complex transition metal complexes have been synthesized to improve selectivity and ease reaction conditions.⁹⁻¹¹

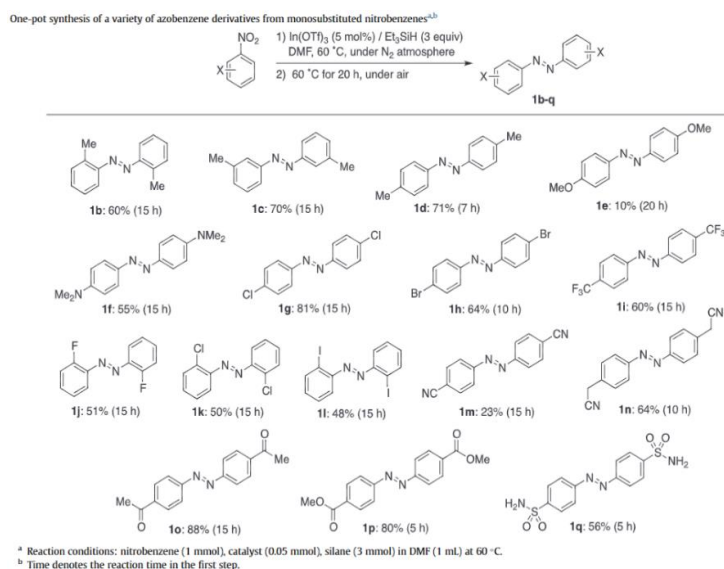


Figure 1.4: Reported procedure for the reductive coupling of nitrobenzenes for the purpose of azobenzene synthesis.⁸

Although diazonium salt is widely preferred in industrial applications, many issues still persist and must be resolved (Figure 1.5). As previously stated, the first step of the diazotization process is the forming of a diazonium salt which is typically done *in situ*. This portion of the reaction is extremely difficult to isolate safely and, thus, the diazotization process is generally proceeded with without any diazonium salt isolation. Furthermore, due to the diazonium salt reactivity, the salt must be held at extremely low

temperatures in inert atmospheres to prevent degradation or explosive reactions of the initial salt. Even when steps like this are taken, however, diazonium salt degradation still occurs. This leads to undesirable reactivity as well as waste prior to a reaction is ever begun. It must be mentioned, however, that recent strides have been made in the increasing of diazonium salt stability. In fact, recent reports have shown promise in utilizing diazonium salts in sensory materials for phenol substrates and shows that in an aqueous solution, these compounds remained stable for up to 13 days.¹²

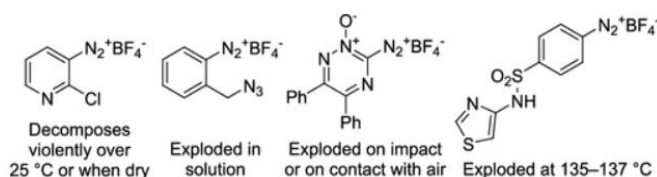


Figure 1.5: Many stability issues remain with diazonium salts, thus leading to a need to replace them with more stable alternatives.¹³

Another issue that plagues traditional synthesis methods is high fossil fuel energy consumption. During the traditional synthesis methods, extreme temperatures are typically utilized to push these reactions forward and stabilize intermediates long enough for the desired reaction to occur.^{5, 14} The heat utilized in these reactions is created by burning large quantities of fossil fuels. Furthermore, the diazotization synthesis method requires extremely low temperatures to preserve the diazonium salt and prevent unwanted reactivity.¹⁵ These extreme temperatures require great precision to all for the reaction to move forward as desired. As such, it is imperative that routes requiring less precise control of temperatures is found so that waste may be limited and energy consumption may be reduced.

Recently, to combat the issues of non-renewable fuels being utilized, the photocatalytic reduction of nitrobenzene compounds to synthesize azobenzenes and azoxybenzenes has been reported.¹⁶ While this route has shown promise when utilizing a renewable energy source, it lacks complete selectivity and requires careful handling of the photocatalyst as it is unstable in air. While this is a promising step into the sustainable synthesis of azobenzene compounds, air sensitivity and selectivity remain priorities when speaking of applicability and green chemistry principles, respectively. Additionally, it is important to remember that currently all three routes typically require the utilization of carcinogenic solvents, high pressures, or a sacrificial electron donor or acceptor. This provides challenges when discussing safe waste disposal and the effect these solvents may have on industrial workers and the environment. While there are methods that are established in the azobenzene synthesis industry, there are also many viable solutions for improving these synthesis methods moving forward and making the processes greener. In this dissertation, I will be discussing one of those possible solutions that has the potential to decrease waste, increase selectivity and broaden the substrate scope all while remaining air stable: photochemical synthesis.

1.5 Photochemistry background

Photochemistry is a growing field due to its ability to potentially use sunlight in order to catalyze reactions forward, replacing the need for the utilization of fossil fuel energy. Recently, photochemistry has made an impact in a broad range of reactions including in uses in Metal Organic Frameworks,¹⁷ in 3D resin printing,¹⁸ and in solar energy¹⁹ as a promising method of replacing traditional fossil fuel consumption for energy purposes.

Photocatalysis works in a one electron transfer mechanism. A photocatalyst begins in its ground state and a light is shined on the photocatalyst to excite it. At this point, the excited electron enters into the lowest unoccupied molecular orbital and the photocatalyst is able to either reduce a substrate by donating the excited electron, or it is able to oxidize a substrate by accepting an electron from the substrate. Once the substrate is oxidized or reduced, it is allowed to react with another substrate and form the desired product. In order for the photocatalyst to be considered a catalyst, however, it must be able to either be reduced or oxidized to the original ground state photocatalyst so that it may repeat this cycle. As such, there are three main components of the reaction that must be looked at when optimizing for specific reactions: the photocatalyst, the sacrificial electron donor or acceptor and the substrates with which you wish to react.

Much of photochemistry focuses on the design of new photocatalysts that are made with exotic ligand moieties or focus on attempting to conduct photochemical reactions with catalysts containing less toxic, more abundant transition metal centers. The research that will be discussed in this dissertation focuses on the improvement of selectivity and reduction of waste utilizing the aforementioned $\text{Ir}(\text{dF-CF}_3\text{-ppy})_2(\text{dtbpy})^+$ photocatalyst for the purpose of azobenzene synthesis applications. It is this reduction in waste and increase in selectivity that allows for a great understanding of how to further improve existing synthesis methods with a drive towards a greener future.

1.6 Elucidating reactivity trends for the anion pool synthesis method

The second project discussed herein focuses on the exploration and understanding of the anion pool method for the synthesis of carbon-nitrogen bonds that are prevalent and desirable in the pharmaceutical and materials industries. The anion pool method was

developed by the Vannucci Research Group as a new electrochemical route to form these carbon-nitrogen bonds via nucleophilic substitution. This synthesis method has previously been shown to be able to react with highly activated anhydride compounds with impressive selectivity (Figure 1.6). As this method is still young, a further understanding of this process is needed to further improve its applicability. However, utilizing electrochemical energy instead of expensive TM catalysts and fossil fuels for energy allows for the limitation of pollutants produced from the reaction.

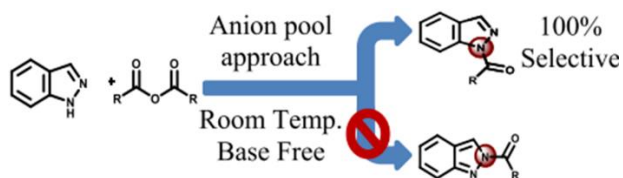


Figure 1.6: The anion pool approach has shown unique selectivity to the N₁ site justifying a deeper understanding of its potential uses. Reprinted from reference.²⁰

In the anion pool method, nitrogen heterocyclic anions are generated during an electrolysis period to produce a pool of anions. During a second step, the electrophile is added into the reaction mixture during the relaxation period to allow for a nucleophilic substitution and the production of aromatic carbon-nitrogen bonds. This chapter explores important aspects of the reaction that must be understood when utilizing it as a synthesis method, namely the importance of the pK_a of the nitrogen containing substrate and its effect on overall reactivity trends. Also shown is the effect the strength of the carbon-fluorine bond has on the overall yields as well as exploration into the effect that the electrolyte has on the stabilization of the generated anion and the effects that the sterics of the electrolyte have in allowing the reaction to move forward. The understanding, exploration and

utilization of the anion pool method offers a promising avenue for the synthesis of highly desirable carbon-nitrogen containing compounds while maintaining a green chemistry centric focus.

1.7 Traditional methods for C-N bond synthesis

The formation of carbon-nitrogen bonds has been of interest for many years. Compounds containing carbon-nitrogen bonds are desirable in materials and medicinal chemistry along with other industries.²¹ Ullmann-type coupling was discovered over 100 years ago and has been used for as long to synthesize desired carbon-nitrogen bonds. This reaction finds frequent utilization in surface-confined polymerization, pharmaceutical reactions and agrochemical synthesis.²² Although novel ligand design is often required, recent reports have found photochemical applications that allow for promising yields up to 77% utilizing a copper/copper(II) oxide catalyst system.²³

Nucleophilic substitutions of activated compounds have also been explored as a promising method for the formation of carbon-nitrogen bonds for the purpose of forming new osmium clusters for organic material synthesis as well as showing promise when cleaving sp^2 carbon-fluorine bonds.²⁴ Other recent research has shown progress in utilizing less activated substrates for the purpose of the synthesis of *N*-arylated compounds via ladderization of fluorinated aromatic compounds.²⁵

Over the past thirty years, the Buchwald-Hartwig synthesis method has grown in popularity due to the generally facile conditions of this reaction.²⁶ The breakthrough advances in the Buchwald-Hartwig catalyst designs have allowed for the utilization of new

biaryl ligands to advance at mild temperatures of 60 °C.²⁷ Many catalysts that have been developed have also allowed for a wider substrate scope to be obtained.

1.8 Challenges facing traditional C-N bond synthesis

While there are several tools in the toolbox for the synthesis of carbon-nitrogen bonds, there is still a desire to broaden the scope of tools. While these traditional methods show promise when looking at asymmetric and ring closure syntheses, several issues remain. Traditional Ullmann-type coupling utilizes a copper catalyst and high reaction temperatures. While the copper catalyst has traditionally led to unpredictable yields, recent advances in copper catalyst chemistry has led to improved catalyst stability and efficiency.²⁷ Although there has been great progress in the design of copper catalyst for the purpose of Ullmann-type coupling, harsh reaction conditions are still commonly required for the reaction to move forward successfully.²³ However, with harsh reaction conditions, there leads a limited substrate scope that may be utilized successfully. Furthermore, one of the issues that has constantly been of issue with Ullman-type coupling reactions is the unpredictability of product yields.

While Buchwald-Hartwig amination is widely used in industrial and academic settings, there has been a recent renewed interest in finding new ways to synthesize carbon-nitrogen bonds due to the desire to utilize more readily available and less-expensive substrates. A lot of research has gone into decreasing catalyst loading for these types of reactions so that they may be less expensive and greener. In this dissertation it is suggested that the utilization of electrochemical methods offer a unique and transformative manner of which to synthesize carbon-nitrogen bonds.

1.9 Electrochemistry background

Electrochemistry has garnered a lot of recent attention with regards to green chemical synthesis research. Recent research has shown that electrochemical synthesis has shown promise in a wide variety of applications including the formation of ammonia in both solid and liquid electrolyte cells,²⁸ the synthesis of ceramic thin films and coatings,²⁹ and in water-splitting reactions utilizing water-splitting photoelectrochemical cells (PECs).³⁰ Electrochemical synthesis involves a closed circuit of continuous electrons that either reduce a substrate, or allow for the oxidation of a substrate, depending on which direction the current is running. As such, electrochemical synthesis can be thought of as a single-electron synthesis process that requires a great amount of conductivity in the solution to push forward. In terms of electrochemical synthesis methods, there are two methods of which scientists traditionally achieve reactivity: bulk electrolysis and split cell electrolysis. While bulk electrolysis is generally preferred due to ease of use, split cell electrolysis typically offers greater reaction control. The focus throughout this portion of my dissertation will be on split cell electrolysis utilizing a two-step synthesis approach.

In split cell electrolysis, there are two cells divided by a membrane. Additionally, there are two electrodes that allow the circuit to close and a reference electrode to measure the reaction potential at the counter electrode. At the anode, an oxidation reaction occurs while at the cathode, a reduction reaction occurs. The method that will be utilized here is the anion pool method which, as the name suggests, focuses on the reduction of a substrate to provide unique reactivity. Therefore, throughout the remainder of this dissertation, the “working” electrode may be used interchangeable with the “cathode” as this is the electrode where the work of interest is being performed.

1.10 Anion pool and its potential

The anion pool synthesis method was developed by the Vannucci Research Group and is analogous to the cation pool synthesis method developed by Yoshida et al.³¹ This anion pool synthesis method is an electrochemical synthesis method that utilizes a nitrogen containing heterocycle that is reduced in order to act as a nucleophile in a nucleophilic substitution reaction. The start of the reaction occurs when the nitrogen containing heterocycle is reduced during the electrolysis period and stabilized by the electrolyte forming the pool of anions that the reaction is named after. After the electrolysis period is complete, an electrophile is added to the solution and a nucleophilic attack occurs forming a new nitrogen-carbon bond (Figure 1.7).

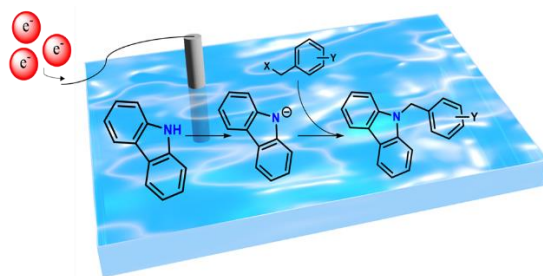


Figure 1.7: General reaction scheme of the anion pool two-step synthesis method.

The Vannucci Research Group has previously reported the ability of this electrochemical synthesis method to activate highly active compound such as anhydride substrates.²⁰ Additionally, it has been reported that the anion pool synthesis method provides unique selectivity. However, since this is a new approach for electrochemical synthesis, a reaction trend has not yet been established. As such, part of this dissertation focuses on the formation of such a reactivity trend so that the limitations of the current method may be understood and further improved upon.

1.11 Determination of benzidine reactivity based on electronics and functionality

The last portion of this dissertation focuses on understanding the reactivity of the benzidine rearrangement for the synthesis of carbon-carbon bonds. In recent years, the Suzuki-Miyaura coupling reaction has taken over the field for its ability to form carbon-carbon bonds with outstanding selectivity. While this method allows for great reactivity, it utilizes a transition metal catalyst that requires strategic design and typically requires great control to prevent unwanted reactivity. Additionally, many applications still require that substrate functionality be expanded on the aromatic substrates. When additional functionality like amines or nitro groups are added to the aromatic substrate and added into a reaction containing transition metal catalysts, there is the issue of the reactant acting as a ligand and poisoning the original transition metal catalyst, thus preventing the reaction from moving forward. This reaction offers an inexpensive and complex transition metal catalyst free system to synthesize sp^2 - sp^2 carbon-carbon bonds while maintaining unique functionality that is desirable in pharmaceuticals and materials industries. This study explores the traditional benzidine rearrangement and its limitations based on the electronic effects and functionality of the substrate substituents.

1.12 Traditional synthesis methods of C-C bonds

Aromatic molecules containing carbon-carbon bonds are of great importance in the pharmaceutical and materials industries. These carbon-carbon bonds are seen in everyday life in the make-up of human DNA to the formation of diamonds and in computer hardware. Due to their unique thermal and mechanical properties, aromatic compounds containing one or more sp^2 - sp^2 carbon-carbon bonds are of great interest in materials. Additionally, these compounds have unique redox properties that widen their application into electronic

devices and OLED applications. Furthermore, due to their prevalence in the human genomic makeup, aromatic compounds containing at least one carbon-carbon bond have been used for many medical applications including in the fight against certain lung-cancers as well as their uses in synthesizing compounds used to fight blood clotting disorders during pregnancy.

Due to the prevalence of carbon-carbon bonds in the biomedical application, it follows that biological enzymes would be well suited to catalyze the synthesis of carbon-carbon bonds. As such, enzymes such as transketolase from *Escherichia coli* has been used for asymmetric carbon-carbon bond synthesis.³² This is of particular interest as biocatalyst do not contain chemicals in a manner that would be toxic to the body. Furthermore, these biocatalysts can be easily grown in a laboratory setting with little cost. However, as seen with many biocatalysts, they require specific environments that must be extremely controlled in order to remain intact. That leads to difficulties when keeping them catalytic and stable in many industrial applications.

Another method that is taught in organic synthetic chemistry for the formation of carbon-carbon bonds is the Grignard reaction. This reaction first requires the creation of a Grignard reagent from an organic halide reacting with magnesium in order to make an organic magnesium halide reaction. This reaction was so important that in 1912 its discoverer, Francois Auguste Victor Grignard, was awarded the Nobel Prize in Chemistry for his work. While this reaction is well established and still of interest, it too requires a controlled environment as it is extremely moisture sensitive.³³

While there are several methods that may be utilized to synthesize compounds containing aromatic sp^2 - sp^2 carbon-carbon bonds, the most widely utilized method

currently is the Suzuki-Miyaura coupling method. This method has been so impactful that its discoverers were awarded the Nobel Prize in 2010 for the impact this reaction has had on the field of organic synthesis. This reaction allows for desirable yields when cross-coupling an aryl halide with a boronic acid while utilizing a palladium catalyst and base.³⁴ While this reaction is of high importance and interest, other methods provide unique and desirable reactivity as well. One of these reactions is the benzidine rearrangement.

1.13 Benzidine rearrangement

The benzidine rearrangement was first discovered in 1862 by August von Hofmann. Since its discovery there has been ample research to determine whether this reaction is an intermolecular or intramolecular reaction.³⁵ As it is now widely accepted that the benzidine rearrangement is in fact an intramolecular reaction, this dissertation does not delve further into this mechanism. Instead, the research presented herein is designed to further understand the role that the electronics and functionality of substituents play on the success of the rearrangement. However, on the basis of how the benzidine rearrangement works, it is well known that the reduction of the azobenzene compound to the hydrazine intermediate occurs first. After this step, it is widely accepted that in the presence of a strong acid and added heat, there is an intramolecular radical transfer to either the para-, meta-, or ortho-position of the benzene ring. Concurrently, the proton at this given position transfers to the hydrazine nitrogen and a new carbon-carbon bond is formed (Figure 1.8).

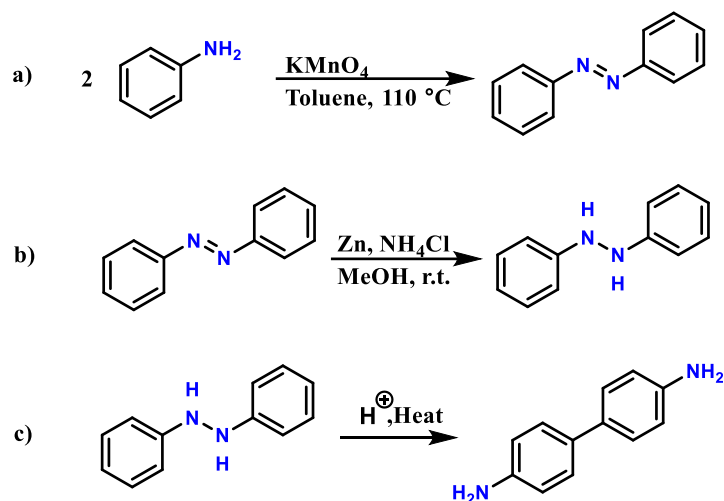


Figure 1.8: Traditional benzidine rearrangement as discovered by August von Hofmann

It is shown herein that the benzidine rearrangement occurs well without any substituents on the azobenzene compound or with substituents like chlorine which offers an electron donating and withdrawing effect. However, as substituents are added that are more electron donating and contain very little electron withdrawing properties, the yields decrease. Additionally, when functionality of the substituents is increased (i.e. a nitro- or amino- substituent) yields decrease. This dissertation aims to form a relative understanding and reactivity trend relating yields to the electron donating effect and functionality of the substituents on the azobenzene utilized.

**CHAPTER 2: PHOTOCATALYTIC OXIDATIVE COUPLING OF
ARYLAMINES FOR THE SYNTHESIS OF AZOAROMATICS AND
THE ROLE OF O₂ IN THE MECHANISM¹**

¹Sitter, J. D. and A. K. Vannucci, 2021. *Journal of the American Chemical Society*. 143, 2938-2943. Reprinted here with permission of the publisher.

2.1 Abstract

The photocatalytic oxidative coupling of aryl amines to selectively synthesize azoaromatic compounds has been realized. Multiple different photocatalysts can be used to perform the general reaction, however, $\text{Ir}(\text{dF-CF}_3\text{-ppy})_2(\text{dtbpy})^+$, where dF-CF₃-ppy is 2-(2,4-difluorophenyl)-5-(trifluoromethyl)pyridine and dtbpy is 4,4'-tertbutyl-2,2'-bipyridine showed the greatest range of reactivity with various amine substrates. Both electron rich and electron deficient amines can be coupled with yields up to 95% under ambient air atmosphere. Oxygen was deemed to be essential for the reaction and is utilized in the regeneration of the photocatalyst. Fluorescence quenching and radical trap experiments indicate an amine radical coupling mechanism that proceeds through a hydrazoaromatic intermediate before further oxidation occurs to form the desired azoaromatic products.

2.2 Introduction

Azoaromatic compounds are vital in many industries, including the textile, medical, optical storage, and dye industries.³⁶⁻³⁹ These compounds are traditionally synthesized via diazotization, which generates unstable diazonium intermediates and stoichiometric waste, and requires harsh conditions and high energy inputs as shown in Figure 2.1a.⁴⁰ More sustainable synthesis routes for azoaromatic compounds that produce higher product yields (>90%) and limit stoichiometric waste continues to be a research goal.^{41, 42} Advances in the understanding and sustainability of azoaromatic synthesis have been made recently with electro-⁴³ and photo-catalytic⁴⁴⁻⁴⁷ reductive coupling of nitrobenzenes. While impressive azoaromatic substrate scopes have been achieved, these processes can still require sacrificial inorganic salts as electron donors.⁴³ Product selectivity to the desired

azoaromatics, instead of azoxyaromatics or nitrosobenzene, has also proven difficult (Figure 2.1b).⁴⁸ It has been shown, however, that product selectivity in photocatalytic systems can be tuned by judicious choice of the light source.^{44, 47} Lastly, due to the reductive coupling nature of these catalytic systems, the reactions must be performed under inert atmosphere to avoid non-productive side reactions with molecular oxygen.

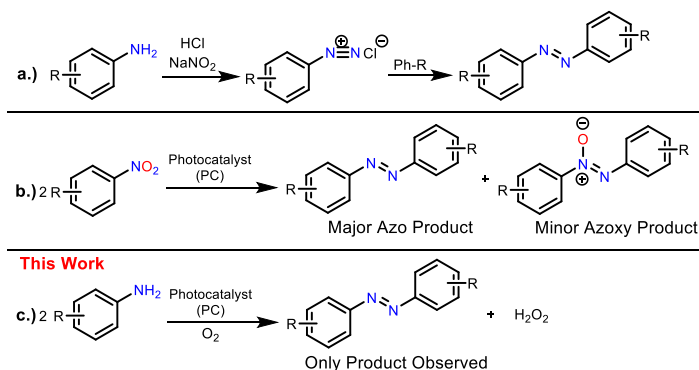


Figure 2.1: Comparison of routes for azoaromatic synthesis.

We thus hypothesized a possible photocatalytic oxidative coupling of aryl amines for the synthesis of azoaromatics (Figure 2.1c). This hypothesis was inspired by recent reports on the photocatalytic formation of aryl amines in which the proposed mechanism involves the oxidation of aryl amines.^{49, 50} Furthermore, photocatalytic oxidative coupling would use renewable light energy input, avoid solid stoichiometric waste from sacrificial electron donors, and be operable under ambient air conditions. Oxidative coupling has been widely explored,⁵¹⁻⁵³ used for N-N bond forming reactions,^{54, 55} and has shown the use of sustainable O_2 as oxidant.⁵⁶ Chemical oxidation of amines for the synthesis of azobenzenes has been reported, but often these processes require elevated temperatures and peroxide oxidants.^{57, 58} Alternatively amines can be oxidized to nitroso- or nitro-compounds and

subsequently coupled to amines for the synthesis of azobenzenes.⁵⁹ Synthesis directly from widely available amine starting materials however, could circumvent product selectivity issues that have been observed starting from nitrosobenzene compounds.

2.3 Results and Discussion

Multiple reactions were performed to achieve and optimize the photocatalytic oxidative coupling of aryl amines. Optimization reactions were carried out with *p*-anisidine as the substrate and are summarized in Table 2.1. Exploration for a suitable photocatalyst (PC) for this reaction examined Eosin Y, Ru(bpy)₃²⁺, where bpy = 2,2'-bipyridine, 9-mesityl-10-methylacridinium, and Ir(dF-CF₃-ppy)₂(dtbpy)⁺ (**Ir**), where dF-CF₃-ppy is 2-(2,4-difluorophenyl)-5-(trifluoromethyl)pyridine and dtbpy is 4,4'-tertbutyl-2,2'-bipyridine. As shown in Table 2.1, all four possible PCs gave good product yields, with the acridinium PC giving the lowest yield at 42% and **Ir** the highest yield at 94%. Subsequent investigations showed that changing the starting substrate from the electron rich *p*-anisidine to electron deficient amines caused the catalytic proficiency of Eosin Y and Ru(bpy)₃²⁺ to greatly decrease. Conversely, **Ir**, in which the **Ir** excited state is a stronger oxidant, maintained catalytic proficiency over a wide range of amine substrates. The acridinium PC, however, generates the strongest excited-state oxidant, however, the acridine neutral species is a poor reductant, and thus regeneration of the acridinium ground-state via oxidation by molecular oxygen is likely inefficient.

The oxidation of amine substrates is accompanied by the subsequent loss of a proton, therefore, the addition of base to the reaction was determined to be advantageous for obtaining optimal yields. Despite limited solubility in acetonitrile solution, K₃PO₄ resulted in the highest yields of desired products when compared to potassium acetate and

pyrrolidine base. Increasing the concentration of K_3PO_4 beyond 3 equivalents relative to the substrate concentration led to a decrease in yields which can be contributed to excess solid K_3PO_4 interfering with penetration of the light source into the reaction solution.

Table 2.1: Optimization of Reaction Conditions



Deviation from Standard Conditions ^a	% Yield ^b
none	94
4 hrs.	88
Eosin Y instead of Ir	64
$Ru(2,2'$ -bipyridine) $_3(PF_6)_2$ instead of Ir	82
Acridinium instead of Ir	42
Potassium Acetate instead of K_3PO_4	44
pyrrolidine instead of K_3PO_4	72
1 eq. of K_3PO_4	36
4 eq of K_3PO_4	82
No base	7
No $h\nu$	0
No photocatalyst	0
Under N_2 atmosphere	0
Under O_2 atmosphere (4 hrs.)	99

^aStandard conditions: 25 mM *p*-anisidine), 5 mL acetonitrile, under air atmosphere. ^bYields determined by GC-MS.

As anticipated, removing the PC or the light source resulted in no product formation or any conversion of the starting substrate. Purging the reaction solution with N₂ also resulted in a complete shutdown of product formation. Therefore, a reaction was performed in which the reaction solution was purged with molecular oxygen and sealed under an O₂ atmosphere. This O₂ saturated reaction led to an increase in product yield for the 4-hour reaction.

With the optimized conditions established, the range of possible amines suitable for photocatalytic oxidative coupling was explored. For the products reported in Figure 2.2, both GC-MS and NMR analysis of the reaction mixtures did not show any evidence of over oxidized azo-products such as azoxy-compounds nor was the formation of nitrobenzenes observed. These results illustrate the selectivity of this photocatalytic approach. All non-quantitative yields were mixtures of desired product and starting material. Figure 2.2 also reports the yields for two separate photocatalytic oxidative coupling reaction conditions. Azoaromatic products can be obtained in 4-hour reaction times by purging the reaction solutions with O₂. This photocatalytic reaction can also be adequately performed in 24 hours when performed in ambient air and the results of those reactions are shown in parentheses in Figure 2.2. In general, electron rich amines couple with good to excellent yields. Substituted azoaromatic products were also obtained starting from *ortho*-*meta*- and *para*-anisidine (rxns. 1 – 3 in Figure 2.1) and from the sterically encumbered trimethyl aniline (rxn. 4, Figure 2.1). Azoaromatic products were also obtained from electron neutral (aniline, rxn. 5) and electron deficient amines (4-fluoroaniline, rxn. 7). For the halogenated anilines (rxns. 7 – 9), no observed side products for C-X bond activation were observed further illustrating the high selectivity of this reaction.

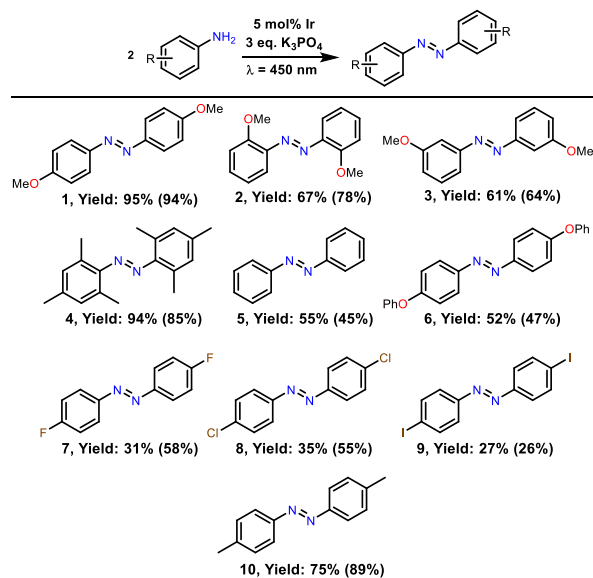


Figure 2.2: Photocatalytic oxidative coupling of arylamines. Yields are reported for reactions performed under an O₂ atmosphere for 4 hours. Yields in parentheses are 24-hour reactions open to ambient air. General conditions: 1.25 mM Ir, 25 mM amine, 3 equiv. K₃PO₄ in 5 mL of acetonitrile irradiated with a blue LED light.

To rationalize the observed trends in product yields from Figure 2.2 (high yields for electron rich amines, lower yields for electron deficient amines), and trends of chosen photocatalyst (high yields for the strong oxidant Ir and lower yields for weaker PC oxidants) we compared the oxidation potentials of the amines to the reduction potentials of the excited-state PCs. Cyclic voltammetry was used to determine the irreversible oxidation potentials for each of the amine substrates and this potential represents the oxidation of neutral amine substrates to the corresponding radical cations. Our data agrees with the few oxidation potentials we could find in the literature.⁶⁰ The largest magnitude oxidation potentials are roughly 0.94 V versus the saturated calomel electrode (SCE) and are associated with 4-chloro- and 4-iodo-aniline. These substrates also result in low yields (8

and 9 in Figure 2.2) when **Ir** is the PC and in no yields when Eosin Y or Ru(bpy)₃ are used as the PC. The magnitude of the excited-state reduction potentials (PC^{*}/PC⁻) for **Ir**, Eosin Y, and Ru(bpy)₃ are 1.21 V, 0.78 V, and 0.77 V versus SCE respectively. Thus the oxidation of 4-iodo-aniline by Eosin Y^{*} and Ru(bpy)₃^{*} is thermodynamically uphill by roughly 0.15 V and explains the lack of observed oxidation products. With respect to the **Ir** PC, higher energy amine radical cations, such as 4-iodo-aniline compared to *para*-anisidine, should be more efficient at unwanted back electron transfer from the radical cations to **Ir**^{*}. Thus, if back electron transfer has an effect on product yields, a direct correlation between amine oxidation potentials and product yields should be observed. Figure A.29 does show a linear trend between amine oxidation potentials and product yields and explains the observed trend in Figure 2.2.

The control reactions in Table 2.1 showed that O₂ was required for catalysis, likely as the oxidant required to regenerate the ground-state PC. Oxygen may play additional roles in the catalytic mechanism, such as the formation of nitroso or nitro intermediates, but no oxygenated side products were observed. Amine and nitroso compounds are known to thermally react to form azo compounds.^{61, 62} To examine this possibility, reactions with equal mixtures of aniline and nitrosobenzene or nitrobenzene respectively were performed as shown in Figure A.1 and discussed in detail in the SI. The reactions containing oxygenated starting materials resulted in product distributions that were quite different from the product distributions obtained from reactions containing only aryl amine starting material. These results thus eliminate the possibility of oxygenated monomer intermediates during the catalytic cycle.

The evidence for the lack of oxygenated intermediates coupled with the requirement for O₂ to be present in the reaction mixture implies that O₂ is involved in the regeneration cycle of the **Ir** photocatalyst. Previous reports on the photocatalytic oxidative coupling of benzylamine to form imines have shown that O₂ can act as a sacrificial electron acceptor and be converted to H₂O₂.⁶³ To test for the presence of H₂O₂ in the reaction mixtures, hydrogen peroxide strips with ppm sensitivity were used. As shown in Figure A.2, the indicator strips only changed color and detect H₂O₂ when a reaction was performed under standard conditions. These results indicate that O₂ is reduced to H₂O₂ during the photocatalytic mechanism and helps explain the major role for O₂ in the reaction mixture. Furthermore, a reaction was performed in which O₂ was replaced by Pt(IV)Cl₆²⁻ as the sacrificial oxidant. Under an N₂ atmosphere, with one equivalent of Pt(IV)Cl₆²⁻, 45% yield of product 4 was obtained. This further illustrates the role of O₂ as the sacrificial oxidant, as well as shows that inexpensive, renewable O₂ may be the superior reaction additive.

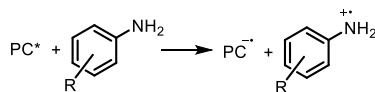


Figure 2.3: The proposed reductive quenching pathway with amine acting to quench the photocatalyst.

The lack of observed oxygenated intermediates also implies the amines are directly oxidized to amine radicals by the photocatalyst through the reductive quenching shown in Figure 2.3. Previous reports have shown that amine radical formation can selectively result in N-N bond forming reactions.⁵⁴ Fluorescence quenching experiments and a Stern-Volmer analysis were performed on the quenching between the **Ir** and *p*-anisidine, aniline, and 4-fluoroaniline respectively to examine how the electron density of the amine affected the

fluorescence of the excited state photocatalyst. The results, presented in Figures 2.4 and A.3 – A.7, show electron transfer quenching with $10^9 - 10^{10}$ M/s quenching rate coefficients in each experiment. Furthermore, as the electron density of the amines increased in the order of 4-fluoranylne < aniline < *p*-anisidine the slope of the Stern-Volmer plot increased. The increased slope indicates increased electron transfer kinetics and correlates well with electron density of the amine substrate.

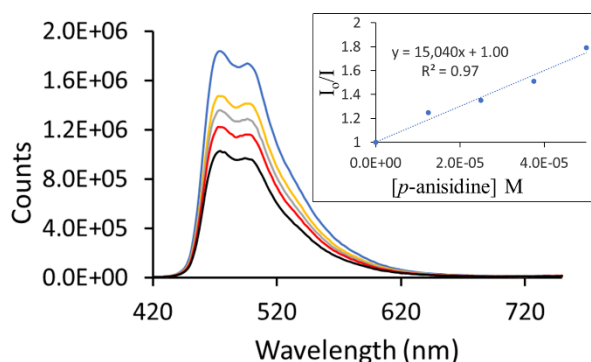


Figure 2.4: Fluorescence quenching data and Stern-Volmer plot for the quenching of **Ir** with *p*-anisidine. Conditions: 1.25×10^{-5} M **Ir** with indicated concentrations of substrate in acetonitrile solvent.

Additionally, quenching studies were performed with added K_3PO_4 base to further understand the role of base in the catalytic mechanism. The Stern-Volmer plots created from the quenching data with added base (Appendix A) show that the magnitude of the quenching kinetics is not significantly changed. This suggests that the base is not directly involved in the quenching mechanism, either through direct quenching of the photocatalyst or through a proton coupled electron transfer oxidation of the amine substrate.⁶⁴ The K_3PO_4 base likely just acts as a proton shuttle and accepts a proton from the amine radical cation substrates.

The fluorescence quenching experiments support the formation of amine radical cation intermediates; thus, radical trap experiments were performed to gain insight into the nature of the possible radical intermediates. 5,5'-dimethylpyrroline-1-oxide (DMPO) was used for the detection of photocatalytically generated amine radicals.⁶⁵ Standard reaction conditions as described in Table 2.1 under ambient atmosphere were used for the photocatalytic oxidative coupling of *p*-anisidine. The addition of a stoichiometric amount of DMPO occurred after 5 minutes of reaction. An aliquot of the reaction mixture was then transferred to a room temperature EPR instrument. The EPR spectrum, shown in Figure A.8, has *g*-values and a splitting pattern consistent with an amine-based radical trapped by DMPO.^{65,66} It is worth noting that the radical trap experiments do not differentiate between the trapping of amine radicals as shown in Figure A.8 or the trapping of amine radical cations, followed by deprotonation as has been previously shown.⁶⁷ Either possible amine species, however, does support the formation of amine radicals.

A likely mechanism for the formation of azobenzene molecules is shown in Figure 2.5. Amine radicals are generated through reductive quenching of the excited state photocatalyst. Radical coupling forms the nitrogen-nitrogen bond and the hydrazobenzene intermediate. This intermediate is then further oxidized by another photocatalyst cycle to the desired azobenzene product. The oxidation of the hydrazobenzene intermediates is likely facile as it has been reported that hydrazobenzenes can readily oxidize under ambient conditions.⁶⁸ It is worth noting that for reactions performed under an N₂ atmosphere, when exposed to oxygen post-reaction, azobenzene products were still not detected. Hence, while O₂ may aid in the oxidation of hydrazobenzene to azobenzene, O₂ must also play another role in the catalytic cycle. The critical role of oxygen then arises in the regeneration of the

ground state photocatalyst. With the formation of each azobenzene molecule generating 4 equivalents of protons and 4 equivalents of electrons, and the indirect detection of H_2O_2 , the fate of the reduced O_2 is the formation of hydrogen peroxide. This highlights a green chemistry aspect of this approach as O_2 acts as a sacrificial electron acceptor and generates relatively benign H_2O_2 by-product.

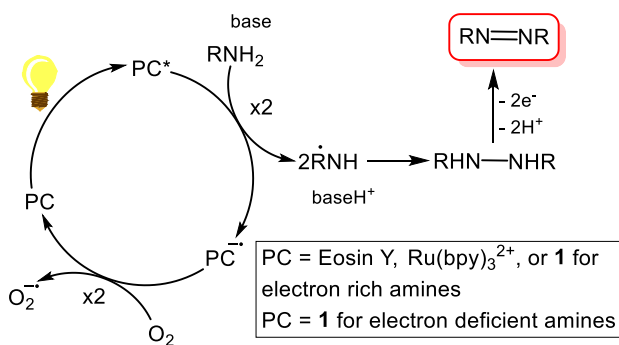


Figure 2.5: Proposed mechanism for the photocatalytic oxidative coupling of amines for the synthesis of azoaromatics.

2.4 Conclusions

The first example of a photocatalytic system for the oxidative coupling of arylamines for the synthesis of azoaromatics has been described. With the proper photocatalyst, electron-rich and electron-deficient amines can be coupled to form a variety of azoaromatic products. The catalytic system highlights a couple green chemistry principles⁶⁹ such as using renewable visible light as the energy input and utilizing renewable O_2 as a sacrificial electron acceptor. Mechanistic studies support nitrogen-based amine radical intermediates that couple to form hydrazobenzene intermediates which are further oxidized to the azoaromatic final products. Oxygenated by-products such as azoxybenzenes were not observed in post reaction mixtures. In addition, nitroso- and nitrobenzenes were shown to be inept for azoaromatic formation under the developed reaction

conditions. Overall, this study gives insight into the photocatalytic oxidation of amines and how to potentially control nitrogen-bond forming reactions.

2.5 Experimental

Materials. All reagents used were used as received from the manufacturer without further purification.

Instrumentation. Gas Chromatography-Mass Spectrometry (GC-MS) analysis was performed on a Shimadzu QP-2010S with a 30 m long Rxi-5 ms (Restek) separation column with a 0.25 mm id. The oven temperature program was 40 °C for 0.5 min, followed by a 10 °C/min ramp to 280 °C and held for 2 min.

NMR spectroscopy was performed using a Bruker Avance III HD 400. Data were processed using Bruker TopSpin software. ¹H NMR spectroscopy was performed using a 400 MHz instrument using deuterated chloroform or deuterated acetone as the solvent with a calibrated peak at 7.26 or 2.05 ppm, respectively. ¹³C NMR was conducted on a 400 MHz instrument set to a frequency of 75 MHz using chloroform or methylene chloride as the solvent and a calibrated solvent peak at 77.33 for deuterated chloroform or 206.7 and 29.9 ppm for deuterated acetone.

Emission spectra were obtained utilizing an Edinburgh FS5 fluorescence spectrometer equipped with a 150 W continuous wave xenon lamp source for excitation. The samples were all degassed and then the emission measurements were collected on the sample utilizing a 1.0 cm quartz cuvette with the SC-05 standard cuvette module.

EPR spectroscopy was performed using an X-band Bruker EMXplus spectrometer (Bruker Bio Spin, Billerica, MA) equipped with an Oxford Instruments ESR900 (Oxfordshire, UK) liquid helium continuous flow cryostat.

General procedure synthesis of symmetrical azo compounds. To a clean, 20-mL reaction vial, 25 mM of the aniline reactant was dissolved in 2.5 mL of acetonitrile. To this, 39.8 mg of K_3PO_4 (75 mM) and 3.5 mg of $(Ir[dF(CF_3)ppy]_2(dtby))PF_6$ catalyst (5 mol %) was dissolved. The reaction vial was then closed to prevent solvent evaporation, and a blue light was placed up to the reaction vessel. The light source used for all experiments was a 34 W Kessil H150W-BLUE light exciting at 400–500 nm with a maximum intensity at 480 nm. A fan was run over the reaction mixture to keep the reaction at room temperature the entire time. The reaction was then stirred at 260 rpm for 4 hrs or 24 hrs. The reaction was then isolated using preparatory thin-layer chromatography. All separations occurred via preparative-scale TLC. The solvent used were ethyl acetate and hexanes of ACS grade or better ($\geq 99\%$). The isolated product was then air dried overnight and submitted for proton and carbon NMR.

General procedure for the synthesis of symmetrical azo compounds with O_2 purge. To a clean, 20-mL reaction vial, 25 mM of the aniline derivative was dissolved in 2.5 mL of acetonitrile. To this, 39.8 mg of K_3PO_4 (75 mM) and 3.5 mg of $(Ir[dF(CF_3)ppy]_2(dtby))PF_6$ catalyst (5 mol %) was dissolved. The reaction vial was then purged with O_2 for 15 minutes, closed, and a blue light was placed up to the reaction vessel. The light source used for all experiments was a 34 W Kessil H150W-BLUE light exciting at 400–500 nm with a maximum intensity at 480 nm. A fan was run over the reaction mixture to keep the reaction at room temperature the entire time. The reaction was then stirred at 260 rpm for 4 hrs or 24 hrs. The reaction was then isolated using preparatory thin-layer chromatography. All separations occurred via preparative-scale TLC. The solvent

used were ethyl acetate and hexanes of ACS grade or better ($\geq 99\%$). The isolated product was then air dried overnight and submitted for proton and carbon NMR.

Fluorescence Quenching Experiments. Fluorescence quenching experiments were conducted with 1.25×10^{-5} M $(\text{Ir}[\text{dF}(\text{CF}_3)\text{ppy}]_2(\text{dtbyp}))\text{PF}_6$ in acetonitrile at room temperature with added substrate as indicated in the Stern-Volmer plots. For quenching experiments with added K_3PO_4 base, the concentration of the base was 2.5×10^{-4} M. The solutions were irradiated at 385 nm, and fluorescence were measured at 420 nm. Data can be found in the Appendix A.

EPR Experiments. Solvent used was dichloromethane as acetonitrile absorbs microwaves. A reaction was set up under standard, ambient air conditions with aniline as the substrate. Reaction was performed for 5 minutes at which point 25 mM 5,5-dimethyl-1-pyrroline N-oxide was added to trap the radical. The reaction was then run for an additional 30 minutes and 100 μL reaction mixture was placed into a quartz EPR tube. Spectra were recorded at room temperature. MatLab was used to fit the spectra.

Experiments with nitrobenzene and nitrosobenzene. To a 20 mL reaction vial, 25 mM total of the indicated starting material in Figure A.1 was dissolved in 5 mL of acetonitrile. To this, 39.8 mg of K_3PO_4 (75 mM) and 3.5 mg of $(\text{Ir}[\text{dF}(\text{CF}_3)\text{ppy}]_2(\text{dtbyp}))\text{PF}_6$ catalyst (5 mol %) was dissolved. The reaction vial was then closed, and a blue light was placed up to the reaction vessel. A fan was run over the reaction mixture to keep the reaction at room temperature the entire time. The reaction was then stirred at 260 rpm for 4 hrs. The reaction mixture was then determined utilizing GC-MS.

For reaction 1 in Figure A.1, a 1:1 mixture of aniline and nitrosobenzene was dissolved in acetonitrile and subjected to the standard reaction conditions under ambient

atmosphere as described in Table 2.1. A GC-MS analysis of the reaction solution after 24 hours of light irradiation showed a 3:1 product mixture of azoxybenzene:azobenzene. This product mixture is considerably different from the observed products when starting with only amines and thus rules out the possibility of nitrosobenzene intermediates in the catalytic mechanism. When reaction 1 in Figure A.1 is performed at room temperature without light irradiation, no substrate consumption or product formation was observed.

Next, a reaction containing equal mixtures of aniline and nitrobenzene (reaction 2, Figure A.1) was performed under standard conditions. For this reaction, the consumption of aniline was observed with the concurrent formation of azobenzene product. The nitrobenzene substrate, however, was not consumed in the reaction.

For the reaction containing nitrosobenzene (reaction 3 Figure A.1), GC-MS analysis did not detect any azobenzene product. Instead roughly 50% of the nitrosobenzene was converted to nitrobenzene. In addition, a small amount of azoxybenzene was formed. This product mixture is entirely different from the products obtained with amine reactants and indicates that nitrosobenzene is not a prominent intermediate in the photocatalytic oxidative cross-coupling of aryl amines.

The attempted reaction containing only nitrobenzene (reaction 4, Figure A.1) did not appear to result in any conversion of nitrobenzene as determined by GC-MS analysis. This result is consistent with the results presented in Scheme 1 of this chapter which also showed that nitrobenzene is inert towards the reaction conditions and further rules out nitrobenzene as an intermediate in the performed photocatalytic reaction.

**CHAPTER 3: INSIGHTS INTO REACTIVITY TRENDS FOR
ELECTROCHEMICALLY GENERATED ANIONIC NITROGEN
NUCLEOPHILES²**

²Sitter, J. D., Lemus-Rivera, E. L. and A. K. Vannucci, 2023. Submitted to Organic & Biomolecular Chemistry.

3.1 Abstract

Electrochemistry is currently of great interest due its potential in synthesizing much needed products while limiting reactant and energy input and providing potentially unique selectivity. Our group has previously reported the development of the “anion pool” synthesis method. As this is a new and unique method for organic synthesis, it is important to understand the reactivity trends and limitations this method provides. In this report we explore the reactivity trends of a series of nitrogen-containing heterocycles under reductive electrochemical conditions. Benzylic halides were utilized as model substrates to probe the reactivity of electrochemically reduced nitrogen-containing heterocycles. By generating nitrogen-centered anions during electrolysis and maintaining them in a “pool”, unique reactivity is observed when followed by the addition of an electrophile. This two-step method allows for sp^3 C-X bonds to be broken and C-N bonds formed. It is discussed herein a general reactivity trend correlating between the pK_a value of the parent nitrogen-containing heterocycle. Generally, as the pK_a of the heterocycle increases, the strength of the resulting anion nucleophile likewise increases. Following that logic, the stronger nucleophiles can activate more thermodynamically stable sp^3 C-X bonds forming the desired C-N cross-coupled products. Additionally, it is shown that the stability of the anion generated is imperative when obtaining high yields and the stability and reactivity of the anions are affected by the choice of electrolyte and temperature.

3.2 Introduction

Electrochemical synthesis has garnered renewed interest in recent years as a tool to access new synthetic routes⁷⁰ while also being able to adhere to green chemistry principles.⁷¹ As a synthesis route, it is able to avoid harsh chemical oxidizers and reducers

and elevated temperature by accessing single electron redox reactions at electrode surfaces under applied potentials.⁷² In addition, electrochemical simulation programs can help elucidate reaction mechanisms and kinetics.⁷³⁻⁷⁴ Recent reviews and reports highlight the versatility of electrochemical synthesis.⁷⁵⁻⁷⁷ For example, electrochemical synthesis has been recently used to selectively synthesize N-N bonds in pyrazolidine-3,5-diones and benzoxazoles allowing for the avoidance of typically high temperature and multi-step processes used in these compounds traditional synthesis routes.⁷⁸ More recently, the usefulness of electrochemical synthesis has been shown when performing the oxidation of methylenes utilizing a hydrogen atom-transfer (HAT) agent to increase substrate scope and functional group compatibility.^{79, 80} Highlighting sustainability, electrochemical reduction was utilized to perform Mizoroki-Heck coupling of aryl halides with a nickel catalyst, thus preventing the utilization of an expensive palladium catalyst for the same route.⁸¹ In addition, early work on electrochemical cross-coupling⁸² has been advanced by chemical reductive cross-coupling,⁸³ then re-adapted to electrochemical cross-coupling.⁸⁴

Within the past few years, our group has developed a catalyst-free electrochemical synthesis method for the formation of C-N bonds. This method has been dubbed the “anion pool” synthesis and it took inspiration from the cation pool synthesis method that was first reported by Suga and Yoshida.^{85, 86} In the anion pool method for electrochemical synthesis, a nitrogen containing reactant is reduced in the cathodic chamber during electrolysis as shown in Figure 3.1. During electrolysis, a half of an equivalent of hydrogen gas is released per equivalent of reactant.⁸⁷ Once enough current has been passed to successfully create a “pool” of nucleophilic anions, a carbon electrophile is added to the cathodic chamber leading to a nucleophilic substitution reaction to form C-N bonds. Previous reports have

shown that ferrocene can be used as a recyclable component in the anodic chamber to balance the overall redox reaction.⁸⁸

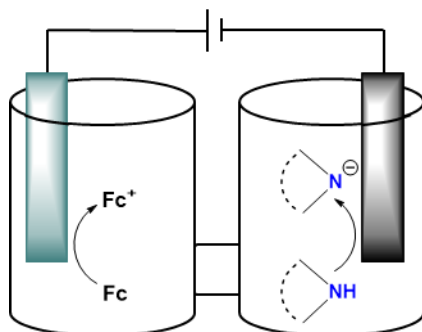


Figure 3.1: Schematic of the anion pool synthesis method showing the electrochemical formation of anionic nitrogen-containing nucleophiles.

The formation of C-N bonds is highly important for use in the pharmaceutical industry as 75% of pharmaceutical compounds contain at least one nitrogen containing heterocycle.⁸⁹ C-N bond formation has been attempted via many different methods. Primarily, Buchwald-Hartwig amination has been utilized for the selective formation of sp^2 C-N bonds.⁹⁰ This route offers good selectivity and overall yields, thus making it highly desirable via industrial applications. Another route that has recently been explored has resulted from advances in photoredox coupling have led to the construction of important sp^2 and sp^3 C-N bonds utilizing ruthenium, iridium, copper and nickel catalysts.⁹¹⁻⁹⁶ Furthermore, ionic liquids as electrochemical solvents have been explored for the purpose of synthesizing desired C-N bonds. Recently, basic ionic liquids have been used for the purpose of C-N bond formation utilizing Huenig's base.⁹⁷ The anion pool synthesis method provides yet another tool in the C-N bond synthesis toolbox and offers a simple, potentially

green approach that circumvents the need for expensive catalysts. This method was also the first to achieve completely selective *N1*-acylation of indazoles,⁹⁸ thus justifying further exploration of this relatively new method.

While the anion pool approach may offer advantages for the formation of C-N bonds in chemical synthesis, to date this method has mainly been utilized with highly reactive electrophiles such as anhydrides. For the purpose of promoting reactivity with wider variety of electrophiles, we must first develop a fundamental understanding of reactivity trends with regard to the anionic nitrogen-containing nucleophiles. In this report, reactivity trends are elucidated for nitrogen-containing heterocycle anions based on pK_a values and extended conjugation of the parent protic heterocycle. The effect the electrolyte has on the reaction as well as the electrophilicity of the halogenated substrates is also explored.

3.3 Results and Discussion

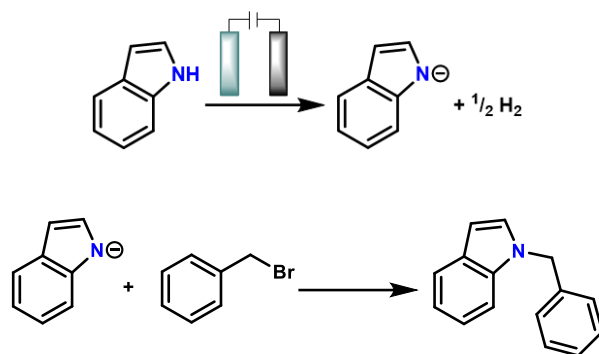
The anion pool method has been previously established by our group as a means to electrochemically generate anionic nitrogen nucleophiles capable of reacting with carbon electrophiles and forming C-N bonds without the need for a metal catalyst.⁸⁷ While we have shown this approach is applicable for selective acylation and ester formation,^{88, 98} fundamental insights into anion formation and reactivity trends have not yet been established. These reactivity trends are necessary for the rational design of new electro-synthetic routes. With this in mind, we chose to study a series of nitrogen-containing heterocycles with a pK_a value range between 16 and 23 in acetonitrile solution. These seven orders of magnitude range of acidity should give a wide range of reactivity of the subsequent nitrogen anion generated upon electrochemical reduction as shown in Figure

3.1. We also chose benzylic halides as a model set of substrates to probe the reactivity of the nitrogen anions. The carbon electrophiles in benzylic halides are less activated than the anhydride substrates utilized in previous reports but should offer ample reactivity to probe trends in the nitrogen containing substrates.

The first step in anion pool synthesis is the generation and buildup of reactive anionic species (Figure 3.1). Preventing decomposition of the anion, or unwanted reactivity with solvent or electrolyte, is obviously important for the success of this two-step electrosynthesis process. Previous reports have eluded to the importance of electrolyte in achieving desired reactivity.⁸⁸ Therefore, it is imperative to understand how the electrolyte may interact with or stabilize the reactive anions. To determine how electrolyte cation size and steric hindrance affect this method, the anion pool coupling between 1*H*-indole and benzylic bromide was explored using three different electrolytes suitable for use in acetonitrile solvent as shown in Table 3.1. As described in the experimental section, the first step of the anion pool synthesis is a constant current electrolysis of the heterocycle, and the second step is the addition of the benzylic halide. For each experiment in Table 3.1 all variables were kept constant with the exception of electrolyte used. The results in Table 3.1 show that the electrolyte with the smallest cation, LiClO₄, led to no product yield, whereas the largest electrolyte cation, Nbu₄PF₆, led to the highest product yield and the intermediate cation size, KPF₆, led to intermediate yield. These results indicate that smaller cations likely over-stabilize the nitrogen anions generated in the first step and prevent efficient reactivity with the carbon electrophiles. Similar reactivity trends of nitrogen nucleophiles with various cation sizes have previously been reported.⁹⁹ Furthermore, the Nbu₄PF₆ electrolyte contains hydrogen atoms that could be susceptible to deprotonation by

strong bases. However, no reactivity between the anionic indole intermediate and the electrolyte was observed by GC-MS analysis of the post reaction mixture. This indicates that the conjugate bases of the nitrogen containing heterocycles examined here are not strong enough bases to deprotonate the electrolyte or acetonitrile solvent.

Table 3.1. Optimization of electrolyte for anion pool synthesis reaction involving nitrogen heterocycles.



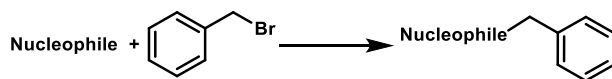
Electrolyte	% Yield
LiClO ₄	0
KPF ₆	49
Bu ₄ NPF ₆	77

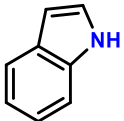
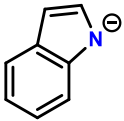
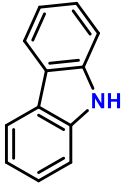
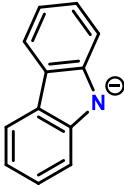
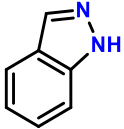
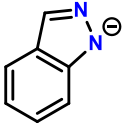
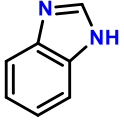
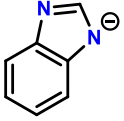
Reaction conditions: Room temperature, 0.1 M electrolyte, 0.375 mmol of indole, excess benzyl bromide in acetonitrile. 0.75 mmol Fe added to anodic chamber. RVC anode and cathode.

Utilizing Nbu₄PF₆ as the electrolyte, a range of nitrogen heterocycles was explored utilizing benzylic bromide as the model electrophile (Table 3.2). The reaction variables in Table 3.2 were kept constant with exception of the heterocycles and the corresponding p*K_a* values in acetonitrile solution.^{100, 101} As shown in Table 3.2, a clear correlation can be seen between the p*K_a* value of the parent heterocycle and the overall yield of the product in the

pK_a range of 16 – 21. The pK_a values of the parent heterocycle are a measure of the electron density of the nitrogen atoms, and thus should directly correlate with the reactivity of the corresponding nucleophiles.

Table 3.2: Anion pool C-N bond forming reaction yields versus pK_a values of parent heterocycle.



Heterocycle	Nucleophile	pK_a	% Yield
		23.0	45
		21.0	77
		19.9	79
		19.0	49
		16.4	0

Reaction conditions: Room temperature, 0.1 M Bu_4NPF_6 , 0.375 mmol of nitrogen containing heterocycle, excess benzyl bromide in acetonitrile. 0.75 mmol Fe added to anodic chamber. RVC anode and cathode.

Up to a pK_a value of 21, this trend appears to hold as product yields in the reaction between the nitrogen nucleophiles and the carbon electrophile increase as pK_a values increase. However, for pyrrole, with a pK_a value of 23, the trend is broken and product yields decrease. This break in the reactivity trend may be due to the anionic pyrrole nucleophile being unstable under the reaction conditions during the anion pool formation during the first step.

With these results, it can be inferred that there is an upper limit with regard to the parent heterocycle pK_a values and its observed reactivity at room temperature. This may occur due to the anion pool method being a two-step process and thus the generated nucleophile must be stable long enough for the electrophile to be added at a later time. This hypothesis was tested by utilizing pyrrole as the nucleophile and comparing the effects of cooling down the reaction during electrolysis to 0 °C. Previous reports of electrochemically generating pools of cations have shown that temperature can help stabilize ion formation.⁸⁵ It was found that the cooling of the reaction during the electrolysis period resulted in an increased yield of desired C-N cross-coupled product of 91%, thus supporting the hypothesis that stability of the nucleophilic anion plays a vital role in overall reaction yields.

To further explore the pK_a reactivity trend, a 5,6-substituted indazole was tested under the standard reaction conditions in Table 3.2. The pK_a value for 6-bromo-5-methoxy-1*H*-indazole is not reported, however, the electron donating properties of the methoxy group, and to a lesser extent the bromide group, should increase the electron density of this molecule compared to 1*H*-indazole. Therefore, the pK_a of 6-bromo-5-methoxy-1*H*-indazole should be > 19 and if the observed pK_a reactivity trends hold product yields from

the anion pool coupling of the substituted indazole with benzyl bromide should be greater than the yields observed for unsubstituted 1*H*-indazole (49%, Table 3.2). To our delight, the 5,6-substituted indazole resulted in an 86% product yield in the anion pool coupling with benzyl bromide. This result further supports the observed pK_a reactivity trend and likely brackets the pK_a of 6-bromo-5-methoxy-1*H*-indazole between 21 and 23.

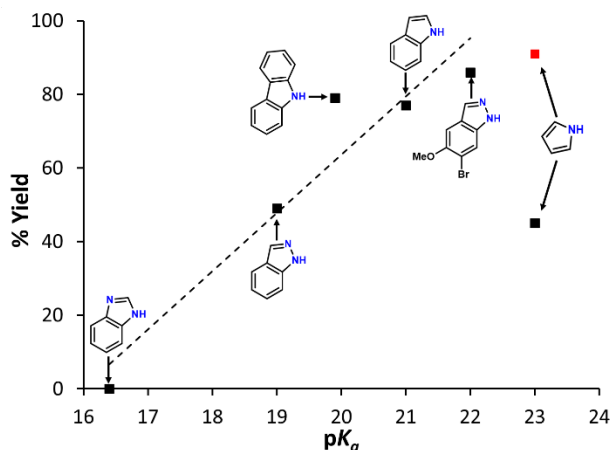
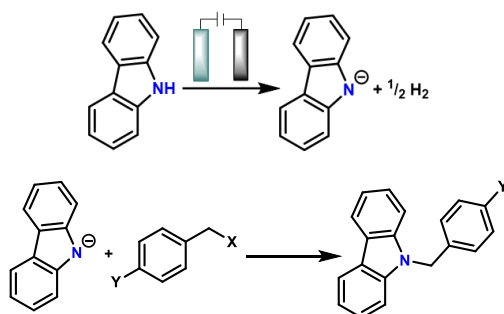


Figure 3.2: Plot of pK_a of parent heterocycle versus % yield of anion pool reaction with benzyl bromide. Red point is pyrrole reaction run at 0 °C.

A summary of the pK_a reactivity trends can be observed in the plot shown in Figure 3.2. The black squares represent product yields obtained with room temperature electrolysis and the red square was a product yield obtained with an electrolysis performed at 0 °C as previously described. A near linear trend is observed for heterocycles with pK_a values between 16 and 22. At a pK_a value of 23, the stability of the anionic nitrogen nucleophile may inhibit reactivity and alternate reaction conditions, such as lower temperatures, are required to obtain optimal yields. These trends provide the basis for the

anion pool methodology that allows for the implementation of improvements on this method in future experiments.

Table 3.3. Summary of % yields in the reactions of carbazole anion nucleophile with various benzylic halide electrophiles.



Rxn.	Electrophile	% Yield
1		92
2		79
3		60
4		82
5		27
6		89
7		39

Reaction conditions: Room temperature, 0.1 M Bu_4NPF_6 , 0.375 mmol of carbazole, excess benzyl bromide in acetonitrile. 0.75 mmol Fe added to anodic chamber. RVC anode and cathode.

With electrolyte and heterocycle trends generally established, reactivity trends with respect to the carbon electrophile coupling partner were explored. Carbazole was chosen as the model heterocycle due to its relatively high product yield in Table 3.2, but with room for potential increase in yields. The range of benzylic electrophiles explored for this study and their corresponding C-N coupled product yields are shown in Table 3.3. Amongst the substrates studied, those substrates that could be considered more electrophilic, with a potentially higher δ^+ on the benzylic carbon, resulted in higher yields. While benzylic bromide showed promising yields, when replaced with a benzylic chloride, yields were improved. This could be attributed to the chlorine atom being more electron withdrawing than the bromine atom on the benzylic sp^3 carbon. Benzylic substrates containing electron withdrawing substituents also consistently led to high product yields. Conversely, when an electron donating groups such as OMe were present on the benzylic substrate, yields were significantly lower compared to unsubstituted benzylic halides. Additionally, the substrate 4-bromo benzyl bromide showed complete selectivity towards the sp^3 benzylic carbon. This result highlights a potential advantage of the anion pool approach to target specific carbon-halogen bonds in complex molecules. Alternatively, the lack of reactivity towards sp^2 C-halogen bonds indicates that more reactive nitrogen nucleophiles are likely necessary to achieve C-N cross-coupling analogous to Buckwald-Hartwig coupling.

In terms for electrochemical efficiency, the Faradaic yields of the reactions reported here scaled directly with product yields. The charge passed during the anion pool generation first step was limited to the charge required to generate enough anions to perform the subsequent reaction with the benzylic halides. Passing excess charge during the electrolysis did not result in increased product yields. Furthermore, the atom economy,

which is a measure of how many atoms in the reactants are incorporated into the products,¹⁰² for reaction 1 in Table 3.3 is 87.5%, which is comparable to many “green” chemistry processes. In addition, we performed reaction 2 in Table 3.3 again, but with a concentration 16 times greater and were able to obtain a 57% product yield, which indicates this reaction can be performed under a range of substrate concentrations. Performing reactions at high concentrations helps improve the process mass index (PMI) of the reaction. PMI is a more direct measure of overall reaction efficiency compared to atom economy and the PMI for reaction 2 was calculated as 81.4 where PMI values under 100 are considered “green” reaction in commercial pharmaceutical processes.^{103, 104}

3.4 Conclusions

Reactivity trends and general principles for the anion pool electrochemical synthesis method have been established. These trends are essential for the rational design of electrochemical synthesis methodology focusing on the reductive activation of substrates. In general, the reactivity of electrochemically generated anionic nitrogen nucleophiles correlated with the pK_a value of the corresponding protonated heterocycles. For heterocycles with a pK_a value under 17, for example benzimidazole (16.4), reactivity with highly activated electrophiles such as acetic anhydride has been previously reported. However, reactivity with less activated electrophiles such as benzylbromide was not observed in this study. Whereas anionic nitrogen nucleophiles with parent pK_a values greater than 23 showed a lack of stability at room temperature and controlled reactivity required lowered temperatures. Alternating the cation size in the reaction electrolyte also offers a route to control reactivity, as smaller cations greatly stabilized the anionic nucleophiles. Overall, the anion pool method for the coupling of nitrogen heterocycles and

carbon electrophiles has been shown as an efficient route and the trends reported here should lead to future studies involving coupling of sp^2 -carbon electrophiles to amines and heterocycles.

3.5 Experimental

Materials. Anhydrous acetonitrile 99.8%, was used for all reactions. All solutions used for electrochemical measurements contained 0.1 M tetrabutylammonium hexafluorophosphate (nBu_4PF_6) further purified via recrystallization from ethanol and dried under vacuum at 80 °C for 24 h. For reactions containing lithium perchlorate ($LiClO_4$), the electrolyte was purified via recrystallization in hot acetonitrile and dried under vacuum at 80 °C for 24 h. For reactions containing potassium hexafluorophosphate (KPF_6), the electrolyte was purified via recrystallization in alkaline deionized water and dried under vacuum at 80 °C for 24 h. All other chemicals were received from the manufacturer without further purification.

Instrumentation. Gas Chromatography-Mass Spectrometry (GC-MS) analysis was performed on a Shimadzu QP-2010S with a 30 m long Rxi-5 ms (Restek) separation column with a 0.25 mm id. The oven temperature program was 40 °C for 0.5 min, followed by a 10 °C/min ramp to 280 °C and held for 2 min.

NMR spectroscopy was performed using a Bruker Avance III HD 400. Data were processed using Bruker TopSpin software. 1H NMR spectroscopy was performed using a 400 MHz instrument using deuterated dimethyl sulfoxide as the solvent with a calibrated peak at 2.50 ppm, respectively. ^{13}C NMR was conducted on a 400 MHz instrument set to

a frequency of 75 MHz using deuterated dimethyl sulfoxide as the solvent and a calibrated solvent peak at 39.52.

General procedure synthesis of products. In an inert atmospheric environment and to a clean, h-cell with 25-mL reaction vials on each side, 0.375 mmol of the nitrogen containing compound was dissolved in 20 mL of acetonitrile on the cathodic side along with 0.1 M of electrolyte and a 1 mm magnetic stir-bar. To the anodic side, 0.75 mmol of ferrocene was added and dissolved in 20 mL of acetonitrile along with 0.1 M of electrolyte and a 1 mm magnetic stir-bar. The reaction was then closed and the pressure was equilibrated utilizing a rubber hose connecting the two reaction sides. In each cap was placed a carbon mesh electrode that was suspended in the solution with a stainless-steel wire. The reaction was placed onto a magnetic stir plate and the stir rate was set to 360 rpm. The electrolysis began at -3 mA and was run for 97.5 minutes. The electrophile was then added to the cathodic side of the reaction and the current was dropped to -0.5 mA for the relaxation period of 2 hours. The reaction was then isolated using preparatory thin-layer chromatography. All separations occurred via preparative-scale TLC. The solvent used were ethyl acetate, dichloromethane and hexanes of ACS grade or better ($\geq 99\%$). The isolated product was then air dried overnight and submitted for proton and carbon NMR.

Procedure for the synthesis of products at 0 °C. In an inert atmospheric environment and to a clean, h-cell with 25-mL reaction vials on each side, 0.375 mmol of the nitrogen containing compound was dissolved in 20 mL of acetonitrile on the cathodic side along with 0.1 M of electrolyte and a 1 mm magnetic stir-bar. To the anodic side, 0.75 mmol of ferrocene was added and dissolved in 20 mL of acetonitrile along with 0.1 M of electrolyte and a 1 mm magnetic stir-bar. The reaction was then closed and the pressure

was equilibrated utilizing a rubber hose connecting the two reaction sides. In each cap was placed a carbon mesh electrode that was suspended in the solution with a stainless-steel wire. The reaction was placed into an ice bath and onto a magnetic stir plate and the stir rate was set to 360 rpm allowing the reaction to cool for 10 minutes. The electrolysis began at -3 mA and was run for 97.5 minutes. The electrophile was then added to the cathodic side of the reaction, the reaction was warmed up to room temperature and the current was dropped to -0.5 mA for the relaxation period of 2 hours. The reaction was then isolated using preparatory thin-layer chromatography. All separations occurred via preparative-scale TLC. The solvent used were ethyl acetate, dichloromethane and hexanes of ACS grade or better ($\geq 99\%$). The isolated product was then air dried overnight and submitted for proton and carbon NMR.

Procedure for PMI calculations for amidation. A separate experiment was setup in an H cell using equivalent volumes of solvent and electrolyte quantity. The volume of acetonitrile used for both cathode and anode was 2.5 mL each. Each compartment contained 70 mM electrolyte. The cathode compartment contained 0.75 mmol of carbazole and anode compartment contained 0.25 mmol ferrocene. After electrolysis was completed, 0.36 mmol of benzyl bromide was added to permit nucleophilic substitution.

Mass of carbazole = 0.0608 g

Mass of benzyl bromide = 0.0622 g

Mass of solvent = 3.93 g

Mass of electrolyte = 0.1356 g

Mass of Ferrocene = 0.0465 g

Mass of the amide = 0.062 g

PMI = total mass/mass of products = 4.235/0.052 = 81.44

**CHAPTER 4: INVESTIGATION INTO THE BENZIDINE
REARRANGEMENT REACTION**

4.1 Abstract

Due to its importance in pharmaceuticals and materials, the development of new and efficient ways for the construction of carbon-carbon bonds is an ever-evolving field of synthetic chemistry. Metal catalyzed cross-coupling reactions is the most common method of synthesis utilized by modern chemist to form carbon-carbon bonds. However, prior to the development of transition metal catalyzed carbon-carbon bond formation, the benzidine rearrangement was a promising route of obtaining the carbon-carbon bond. This benzidine rearrangement reaction forms biphenyl amine products which leads to interesting applications due to highly functional substituents. This research aims to understand and establish reactivity trends for the formation of substituted biphenyl amines via the utilization of the benzidine rearrangement reaction. It has been found that while chlorine substituents offer good reactivity and product yield, other halides like a fluorine and iodine substituent offer far less promise. This is likely due to the difficulties in synthesizing the parent azobenzene molecule as well as the unique donating and withdrawing effects attributed to the chlorine substituent. Furthermore, it has been found that electronically rich azobenzene molecules are able to rearrange but with less apparent yields. Another major effect that has been observed on poor overall yields is azobenzene substituent functionality. When the additional functional groups, like amines, are protected and then exposed to the heats necessary to form the rearranged product, ring closure has been observed as the main product thus leaving this route impractical for industrial applications. This report has been able to establish a general trend between electron density of the parent azobenzene compound as well as the functionality of said compounds and the overall rearrangement yields.

4.2 Introduction

The formation of aromatic carbon-carbon bonds is one of the most desirable bonds to make for industrial purposes. Its thermal and mechanical properties have been of use in the material industries¹⁰⁵ for years while more recently certain aromatic compounds with amine substituents are being explored for the purpose of OLED application due to their unique redox properties.¹⁰⁶ More recently, aromatic compounds containing carbon-carbon bonds have been of interest in the fight against non-small cell lung cancers that were previously thought to be incurable.¹⁰⁷ In recent years, the Suzuki-Miyaura reaction has become the de facto leader when speaking of carbon-carbon synthesis in pharmaceuticals, agrochemicals and polymers. It was such an important discovery that its discovery led to the awarding of the Nobel Prize in 2010. While this reaction is and will remain an important tool in the aromatic carbon-carbon bond formation toolbox, it does have its limitations.

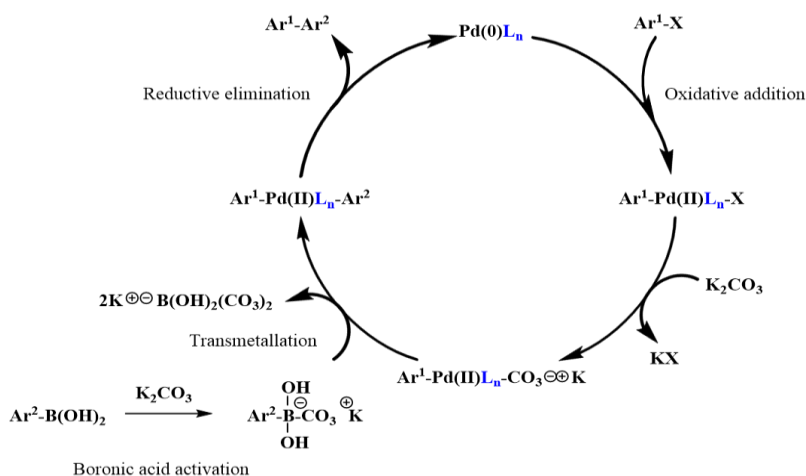


Figure 4.1: The traditional catalytic cycle when conducting Suzuki-Miyaura coupling with a palladium(II) catalyst.

Metal catalyzed cross-coupling reactions are a set of reactions that include the Suzuki-Miyaura coupling reaction and have the distinct advantage of being able to form a wide range of carbon-carbon bonds.¹⁰⁸ The Suzuki-Miyaura coupling reaction in particular utilizes a base and a palladium catalyst to synthesize new biphenyl compounds from aryl halides (Figure 4.1). Typically, however, the reaction is thought to be extremely oxygen sensitive, and the addition of the substrates require precise control for the reaction to work as desired.¹⁰⁹ Additionally, the reaction is limited to substituents that would not act as a ligand to the palladium catalyst as amine substituted aryl compounds are well known to be good ligands for transition metal complexes. The addition of amine aryl-halides compounds to the reaction mixture would likely lead to competition between the amine of the aryl halide and the halide substituent during the oxidative addition step of the reaction. If the equilibrium lies towards the coordination of the amine substrate rather than the halide coordination, the palladium catalyst would be rendered useless for cross-coupling reactions (Figure 4.2).

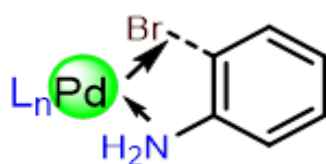


Figure 4.2: Competition between coordinating substituents of a palladium square planar catalyst.

The benzidine rearrangement is a reaction that was discovered by August von Hofmann in 1862 and is ubiquitously used when referring to the replacement of a hydrazine nitrogen-nitrogen bond with a new sp^2 carbon-carbon bond.^{110, 111} One way that this can be

achieved is via the oxidative coupling of aryl amines to an azobenzene (Figure 4.3a) compound followed by the reduction of the azobenzene compound to a hydrazine (Figure 4.3b). After the reduction is completed, the addition of a strong acid and heat complete the benzidine rearrangement (Figure 4.3c).

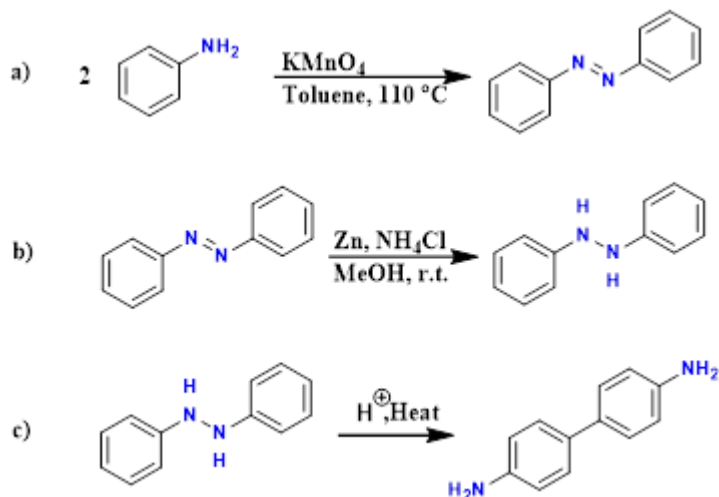


Figure 3: Traditional benzidine rearrangement as discovered by August von Hofmann

Since this time, benzidine products have become widely used in the materials¹¹², dyes¹¹³, pharmaceuticals and OLEDs.¹¹⁴ Although the exact mechanism of the benzidine rearrangement is not known, it is hypothesized to occur via an intramolecular pathway.^{110, 115} Much research has been conducted to fully understand the mechanism of this rearrangement. Recent Density Functional Theory (DFT) calculations have surmised that utilizing a Frustrated Lewis Pair (FLP), the mechanism must be intramolecular and further depends on the bond torsion angle of the resulting adduct.¹¹⁶ Other reports have focused on understanding the mechanism of the benzidine rearrangement and the role that the concentration of acid plays in the reaction determining that there are possibly two

mechanisms of reaction that occur simultaneously as the rate of rearrangement has been found to have been both first and second degree with respect to acid concentration.¹¹⁷ Our research hopes to add to the understanding of the mechanism of reaction for the benzidine rearrangement by focusing on and determining the reactivity trend of the rearrangement based on the electronics and functionality of the azobenzene substituents. While the benzidine rearrangement has been extensively used and studied, the understanding of reaction trends and experimental design is important for the ease of experimental design.

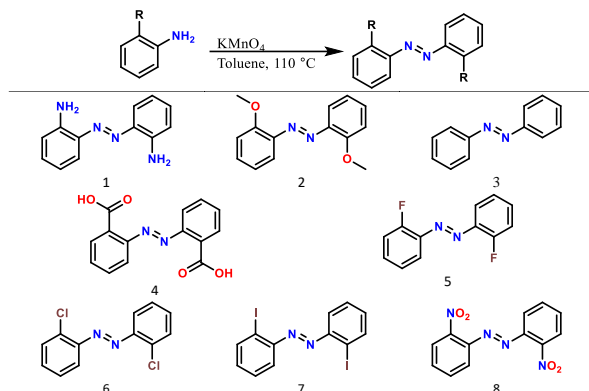
Thus far, we have shown successful rearrangements with electron deficient azo compounds and electron rich compounds, but not with highly functional amine or nitro substituted molecules. The goal of this chapter is to better layout the limitations of current substrate scopes and to understand why these limitations exist in order to help with a fundamental understanding of reaction trends so that the process can be further improved upon in the future.

4.3 Results and Discussion

To first understand the techniques from prior benzidine rearrangement reports, the synthesis of azobenzene from aniline followed by the hydrogenation of a standard azobenzene and its subsequent rearrangement were attempted as previously reported. Once unsubstituted azobenzene was on hand and confirmed via GC-MS, the reduction of the azobenzene compounds to their hydrazine compound was attempted exactly as previously reported in literature.¹¹⁸ The reduction of azobenzene utilizing zinc and ammonium chloride resulted in the quantitative yield of hydrazine. Following the hydrogenation of azobenzene to hydrazobenzene, the rearrangement was conducted by following a previously reported procedure.^{119,120} Yields obtained for the desired benzidine product as

estimated via LC-MS was 60% between 3,3'- and 4,4' rearranged product which was within experimental error when compared to previous reported yields.

Table 4.1: Figure showing scopes of products synthesized.



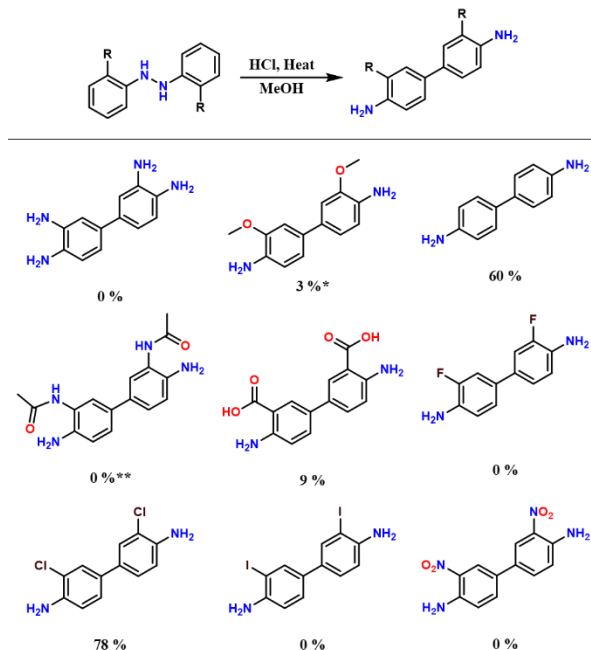
Products synthesized following previously stated procedure. Reaction run for 12 hours prior to separations.

Once previous methods of synthesis were successfully repeated utilizing unsubstituted azobenzene as a standard, a broad range of azobenzene compounds were explored to determine how electronics and functionality would affect the rearrangement reaction. Prior to the rearrangement reaction the parent azobenzene compounds were synthesized (Table 4.1) in the manner previously stated and separated via column chromatography. These products were then utilized in the previously stated hydrazine and benzidine rearrangement reactions. The reactions were then submitted LC-MS for general yields to then determine relative reaction success (Table 4.2). Overall, yields were about 10% from previously reported rearrangement yields.

Many lessons were learned regarding the substituent on the parent azobenzene compound and its readiness to rearrange successfully. The presence of the chlorine substituent allowed for successful rearrangement of the azobenzene compound with the

LC-MS offering evidence of the proper fragmentation in masses that suggest both a 4,4'- and a 3,3'-rearrangement. However, the rearrangement of the 2,2'-iodoazobenzene led to no yields of the desired product due to the activation of the iodo substituents.

Table 4.2: Yields estimated via LC-MS.



Yield is total yield of 2, 3, and 4 substituted rearranged products. *Yield estimated via GC-MS. **Ring closed product gave 68 % yield but no desired ring opened product was obtained.

As far as oxygen containing molecules, the methoxy substituted azobenzene unsurprisingly led to decreased yields when compared to the unsubstituted benzidine product. Next, a weaker electron donating group, 2,2'-(diazene-1,2-diyl)dibenzoic acid, was attempted and led to surprising results although in lower yields than the 2,2'-dichloroazobenzene. Expectedly, when 2, 2'-nitroaminoazoxybenzene was utilized, no product was observed. This was likely due to the extreme electron withdrawing effects of the substituents making it difficult to initially reduce to a hydrazobenzene or, more likely,

the added functionality of the groups that could then react with the reductant prior to reacting with neighboring nitro substituents or similarly reduced amine substituents from its neighboring benzene molecule. Similarly, when 2,2'-aminoazobenzene was utilized, no product was observed under varying conditions of temperature, time and reductant equivalents. This is likely due to the extreme electron donating effect and added functionality of the amine group resulting in reactions with itself or neighboring azobenzene compounds. To eliminate other routes of reactivity, a protecting ketone group was attached to the free amine. This was to provide steric bulk to the molecule and prevent ring closure. Once the rearrangement was attempted, the mass spectrometry suggested that there was rearrangement, but that the ketone led to a ring closure condensation reaction thus eliminating the desired functionality of having free amines on the benzidine compound.

4.4 Conclusion

While the benzidine rearrangement has long been of interest due to its unique ability to provide intramolecular formations of C-C bonds, it still provides difficulty when understanding overall reactivity trends and how to improve them. While the halogenated substituents rearranged successfully, the dichlorobenzene product that resulted is not allowed to be used in major industrial applications in most of the world due to it being a known carcinogen. While trying to replicate the results of the rearrangement with electron donating substituents, the resulting rearrangement was difficult to obtain desirable yields. This is likely due to the electron donating effect and/or the added functionality of certain substituents interfering with the intramolecular pathway of rearrangement. While the addition of sterically hindering moieties like ketones provide higher rearrangement yields,

the reaction of these molecules resulted in the undesirable effect of ring closure. These trends suggest that while benzidine rearrangements may be realized with both electron rich and deficient substituents, electronics and functionality play a major role in overall yields. The electronic effect on overall yields support that this is indeed likely to be an intramolecular pathway.

4.5 Materials and Methods

All solvents were used without distillation and as received directly from the manufacturer. All reactions for the azobenzene compounds and subsequent benzidine rearrangement utilized materials as received from the manufacturer without further purification.

Instrumentation. NMR spectroscopy was performed using a Bruker Avance III HD 400. Data were processed using Bruker TopSpin software. ^1H NMR spectroscopy was performed using a 400 MHz instrument using deuterated dimethyl sulfoxide as the solvent with a calibrated peak at 2.50 ppm, respectively.

General procedure synthesis of azobenzene compounds. 0.5 M of amine substrate was added to a clean 250-mL round bottom flask fitted with a 1" magnetic stir-bar. 2 M of oxidant was then added to the reaction mixture followed by 50 mL of solvent. The reaction was placed onto a reflux condenser and heated to 110 °C and allowed to run overnight at a stir-rate of 360 rotations per minute (rpm). The reaction was then cooled down and the solid was filtered off before the solvent was evaporated off. The remaining solid was separated via column chromatography utilizing hexanes and ethyl acetate (3:1) to obtain the solid product. The product was confirmed utilizing ^1H NMR.

General procedure synthesis of rearranged products. 40 mM of zinc powder was placed into a clean and dry 100-mL round bottom flask fitted with a 1” magnetic stir-bar. To a separate clean round bottom flask, 5 mM of azobenzene, 40 mM of ammonium chloride and 50 mL of solvent was added and sonicated until all solid was dissolved. Both vessels were sealed and purged for 30 minutes. After the vessels were purged, the solution was canula transferred to the reaction vessel with zinc and the reaction was allowed to stir at 360 rpm until the red solution was colorless (approximately 30 minutes). The clear reaction mixture was then canula transferred again into an empty 100 mL purged round bottom that was fitted with a 1” magnetic stir bar in order to remove the majority of zinc powder from the reaction. 1 mL of concentrated HCl was then added to the reaction mixture and the reaction was heated to reflux for 2 hours at a stir rate of 360 rpm. The reaction was then neutralized to a pH of 10 with a solution of saturated sodium hydroxide. The solvent was then evaporated off and the sample was submitted for liquid chromatography-mass spectrometry (LC-MS) analysis.

CHAPTER 5: CONCLUSION AND FUTURE OUTLOOKS

5.1 Conclusions

The work contained in this dissertation explored sustainable approaches to synthesizing new nitrogen-nitrogen, carbon-nitrogen and carbon-carbon bonds. Utilizing photo-, electro- and thermo-chemical means for the synthesis of these compounds, mechanistic insights have been achieved that add fundamental understanding to new and existing green chemistry synthesis routes.

The ability to oxidatively couple a wide range of azobenzene products utilizing light as an energy source has been shown. This work has shown great selectivity for a broad range of substrates that has previously not been achieved. Additionally, it has been shown that oxygen is required to act as a sacrificial electron acceptor for the completion of the catalytic cycle. The combination of the elimination of waste from fossil fuel consumption combined with the sustainable aspects of high selectivity eliminating waste and the ability to conduct the synthesis of these compounds without halogenated or hazardous waste is an important discovery for the green synthesis of these compounds that provide promise for further application.

Following the oxidative coupling of aniline derivatives, the reactivity trends of the anion pool synthesis methods for the purpose of synthesizing new carbon-nitrogen bonds was established. A direct correlation between nitrogen heterocycle's pK_a and their ability to activate benzylic halides was shown as well as the limitations of high pK_a 's and the affect on the anion lifetime. This was counteracted by cooling the reaction down during the electrolysis to increase the lifetime of the generated anion. Furthermore, the size of the electrolyte cation was determined to play a major role in allowing the generated anion to react with the added electrophile. Lastly, the relationship between the δ^+ charge on the

benzylic carbon and the electrophilicity of the benzylic halide has been explored. This research offers a sustainable route for the synthesis of carbon-nitrogen bonds without the utilization of expensive transition metal catalysts and energy waste produced via traditional carbon-nitrogen synthesis routes.

Lastly, the determination of the effect of electronics and substituent functionality has been explored in the traditional benzidine rearrangement reaction. The increase in electron density on parent azobenzene compounds was determined to significantly decrease the desired product yield while electron-deficient parent azobenzene compounds significantly improved overall yield. Once added functionality was added to the azobenzene substituents, however, reactivity disappeared due to the formation of undesirable side-products. Attempts to protect the functional amine substituents to prevent unwanted reactivity resulted in higher yields for the rearrangement, but did not result in the desired product. Instead, a ring-closure occurred for the rearranged product.

5.2 Future Works

While much progress has been made with regards to sustainable synthesis routes for the purpose of synthesizing new nitrogen-nitrogen, carbon-nitrogen and carbon-carbon bonds, the continued research into increasing reactivity and sustainability is imperative.

The synthesis of azobenzene compounds with high selectivity utilizing light as a renewable energy source is important. One manner of progression for this process relies on the development of a new photocatalyst that does not utilize expensive or toxic transition metal catalyst centers. The ability to utilize an organic photocatalyst will lead to increased applicability for large-scale applications. Additionally, the ability to make unsymmetrical

azobenzene products will be explored. While symmetrical azobenzene compounds are important, the ability to increase the diversity of products is essential when looking at wide-scale adoption of synthesis methods. Unsymmetrical azobenzene compounds will also allow for increased functionality via the addition of substituents that can be utilized to further alter the chromophoric and medicinal properties of these compounds by either altering the electronic properties or offering additional reactivity for substitutions to occur selectively in following reactions.

The anion pool synthesis method is a promising route for increasing selectivity and providing unique bond breakage that has previously only been successfully achieved via the utilization of expensive transition metal catalysts and high temperatures. Future research for this method will lie in the ability to stabilize anions of high pK_a like aniline or cyclohexylamine in order to provide enough basicity to activate sp^2 carbon-halogen bonds. Additionally, the activation of sp^2 carbon-hydrogen bonds can be explored. The stabilization of these anions can occur by exploring different stabilizing agents that can then result in less reactive intermediates being formed. Another approach that can be explored is the combining of the anion pool synthesis method with a flow system so that once an anion is formed it is immediately transported to another cell to react with an electrophile. The expansion of applicability that may be obtained from these reactions have great potential implications on pharmaceutical and material synthesis processes.

The benzidine rearrangement has been a known reaction for years. While most of the research focuses on trying to understand the exact mechanism by which it works, this research has tried to understand the scopes of its applicability as a potential green synthesis method for carbon-carbon bond synthesis. Future research will aim to determine if starting

with asymmetric azobenzene compounds can compensate for some of the negative effects that electron rich substituents have on the overall success of the reaction. That is to say if one side of an asymmetric azobenzene contained a methoxy substituent while the other contained a chlorine substituent, the effect on the overall success is still unknown. Although current methods of carbon-carbon bond synthesis will likely not be replaced, the benzidine rearrangement still has academic and industrial application if it is further understood and optimized.

REFERENCES

1. Lipskikh, O. I., Korotkova, E. I., Khristunova, Y. P., Barek, J., & Kratochvil, B. (2018) Sensors for voltammetric determination of food azo dyes - A critical review. *Electrochimica Acta*, 260, 974-985.
2. Kim, Y., Jeong, D., Shinde, V. V., Hu, Y., Kim, C., & Jung, S. (2020) Azobenzene-grafted carboxymethyl cellulose hydrogels with photo-switchable, reduction-responsive and self-healing properties for a controlled drug release system. *International Journal of Biological Macromolecules*, 163, 824-832.
3. Yamada, S., Bessho, J., Nakasato, H., & Tsutsumi, O. (2018) Color tuning donor-acceptor-type azobenzene dyes by controlling the molecular geometry of the donor moiety. *Dyes and Pigments*, 150, 89-96.
4. Cao, L., Jiang, Y., Dai, X., Zhang, X., Peng, Y., & Liu, X. (2020) Using Azo-Compounds to Endow Biobased Thermosetting Coatings with Potential Application for Reversible Information Storage. *ACS Applied Polymer Materials*, 2 (11), 4551-4558.
5. Wang, M., Ma, J., Yu, M., Zhang, Z., & Wang, F. (2016) Oxidative coupling of anilines to azobenzenes using heterogeneous manganese oxide catalysts. *Catalysis Science & Technology*, 6 (6), 1940-1945.

6. Hudwekar, A. D., Verma, P. K., Kour, J., Balgotra, S., & Sawant, S. D. (2019) Transition Metal-Free Oxidative Coupling of Primary Amines in Polyethylene Glycol at Room Temperature: Synthesis of Imines, Azobenzenes, Benzothiazoles, and Disulfides. *European Journal of Organic Chemistry*, 2019 (6), 1242-1250.
7. Cai, S., Rong, H., Yu, X., Liu, X., Wang, D., He, W., & Li, Y. (2013) Room Temperature Activation of Oxygen by Monodispersed Metal Nanoparticles: Oxidative Dehydrogenative Coupling of Anilines for Azobenzene Syntheses. *ACS Catalysis*, 3 (4), 478-486.
8. Sakai, N., Asama, S., Anai, S., & Konakahara, T. (2014) One-pot preparation of azobenzenes from nitrobenzenes by the combination of an indium-catalyzed reductive coupling and a subsequent oxidation. *Tetrahedron*, 70 (11), 2027-2033.
9. Gao, B.-B., Zhang, M., Chen, X.-R., Zhu, D.-L., Yu, H., Zhang, W.-H., & Lang, J.-P. (2018) Preparation of carbon-based AuAg alloy nanoparticles by using the heterometallic [Au₄Ag₄] cluster for efficient oxidative coupling of anilines. *Dalton Transactions*, 47 (16), 5780-5788.
10. Patel, A. R., Patel, G., Maity, G., Patel, S. P., Bhattacharya, S., Putta, A., & Banerjee, S. (2020) Direct Oxidative Azo Coupling of Anilines Using a Self-Assembled Flower-like CuCo₂O₄ Material as a Catalyst under Aerobic Conditions. *ACS Omega*, 5 (47), 30416-30424.
11. Zhang, L., Xia, J., Li, Q., Li, X., & Wang, S. (2011) Fast Synthesis of Hydrazine and Azo Derivatives by Oxidation of Rare-Earth-Metal–Nitrogen Bonds. *Organometallics*, 30 (3), 375-378.

12. Bustamante, S. E., Vallejos, S., Pascual-Portal, B. S., Muñoz, A., Mendia, A., Rivas, B. L., García, F. C., & García, J. M. (2019) Polymer films containing chemically anchored diazonium salts with long-term stability as colorimetric sensors. *Journal of Hazardous Materials*, 365, 725-732.
13. Firth, J. D., & Fairlamb, I. J. S. (2020) A Need for Caution in the Preparation and Application of Synthetically Versatile Aryl Diazonium Tetrafluoroborate Salts. *Organic Letters*, 22 (18), 7057-7059.
14. Chung, T. F., Wu, Y. M., & Cheng, C. H. (1984) Reduction of aromatic nitro compounds by ethylenediamine. A new selective reagent for the synthesis of symmetric azo compounds. *The Journal of Organic Chemistry*, 49 (7), 1215-1217.
15. Merino, E. (2011) Synthesis of azobenzenes: the coloured pieces of molecular materials. *Chemical Society Reviews*, 40 (7), 3835-3853.
16. Liu, Z., Huang, Y., Xiao, Q., & Zhu, H. (2016) Selective reduction of nitroaromatics to azoxy compounds on supported Ag–Cu alloy nanoparticles through visible light irradiation. *Green Chemistry*, 18 (3), 817-825.
17. Dolgoplova, E. A., Rice, A. M., Martin, C. R., & Shustova, N. B. (2018) Photochemistry and photophysics of MOFs: steps towards MOF-based sensing enhancements. *Chemical Society Reviews*, 47 (13), 4710-4728.
18. Wei, H., Lei, M., Zhang, P., Leng, J., Zheng, Z., & You, Y. (2021) Orthogonal photochemistry-assisted printing of 3D tough and stretchable conductive hydrogels. *Nature Communications*, 12 (1).

19. Balzani, V., Credi, A., & Venturi, M. (2008) Photochemical Conversion of Solar Energy. *ChemSusChem*, 1 (1-2), 26-58.
20. Stoll, T., Castillo, C. E., Kayanuma, M., Sandroni, M., Daniel, C., Odobel, F., Fortage, J., & Collomb, M.-N. (2015) Photo-induced redox catalysis for proton reduction to hydrogen with homogeneous molecular systems using rhodium-based catalysts. *Coordination Chemistry Reviews*, 304-305, 20-37.
21. Dissanayake, D. M. M. M., & Vannucci, A. K. (2019) Selective N1-Acylation of Indazoles with Acid Anhydrides Using an Electrochemical Approach. *Organic Letters*, 21 (2), 457-460.
22. Bariwal, J., & Van der Eycken, E. (2013) C-N Bond Forming Cross-Coupling Reactions: An Overview. *Chemical Society Reviews*, 42, 9283-9303.
23. Yashwantrao, G., & Saha, S. (2021) Sustainable strategies of C–N bond formation via Ullmann coupling employing earth abundant copper catalyst. *Tetrahedron*, 97, 132406.
24. Yang, Q., Zhao, Y., & Ma, D. (2022) Cu-Mediated Ullmann-Type Cross-Coupling and Industrial Applications in Route Design, Process Development, and Scale-up of Pharmaceutical and Agrochemical Processes. *Organic Process Research & Development*, 26 (6), 1690-1750.
25. Afonin, M. Y., Savkov, B. Y., Virovets, A. V., Korenev, V. S., Golovin, A. V., & Maksakov, V. A. (2017) Transformation of Chlorohydrocarbons and Amines in the Coordination Sphere of $[(\mu\text{-H})_2\text{Os}_3(\text{CO})_{10}]$. *European Journal of Inorganic Chemistry*, 2017 (24), 3105-3114.

26. Feofanov, M., Akhmetov, V., Takayama, R., & Amsharov, K. (2021) Transition-metal free synthesis of N-aryl carbazoles and their extended analogs. *Organic & Biomolecular Chemistry*, 19 (33), 7172-7175.
27. Wagaw, S., & Buchwald, S. L. (1996) The Synthesis of Aminopyridines: A Method Employing Palladium-Catalyzed Carbon–Nitrogen Bond Formation. *The Journal of Organic Chemistry*, 61 (21), 7240-7241.
28. Forero-Cortés, P. A., & Haydl, A. M. (2019) The 25th Anniversary of the Buchwald–Hartwig Amination: Development, Applications, and Outlook. *Organic Process Research & Development*, 23 (8), 1478-1483.
29. Kyriakou, V., Garagounis, I., Vasileiou, E., Vourros, A., & Stoukides, M. (2017) Progress in the Electrochemical Synthesis of Ammonia. *Catalysis Today*, 286, 2-13.
30. Therese, G. H. A., & Kamath, P. V. (2000) Electrochemical Synthesis of Metal Oxides and Hydroxides. *Chemistry of Materials*, 12 (5), 1195-1204.
31. Wang, S., Liu, G., & Wang, L. (2019) Crystal Facet Engineering of Photoelectrodes for Photoelectrochemical Water Splitting. *Chemical Reviews*, 119 (8), 5192-5247.
32. Yoshida, J.-i., Suga, S., Suzuki, S., Kinomura, N., Yamamoto, A., & Fujiwara, K. (1999) Direct Oxidative Carbon–Carbon Bond Formation Using the “Cation Pool” Method. 1. Generation of Iminium Cation Pools and Their Reaction with Carbon Nucleophiles. *Journal of the American Chemical Society*, 121 (41), 9546-9549.

33. Brocklebank, S., Woodley, J. M., & Lilly, M. D. (1999) Immobilised transketolase for carbon–carbon bond synthesis: biocatalyst stability. *Journal of Molecular Catalysis B: Enzymatic*, 7 (1), 223-231.
34. Seyferth, D. (2009) The Grignard Reagents. *Organometallics*, 28 (6), 1598-1605.
35. Murray, J. I., Zhang, L., Simon, A., Silva Elipe, M. V., Wei, C. S., Caille, S., & Parsons, A. T. (2022) Kinetic and Mechanistic Investigations to Enable a Key Suzuki Coupling for Sotorasib Manufacture—What a Difference a Base Makes. *Organic Process Research & Development*.
36. Ghigo, G., Osella, S., Maranzana, A., & Tonachini, G. (2011) The Mechanism of the Acid-Catalyzed Benzidine Rearrangement of Hydrazobenzene: A Theoretical Study. *European Journal of Organic Chemistry*, 2011 (12), 2326-2333.
37. Zhang, L. Y., Zou, S. J., & Sun, X. H. (2018) Efficient azobenzene co-sensitizer for wide spectral absorption of dye-sensitized solar cells. *RSC Advances*, 8 (12), 6212-6217.
38. Wang, G., Yuan, D., Yuan, T., Dong, J., Feng, N., & Han, G. (2015) A visible light responsive azobenzene-functionalized polymer: Synthesis, self-assembly, and photoresponsive properties. *Journal of Polymer Science, Part A: Polymer Chemistry*, 53 (23), 2768-2775.
39. Blanco, B., Palasis, K. A., Adwal, A., Callen, D. F., & Abell, A. D. (2017) Azobenzene-containing photoswitchable proteasome inhibitors with selective activity and cellular toxicity. *Bioorganic Medicinal Chemistry*, 25 (19), 5050-5054.

40. Amit, B., Sivanesan Saravana, D., & Tapan, C. (2011) Azo dyes: past, present and the future. *Environmental Reviews*, 19, 350-370.
41. Merino, E. (2011) Synthesis of azobenzenes: the coloured pieces of molecular materials. *Chemical Society Reviews*, 40 (7), 3835-3853.
42. Grrirane, A., Corma, A., & García, H. (2008) Gold-Catalyzed Synthesis of Aromatic Azo Compounds from Anilines and Nitroaromatics. *Science*, 322 (5908), 1661.
43. Saba, S., Dos Santos, C. R., Zavarise, B. R., Naujorks, A. A. S., Franco, M. S., Schneider, A. R., Scheide, M. R., Affeldt, R. F., Rafique, J., & Braga, A. L. (2020) Photoinduced, Direct C(sp²)–H Bond Azo Coupling of Imidazoheteroarenes and Imidazoanilines with Aryl Diazonium Salts Catalyzed by Eosin Y. *Chemistry - A European Journal*, 26 (20), 4461-4466.
44. Zhang, Y.-F., & Mellah, M. (2017) Convenient Electrocatalytic Synthesis of Azobenzenes from Nitroaromatic Derivatives Using SmI₂. *ACS Catalysis*, 7 (12), 8480-8486.
45. Dai, Y., Li, C., Shen, Y., Lim, T., Xu, J., & Li, Y. (2018) Niemantsverdriet, H.; Besenbacher, F.; Lock, N.; Su, R., Light-tuned selective photosynthesis of azo- and azoxy-aromatics using graphitic C₃N₄. *Nature Communications*, 9 (1), 60.
46. Mondal, B., & Mukherjee, P. S. (2018) Cage Encapsulated Gold Nanoparticles as Heterogeneous Photocatalyst for Facile and Selective Reduction of Nitroarenes to Azo Compounds. *Journal of the American Chemical Society*, 140 (39), 12592-12601.

47. Guo, X., Hao, C., Jin, G., Zhu, H.-Y., & Guo, X.-Y. (2014) Copper Nanoparticles on Graphene Support: An Efficient Photocatalyst for Coupling of Nitroaromatics in Visible Light. *Angewandte Chemie International Edition*, 53 (7), 1973-1977.
48. Zhu, H., Ke, X., Yang, X., Sarina, S., & Liu, H. (2010) Reduction of Nitroaromatic Compounds on Supported Gold Nanoparticles by Visible and Ultraviolet Light. *Angewandte Chemie International Edition*, 49 (50), 9657-9661.
49. Pal, B., Torimoto, T., Okazaki, K.-i., & Ohtani, B. (2007) Photocatalytic syntheses of azoxybenzene by visible light irradiation of silica-coated cadmium sulfide nanocomposites. *Chemical Communications*, (5), 483-485.
50. Oderinde, M. S., Jones, N. H., Juneau, A., Frenette, M., Aquila, B., Tentarelli, S., Robbins, D. W., & Johannes, J. W. (2016) Highly Chemoselective Iridium Photoredox and Nickel Catalysis for the Cross-Coupling of Primary Aryl Amines with Aryl Halides. *Angewandte Chemie International Edition*, 55, 13219-13223.
51. Key, R. J., & Vannucci, A. K. (2018) Nickel Dual Photoredox Catalysis for the Synthesis of Aryl Amines. *Organometallics*, 37 (9), 1468-1472.
52. Liu, C., Yuan, J., Gao, M., Tang, S., Li, W., Shi, R., & Lei, A. (2015) Oxidative Coupling between Two Hydrocarbons: An Update of Recent C–H Functionalizations. *Chemical Reviews*, 115 (22), 12138-12204.
53. Huang, C.-Y., Kang, H., Li, J., & Li, C.-J. (2019) En Route to Intermolecular Cross-Dehydrogenative Coupling Reactions. *Journal of Organic Chemistry*, 84 (20), 12705-12721.

54. Funes-Ardoiz, I., & Maseras, F. (2018) Oxidative Coupling Mechanisms: Current State of Understanding. *ACS Catalysis*, 8 (2), 1161-1172.
55. Wang, F., Gerken, J. B., Bates, D. M., Kim, Y. J., & Stahl, S. S. (2020) Electrochemical Strategy for Hydrazine Synthesis: Development and Overpotential Analysis of Methods for Oxidative N–N Coupling of an Ammonia Surrogate. *Journal of the American Chemical Society*, 142 (28), 12349-12356.
56. Gieshoff, T., Kehl, A., Schollmeyer, D., Moeller, K. D., & Waldvogel, S. R. (2017) Insights into the Mechanism of Anodic N–N Bond Formation by Dehydrogenative Coupling. *Journal of the American Chemical Society*, 139 (35), 12317-12324.
57. Yi, H., Liu, T., Zilu, T., Singh, A. K., & Lei, A. (2019) *Green Oxidation in Organic Synthesis*. John Wiley & Sons.
58. Lin, M., Wang, Z., Fang, H., Liu, L., Yin, H., Yan, C.-H., & Fu, X. (2016) Metal-free aerobic oxidative coupling of amines in dimethyl sulfoxide via a radical pathway. *RSC Advances*, 6 (13), 10861-10864.
59. Wang, L., Ishida, A., Hashidoko, Y., & Hashimoto, M. (2017) Dehydrogenation of the NH–NH Bond Triggered by Potassium tert-Butoxide in Liquid Ammonia. *Angewandte Chemie International Edition*, 56 (3), 870-873.
60. Hunger, K., Mischke, P., Rieper, W., Raue, R., Kunde, K., & Engel, A. (2000) Azo Dyes. *Ullmann's Encyclopedia of Industrial Chemistry*.

61. Jones, P. R., Drews, M. J., Johnson, J. K., & Wong, P. S. (1972) Bonding studies in group IV substituted anilines. I. Comparison of charge-transfer and electrochemical methods for determining ground-state energies. *Journal of the American Chemical Society*, 94 (13), 4595-4599.
62. Kondo, M., Takizawa, S., Jiang, Y., & Sasai, H. (2019) Room-Temperature, Metal-Free, and One-Pot Preparation of 2H-Indazoles through a Mills Reaction and Cyclization Sequence. *Chemistry - A European Journal*, 25 (42), 9866-9869.
63. Priewisch, B., & Rück-Braun, K. (2005) Efficient Preparation of Nitrosoarenes for the Synthesis of Azobenzenes. *Journal of Organic Chemistry*, 70 (6), 2350-2352.
64. Su, F., Mathew, S. C., Möhlmann, L., Antonietti, M., Wang, X., & Blechert, S. (2011) Aerobic Oxidative Coupling of Amines by Carbon Nitride Photocatalysis with Visible Light. *Angewandte Chemie International Edition*, 50 (3), 657-660.
65. Yayla, H. G., Wang, H., Tarantino, K. T., Orbe, H. S., & Knowles, R. R. (2016) Catalytic Ring-Opening of Cyclic Alcohols Enabled by PCET Activation of Strong O–H Bonds. *Journal of the American Chemical Society*, 138 (34), 10794-10797.
66. Migita, C. T., & Migita, K. (2003) Spin Trapping of the Nitrogen-centered Radicals. Characterization of the DMPO/DEPMPO Spin Adducts. *Chemical Letters*, 32 (5), 466-467.
67. Lin, T.-S., Rajagopalan, R., Shen, Y., Park, S., Poreddy, A. R., Asmelash, B., Karwa, A. S., & Taylor, J.-S. A. (2013) Roles of Free Radicals in Type 1

- Phototherapeutic Agents: Aromatic Amines, Sulfenamides, and Sulfenates. *The Journal of Physical Chemistry A*, 117 (26), 5454-5462.
68. Newcomb, M., Miranda, N., Huang, X., & Crich, D. (2000) Laser Flash Photolysis Kinetic Studies of α -Methoxy- β -phosphatoxyalkyl Radical Heterolysis Reactions: A Method for Alkoxyalkyl Radical Cation Detection. *Journal of the American Chemical Society*, 122 (25), 6128-6129.
69. Hamon, F., Djedaini-Pilard, F., Barbot, F., & Len, C. (2009) Azobenzenes—synthesis and carbohydrate applications. *Tetrahedron*, 65 (49), 10105-10123.
70. Bryan, M. C., Dunn, P. J., Entwistle, D., Gallou, F., Koenig, S. G., Hayler, J. D., Hickey, M. R., Hughes, S., Kopach, M. E., Moine, G., Richardson, P., Roschangar, F., Steven, A., & Weiberth, F. J. (2018) Key Green Chemistry research areas from a pharmaceutical manufacturers' perspective revisited. *Green Chemistry*, 20 (22), 5082-5103.
71. Kingston, C., Palkowitz, M. D., Takahira, Y., Vantourout, J. C., Peters, B. K., Kawamata, Y., & Baran, P. S. (2020) A Survival Guide for the “Electro-curious”. *Accounts of Chemical Research*, 53 (1), 72-83.
72. Li, C.-J., & Trost, B. M. (2008) Green Chemistry for Chemical Synthesis. *Proceedings of the National Academy of Sciences*, 105 (36), 13197-13202.
73. Rafiee, M., Mayer, M. N., Punchihewa, B. T., & Mumau, M. R. (2021) Constant Potential and Constant Current Electrolysis: An Introduction and Comparison of Different Techniques for Organic Electrosynthesis. *The Journal of Organic Chemistry*, 86 (22), 15866-15874.

74. Mayall, R. M., Birss, V. I., & Creager, S. E. (2020) Digital Simulation and Experimental Validation of Redox Mediation at an Electroactive Monolayer-Coated Electrode. *Journal of the Electrochemical Society*, 167 (4), 046512.
75. Felton, G. A. N., Vannucci, A. K., Chen, J., Lockett, L. T., Okumura, N., Petro, B. J., Zakai, U. I., Evans, D. H., Glass, R. S., & Lichtenberger, D. L. (2007) Hydrogen Generation from Weak Acids: Electrochemical and Computational Studies of a Diiron Hydrogenase Mimic. *Journal of the American Chemical Society*, 129 (41), 12521-12530.
76. Yu, Y., Zhong, J.-S., Xu, K., Yuan, Y., & Ye, K.-Y. (2020) Recent Advances in the Electrochemical Synthesis and Functionalization of Indole Derivatives. *Advanced Synthesis & Catalysis*, 362 (11), 2102-2119.
77. Siahrostami, S., Villegas, S. J., Bagherzadeh Mostaghimi, A. H., Back, S., Farimani, A. B., Wang, H., Persson, K. A., & Montoya, J. (2020) A Review on Challenges and Successes in Atomic-Scale Design of Catalysts for Electrochemical Synthesis of Hydrogen Peroxide. *ACS Catalysis*, 10 (14), 7495-7511.
78. Yount, J., & Piercey, D. G. (2022) Electrochemical Synthesis of High-Nitrogen Materials and Energetic Materials. *Chemical Reviews*, 122 (9), 8809-8840.
79. Gieshoff, T., Kehl, A., Schollmeyer, D., Moeller, K. D., & Waldvogel, S. R. (2017) Insights into the Mechanism of Anodic N–N Bond Formation by Dehydrogenative Coupling. *Journal of the American Chemical Society*, 139 (35), 12317-12324.

80. Hoque, M. A., Twilton, J., Zhu, J., Graaf, M. D., Harper, K. C., Tuca, E., DiLabio, G. A., & Stahl, S. S. (2022) Electrochemical PINOylation of Methylarenes: Improving the Scope and Utility of Benzylic Oxidation through Mediated Electrolysis. *Journal of the American Chemical Society*, *144* (33), 15295-15302.
81. Gnaim, S., Bauer, A., Zhang, H.-J., Chen, L., Gannett, C., Malapit, C. A., Hill, D. E., Vogt, D., Tang, T., Daley, R. A., Hao, W., Zeng, R., Quertenmont, M., Beck, W. D., Kandahari, E., Vantourout, J. C., Echeverria, P.-G., Abruna, H. D., Blackmond, D. G., Minter, S. D., Reisman, S. E., Sigman, M. S., & Baran, P. S. (2022) Cobalt-electrocatalytic HAT for functionalization of unsaturated C–C bonds. *Nature*, *605* (7911), 687-695.
82. Walker, B. R., & Sevov, C. S. (2019) An Electrochemically Promoted, Nickel-Catalyzed Mizoroki–Heck Reaction. *ACS Catalysis*, *9* (8), 7197-7203.
83. Amatore, C., & Jutand, A. (1988) Rates and mechanism of biphenyl synthesis catalyzed by electrogenerated coordinatively unsaturated nickel complexes. *Organometallics*, *7* (10), 2203-2214.
84. Everson, D. A., Shrestha, R., & Weix, D. J. (2010) Nickel-Catalyzed Reductive Cross-Coupling of Aryl Halides with Alkyl Halides. *Journal of the American Chemical Society*, *132*, 920-921.
85. Franke, M. C., Longley, V. R., Rafiee, M., Stahl, S. S., Hansen, E. C., & Weix, D. J. (2022) Zinc-free, Scalable Reductive Cross-Electrophile Coupling Driven by Electrochemistry in an Undivided Cell. *ACS Catalysis*, *12* (20), 12617-12626.

86. Yoshida, J.-i., Shimizu, A., & Hayashi, R. (2018) Electrogenerated Cationic Reactive Intermediates: The Pool Method and Further Advances. *Chemical Reviews*, *118* (9), 4702-4730.
87. Yoshida, J.-i., Suga, S., Suzuki, S., Kinomura, N., Yamamoto, A., & Fujiwara, K. (1999) Direct Oxidative Carbon–Carbon Bond Formation Using the “Cation Pool” Method. 1. Generation of Iminium Cation Pools and Their Reaction with Carbon Nucleophiles. *Journal of the American Chemical Society*, *121* (41), 9546-9549.
88. Dissanayake, D. M. M. M., & Vannucci, A. K. (2018) Transition-Metal-Free and Base-Free Electrosynthesis of 1H-Substituted Benzimidazoles. *ACS Sustainable Chemistry & Engineering*, *6* (1), 690-695.
89. Dissanayake, D. M. M. M., Melville, A. D., & Vannucci, A. K. (2019) Electrochemical anion pool synthesis of amides with concurrent benzyl ester synthesis. *Green Chemistry*, *21* (11), 3165-3171.
90. Kerru, N., Gummidi, L., Maddila, S., Gangu, K. K., & Jonnalagadda, S. B. (2020) A Review on Recent Advances in Nitrogen-Containing Molecules and Their Biological Applications. *Molecules*, *25* (8), 1909.
91. Dorel, R., Grugel, C. P., & Haydl, A. M. (2019) The Buchwald–Hartwig Amination After 25 Years. *Angewandte Chemie International Edition*, *58* (48), 17118-17129.

92. Pandey, G., Laha, R., & Singh, D. (2016) Benzylic C(sp³)–H Functionalization for C–N and C–O Bond Formation via Visible Light Photoredox Catalysis. *The Journal of Organic Chemistry*, *81* (16), 7161-7171.
93. Zhou, S., Lv, K., Fu, R., Zhu, C., & Bao, X. (2021) Nickel/Photoredox Dual Catalytic Cross-Coupling of Alkyl and Amidyl Radicals to Construct C(sp³)–N Bonds. *ACS Catalysis*, *11* (9), 5026-5034.
94. Corcoran, E. B., Pirnot, M. T., Lin, S., Dreher, S. D., DiRocco, D. A., Davies, I. W., Buchwald, S. L., & MacMillan, D. W. C. (2016) Aryl amination using ligand-free Ni(II) salts and photoredox catalysis. *Science*, *353*, 279-283.
95. Till, N. A., Tian, L., Dong, Z., Scholes, G. D., & MacMillan, D. W. C. (2020) Mechanistic Analysis of Metallaphotoredox C–N Coupling: Photocatalysis Initiates and Perpetuates Ni(I)/Ni(III) Coupling Activity. *Journal of the American Chemical Society*, *142* (37), 15830-15841.
96. Liang, Y., Zhang, X., & MacMillan, D. W. C. (2018) Decarboxylative sp³ C–N coupling via dual copper and photoredox catalysis. *Nature*, *559* (7712), 83-88.
97. Key, R. J., & Vannucci, A. K. (2018) Nickel Dual Photoredox Catalysis for the Synthesis of Aryl Amines. *Organometallics*, *37* (9), 1468-1472.
98. McNeice, P., Marr, P. C., & Marr, A. C. (2021) Basic ionic liquids for catalysis: the road to greater stability. *Catalysis Science & Technology*, *11* (3), 726-741.

99. Dissanayake, D. M. M. M., & Vannucci, A. K. (2019) Selective N1-Acylation of Indazoles with Acid Anhydrides Using an Electrochemical Approach. *Organic Letters*, 21 (2), 457-460.
100. Hunt, K. W., Moreno, D. A., Suiter, N., Clark, C. T., & Kim, G. (2009) Selective Synthesis of 1-Functionalized-alkyl-1H-indazoles. *Organic Letters*, 11 (21), 5054-5057.
101. Bordwell, F. G. (1988) Equilibrium acidities in dimethyl sulfoxide solution. *Accounts of Chemical Research*, 21 (12), 456-463.
102. Bordwell, F. G., Drucker, G. E., & Fried, H. E. (1981) Acidities of carbon and nitrogen acids: the aromaticity of the cyclopentadienyl anion. *The Journal of Organic Chemistry*, 46 (3), 632-635.
103. Trost, B. M. (1991) The Atom Economy—A Search for Synthetic Efficiency. *Science*, 254 (5037), 1471-1477.
104. Constable, D. J. C., Dunn, P. J., Hayler, J. D., Humphrey, G. R., Leazer, J. J. L., Linderman, R. J., Lorenz, K., Manley, J., Pearlman, B. A., Wells, A., Zaks, A., & Zhang, T. Y. (2007) Key green chemistry research areas—a perspective from pharmaceutical manufacturers. *Green Chemistry*, 9 (5), 411-420.
105. Roschangar, F., Sheldon, R. A., & Senanayake, C. H. (2015) Overcoming barriers to green chemistry in the pharmaceutical industry – the Green Aspiration Level™ concept. *Green Chemistry*, 17 (2), 752-768.

106. Vasconcelos, S. N. S., Reis, J. S., de Oliveira, I. M., Balfour, M. N., & Stefani, H. A. (2019) Synthesis of symmetrical biaryl compounds by homocoupling reaction. *Tetrahedron*, 75 (13), 1865-1959.
107. Chen, C.-H., Huang, W.-S., Lai, M.-Y., Tsao, W.-C., Lin, J. T., Wu, Y.-H., Ke, T.-H., Chen, L.-Y., & Wu, C.-C. (2009) Versatile, Benzimidazole/Amine-Based Ambipolar Compounds for Electroluminescent Applications: Single-Layer, Blue, Fluorescent OLEDs, Hosts for Single-Layer, Phosphorescent OLEDs. *Advanced Functional Materials*, 19 (16), 2661-2670.
108. Kovvuri, J., Nagaraju, B., Nayak, V. L., Akunuri, R., Rao, M. P. N., Ajitha, A., Nagesh, N., & Kamal, A. (2018) Design, synthesis and biological evaluation of new β -carboline-bisindole compounds as DNA binding, photocleavage agents and topoisomerase I inhibitors. *European Journal of Medicinal Chemistry*, 143, 1563-1577.
109. Lennox, A. J. J., & Lloyd-Jones, G. C. (2013) Transmetalation in the Suzuki–Miyaura Coupling: The Fork in the Trail. *Angewandte Chemie International Edition*, 52 (29), 7362-7370.
110. Kumar, A., Rao, G. K., Kumar, S., & Singh, A. K. (2013) Organosulphur and related ligands in Suzuki–Miyaura C–C coupling. *Dalton Transactions*, 42 (15), 5200-5223.
111. Ghigo, G., Maranzana, A., & Tonachini, G. (2012) A change from stepwise to concerted mechanism in the acid-catalysed benzidine rearrangement: a theoretical study. *Tetrahedron*, 68 (9), 2161-2165.

112. Ghigo, G., Osella, S., Maranzana, A., & Tonachini, G. (2011) The Mechanism of the Acid-Catalyzed Benzidine Rearrangement of Hydrazobenzene: A Theoretical Study. *European Journal of Organic Chemistry*, 2011 (12), 2326-2333.
113. Vermisoglou, E. C., Giannakopoulou, T., Romanos, G., Boukos, N., Psycharis, V., Lei, C., Lekakou, C., Petridis, D., & Trapalis, C. (2017) Graphene-based materials via benzidine-assisted exfoliation and reduction of graphite oxide and their electrochemical properties. *Applied Surface Science*, 392, 244-255.
114. Chung, K.-T., Chen, S.-C., & Claxton, L. D. (2006) Review of the Salmonella typhimurium mutagenicity of benzidine, benzidine analogues, and benzidine-based dyes. *Mutation Research/Reviews in Mutation Research*, 612 (1), 58-76.
115. Jeong, K. W., Kim, H. S., Yi, G. R., & Kim, C. K. (2018) Enhancing the electroluminescence of OLEDs by using ZnO nanoparticle electron transport layers that exhibit the Auger electron effect. *Molecular Crystals and Liquid Crystals*, 663 (1), 61-70.
116. Hou, S., Li, X., & Xu, J. (2014) N[1,3]-sigmatropic shift in the benzidine rearrangement: experimental and theoretical investigation. *Organic & Biomolecular Chemistry*, 12 (27), 4952-4963.
117. Wickemeyer, L., Fernández, I., Neumann, B., Stammer, H.-G., & Mitzel, N. W. (2023) Selective 3,3-Rearrangement of Azobenzenes upon Complexation by a Frustrated Lewis Pair. *Angewandte Chemie International Edition*, e202216943.

118. M J S Dewar, A., & Marchand, A. P. (1965) Physical Organic Chemistry: II-Complexes as Intermediates in Organic Reactions. *Annual Review of Physical Chemistry*, 16 (1), 321-346.
119. Tapaswi, P. K., Choi, M.-C., Jeong, K.-M., Ando, S., & Ha, C.-S. (2015) Transparent Aromatic Polyimides Derived from Thiophenyl-Substituted Benzidines with High Refractive Index and Small Birefringence. *Macromolecules*, 48 (11), 3462-3474.
120. Leung, G. Y. C., William, A. D., & Johannes, C. W. (2014) Improved synthesis of pyridyl–biaryl ring systems via benzidine rearrangements. *Tetrahedron Letters*, 55 (29), 3950-3953.

APPENDIX A: SUPPORTING INFORMATION FOR CHAPTER 2

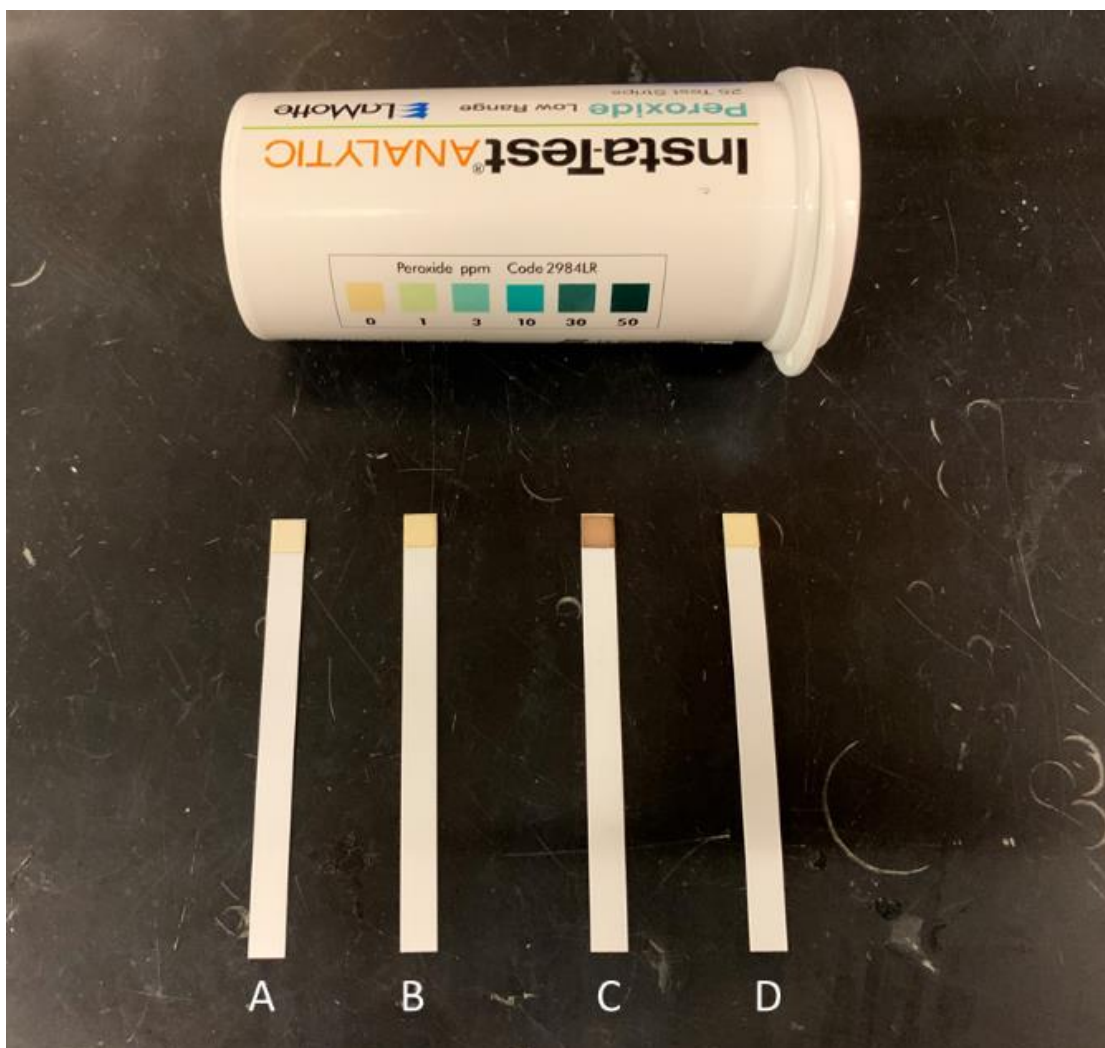


Figure A.2: Picture of the hydrogen peroxide test strips. A) Dry peroxide strip without measurement. B) Peroxide strip tested at the beginning of a standard photocatalytic reaction for the coupling of *p*-anisidine showing no detection of H₂O₂. C) Peroxide strip 4 hours into the photocatalytic reaction for the coupling of *p*-anisidine under an O₂ atmosphere. The change in color in the strip indicates the presence of H₂O₂ in the reaction solution. D) Peroxide strip 4 hours into the photocatalytic reaction for the coupling of *p*-anisidine under an N₂ atmosphere. The lack of oxygen present in this reaction prevents the possible formation of H₂O₂ and the peroxide strip does not change color.

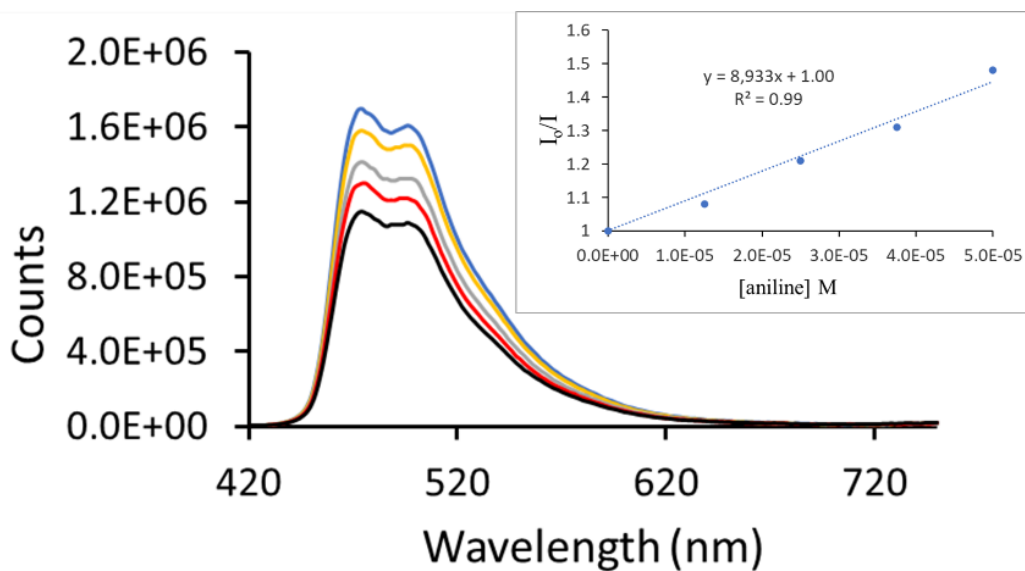


Figure A.3: Fluorescence quenching data and Stern-Volmer plot for the quenching of **Ir** with aniline.

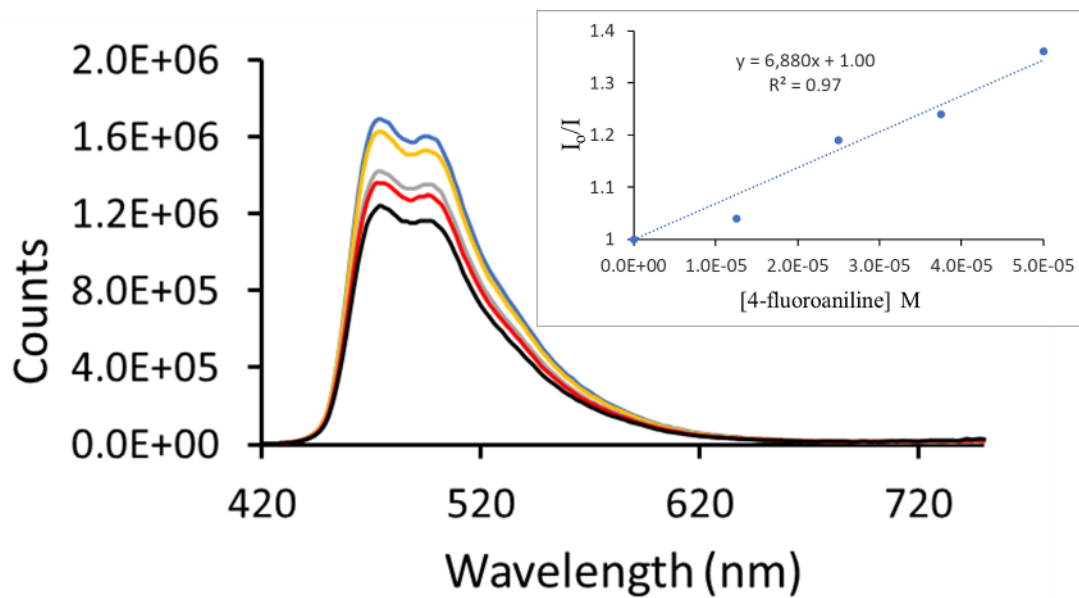


Figure A.4: Fluorescence quenching data and Stern-Volmer plot for the quenching of **Ir** with 4-fluoroaniline.

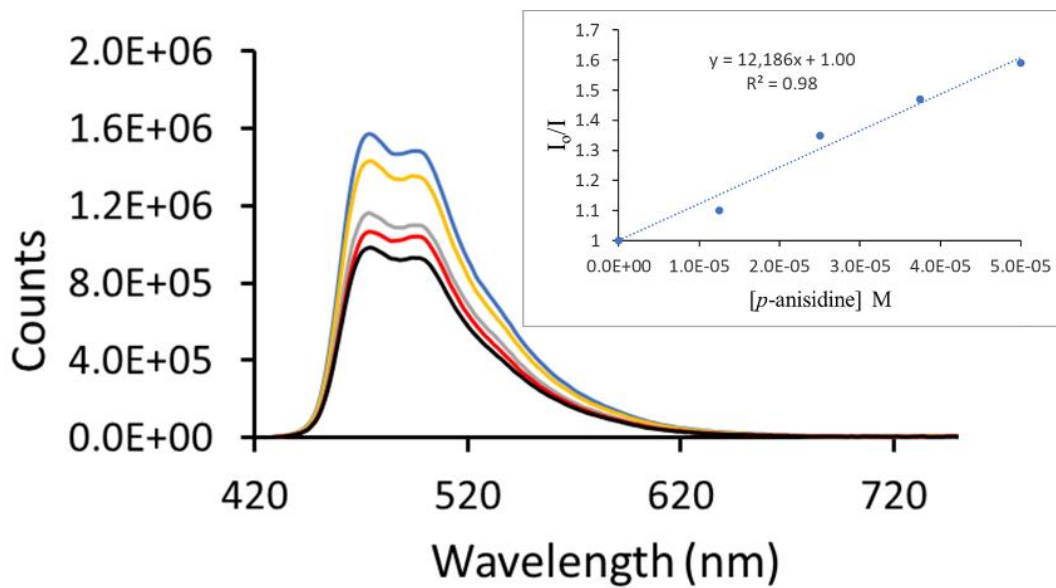


Figure A.5: Fluorescence quenching data and Stern-Volmer plot for the quenching of **Ir** with p-anisidine with 2.5×10^{-4} M K_3PO_4 base added.

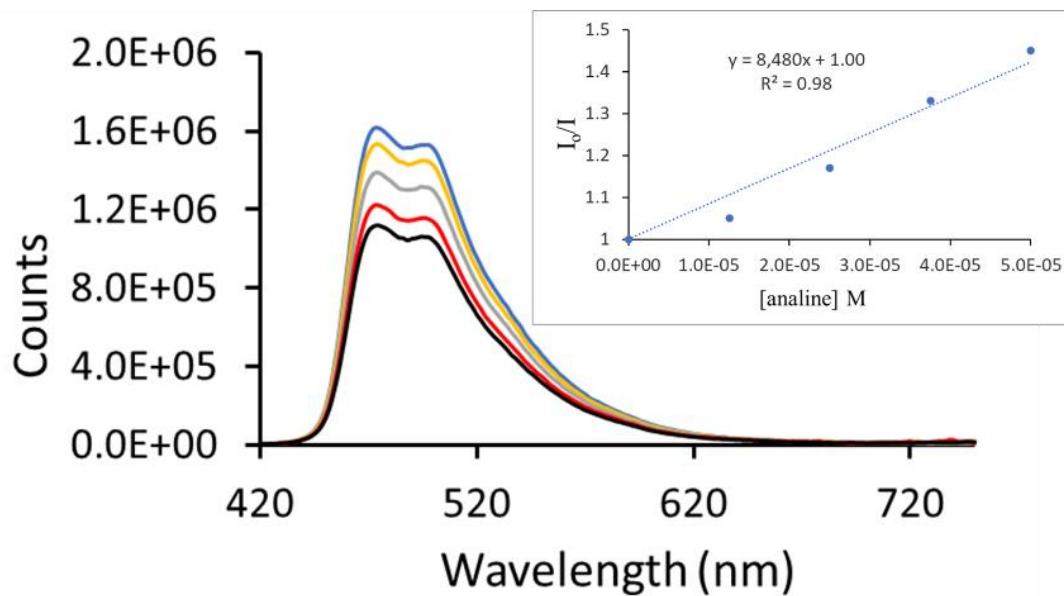


Figure A.6: Fluorescence quenching data and Stern-Volmer plot for the quenching of **Ir** with aniline with 2.5×10^{-4} M K_3PO_4 base added.

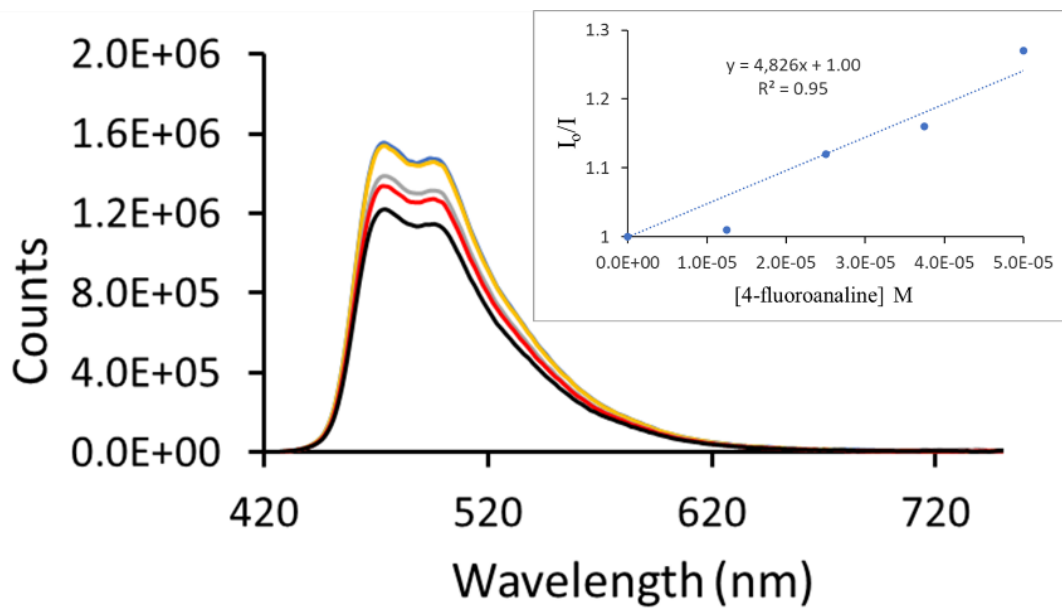


Figure A.7: Fluorescence quenching data and Stern-Volmer plot for the quenching of **Ir** with 4-fluoroaniline with 2.5×10^{-4} M K_3PO_4 base added.

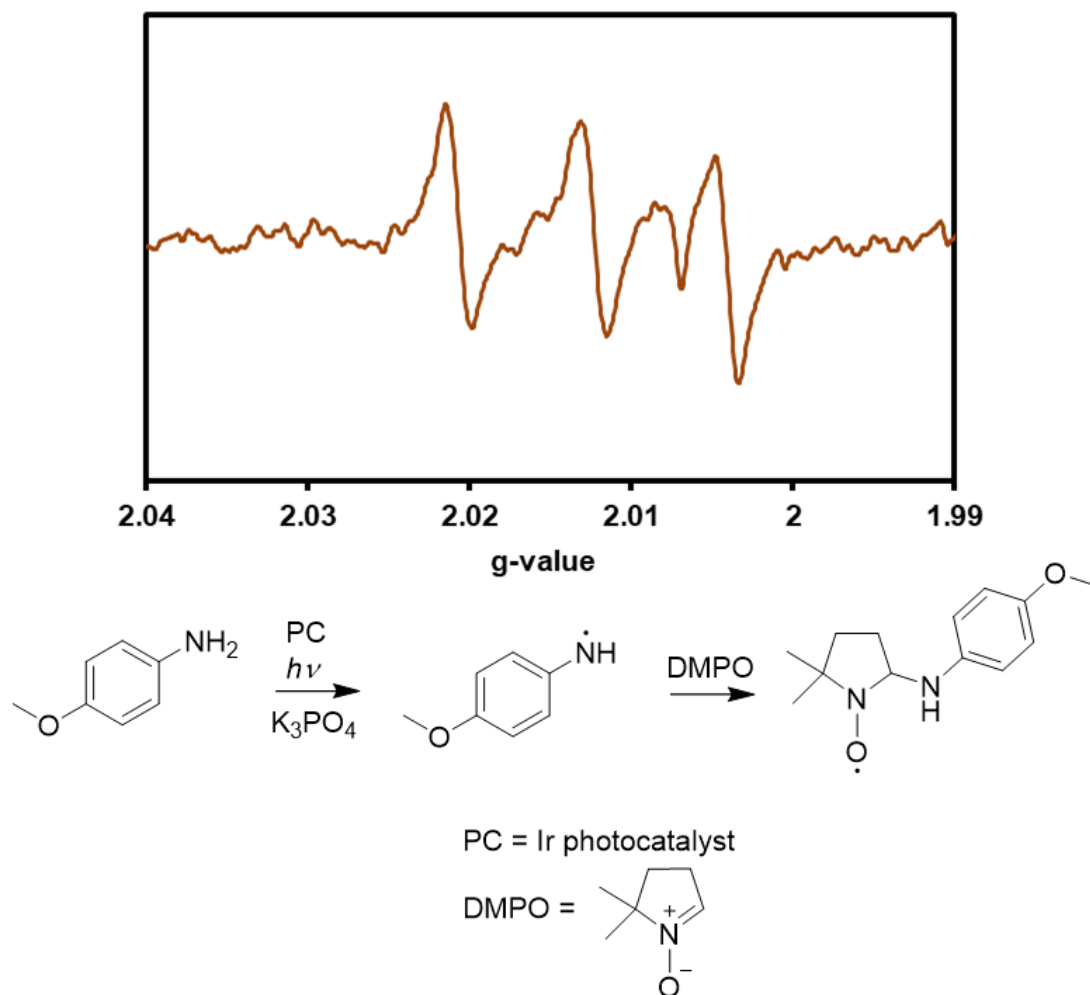


Figure A.8: Room temperature X-band (9.38 GHz) spectrum of reaction solution containing *p*-anisidine, DMPO, K₃PO₄ and **Ir** in dichloromethane after 35 minutes of irradiation with blue light with the proposed reaction leading to the EPR signal.

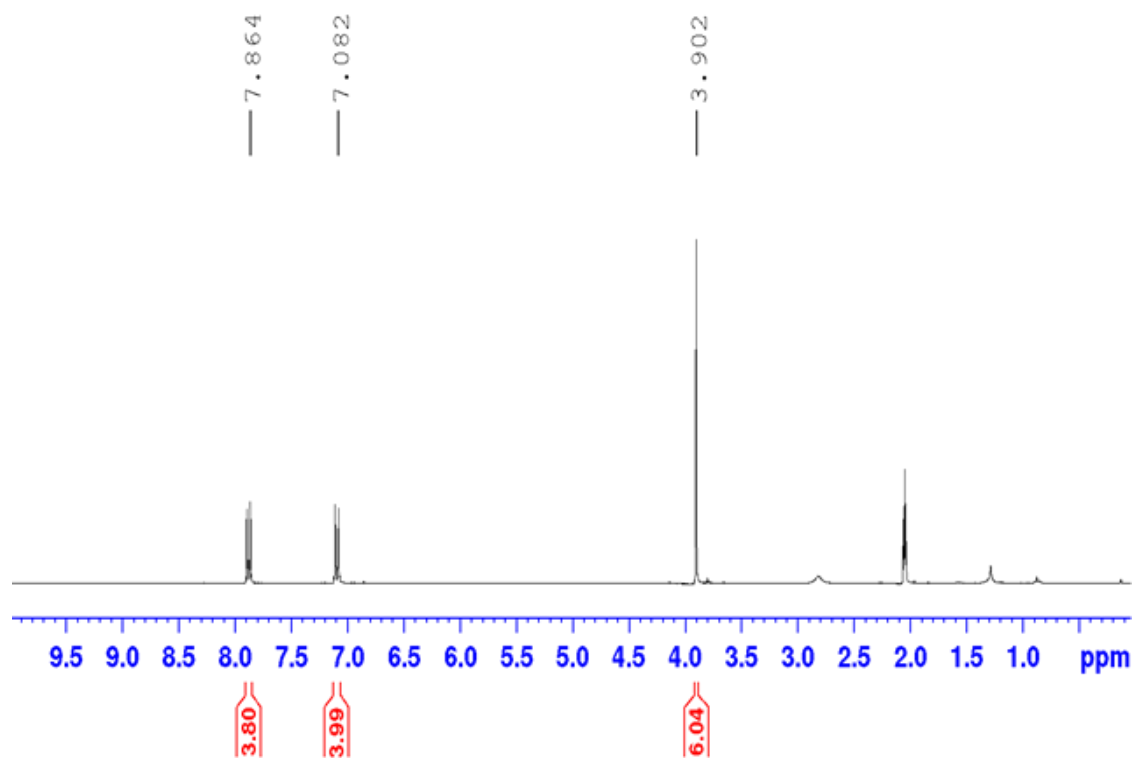


Figure A.9: ^1H NMR spectra of product 2.1 in $(\text{CD}_3)_2\text{CO}$ with solvent peak at 2.05 ppm.

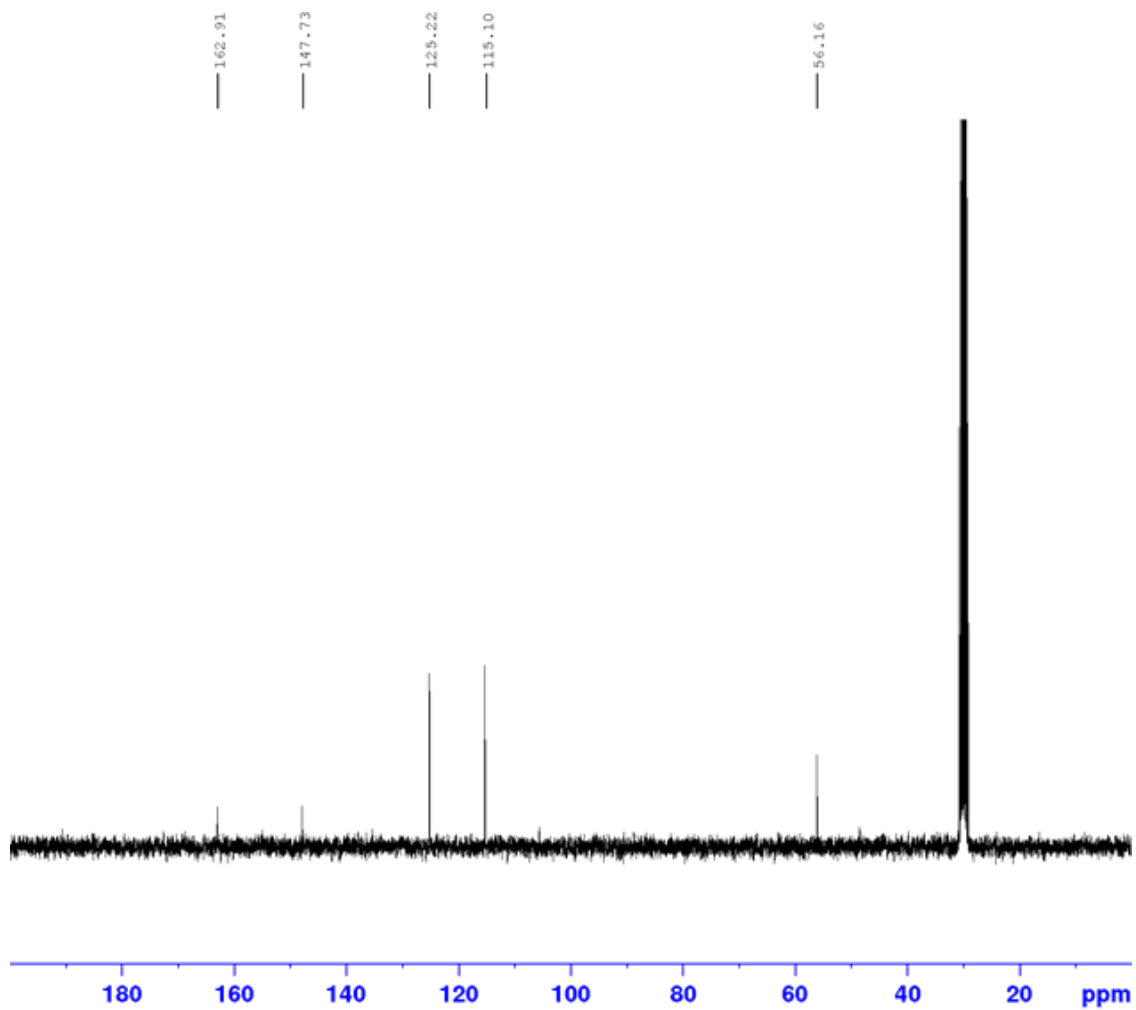


Figure A.10: ^{13}C NMR spectra of product 2.1 in $(\text{CD}_3)_2\text{CO}$ with solvent peak at 30.0 ppm.

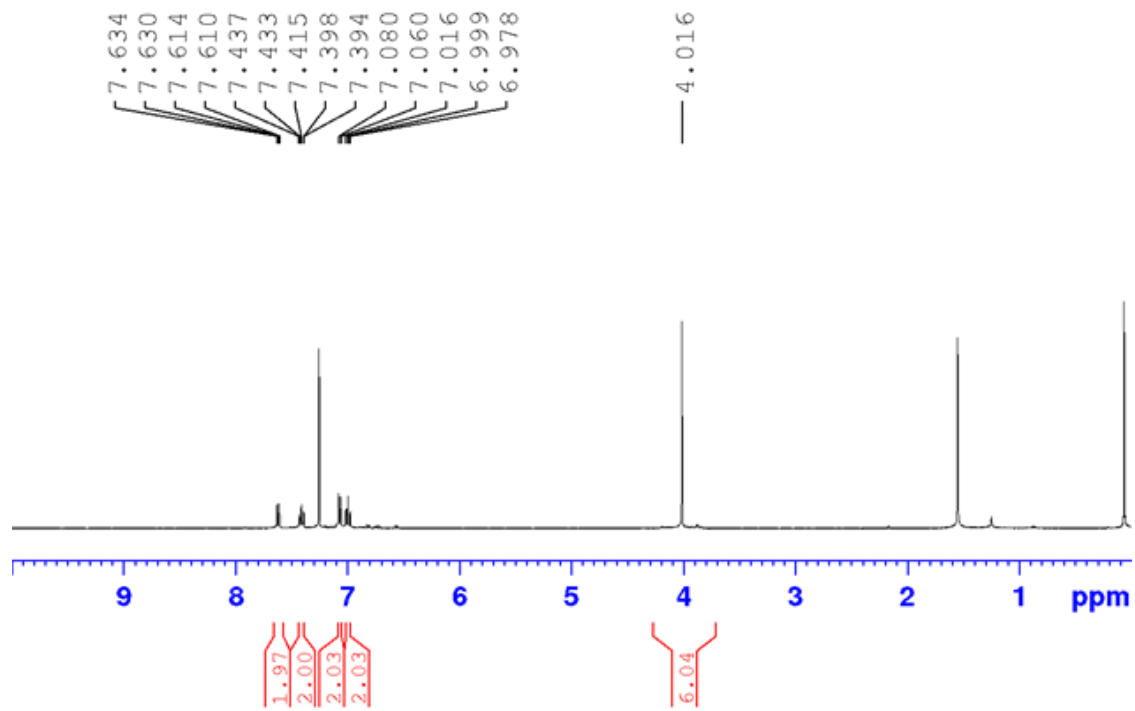


Figure A.11: ^1H NMR spectra of product 2.2.

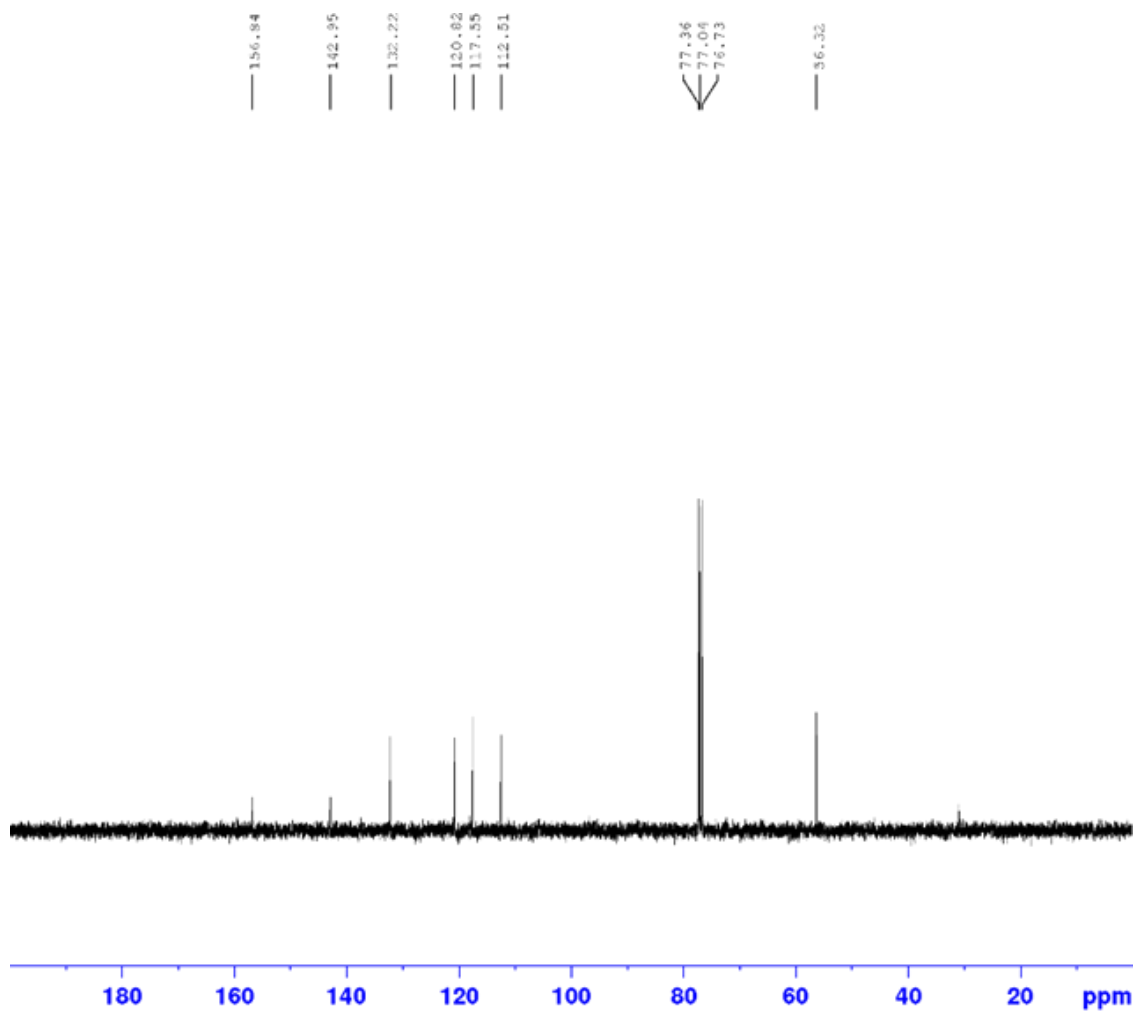


Figure A.12: ^{13}C NMR spectra of product 2.2.

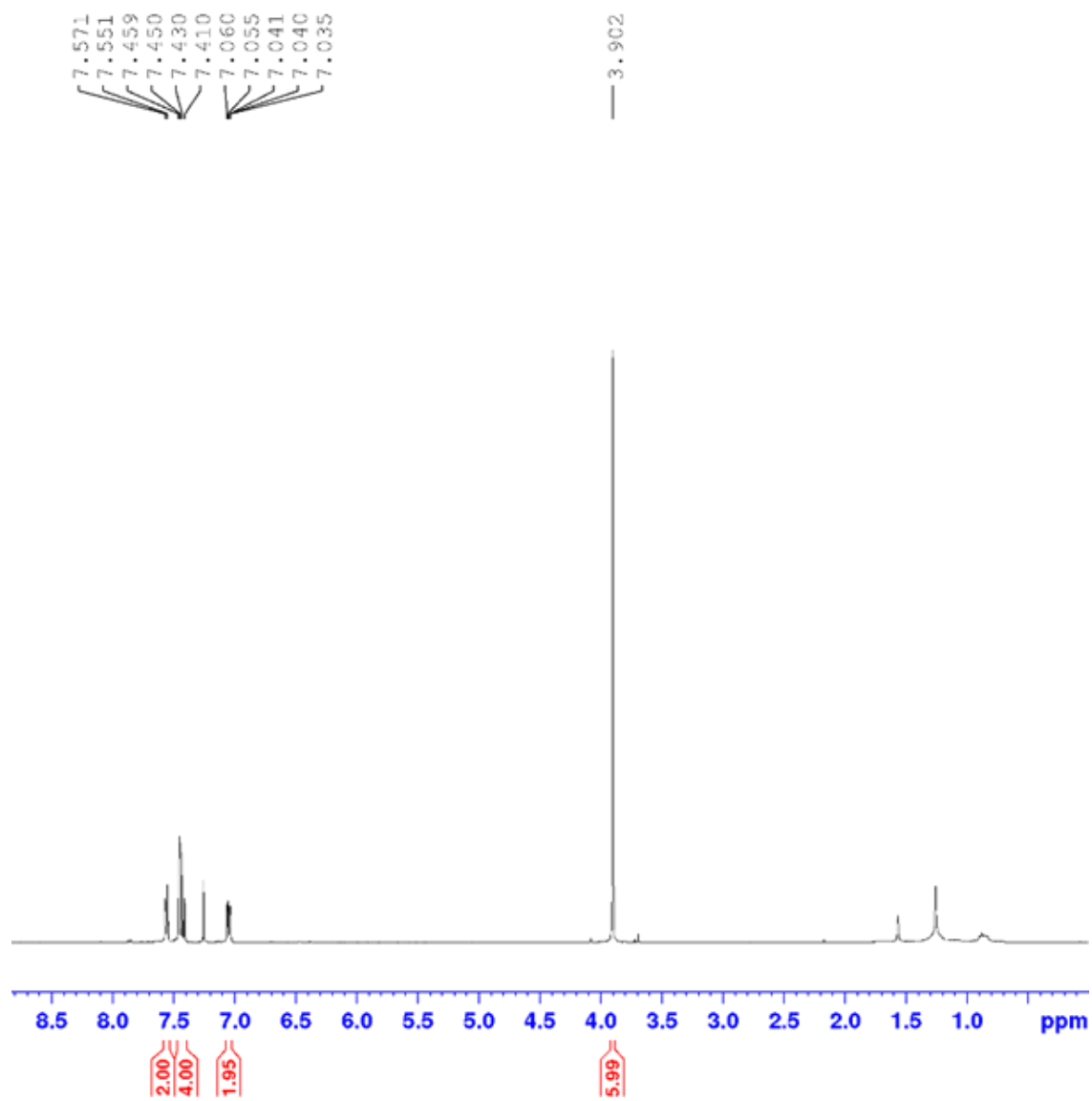


Figure A.13: ^1H NMR spectra of product 2.3.

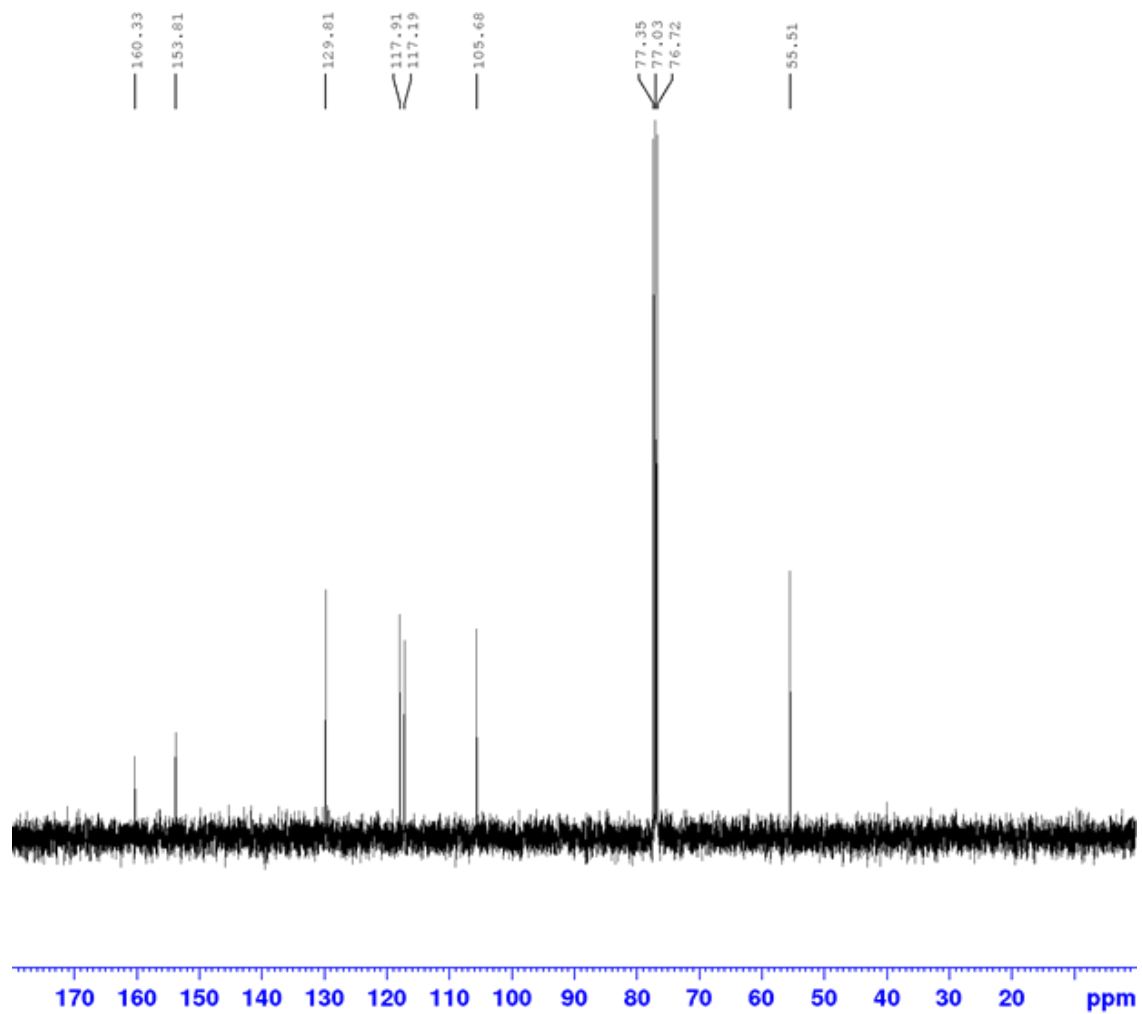


Figure A.14: ^{13}C NMR spectra of product 2.3.

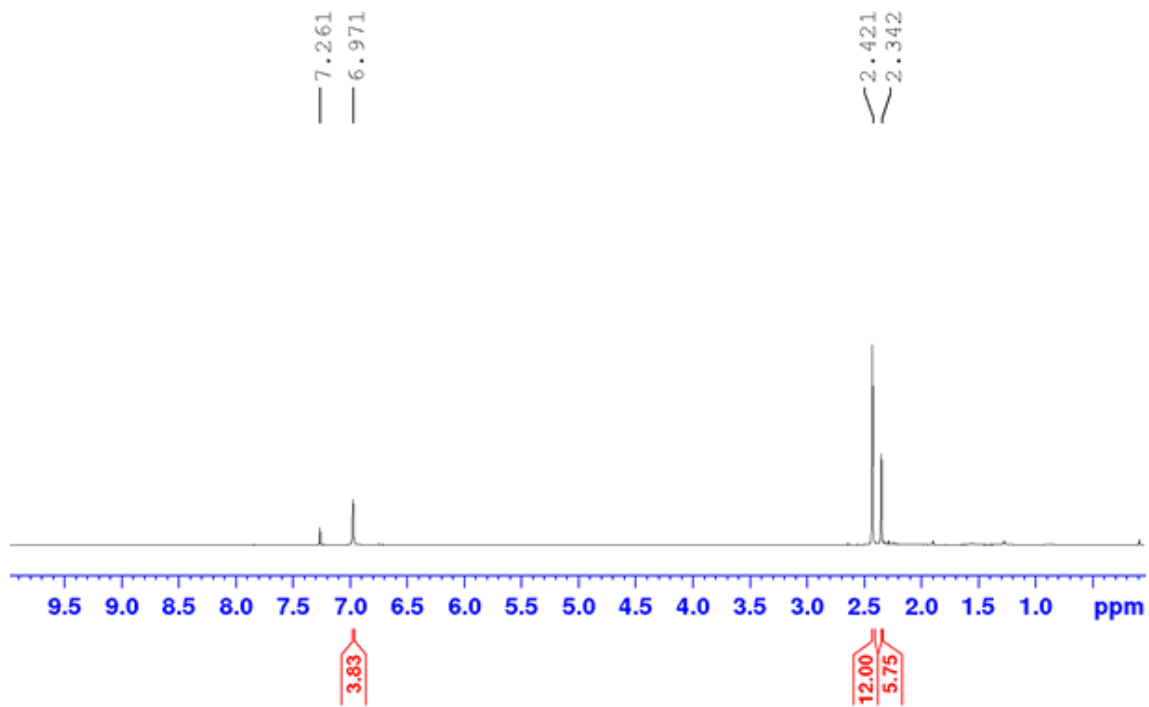


Figure A.15: ¹H NMR spectra of product 2.4 in CDCl₃ with solvent peak at 7.26 ppm.

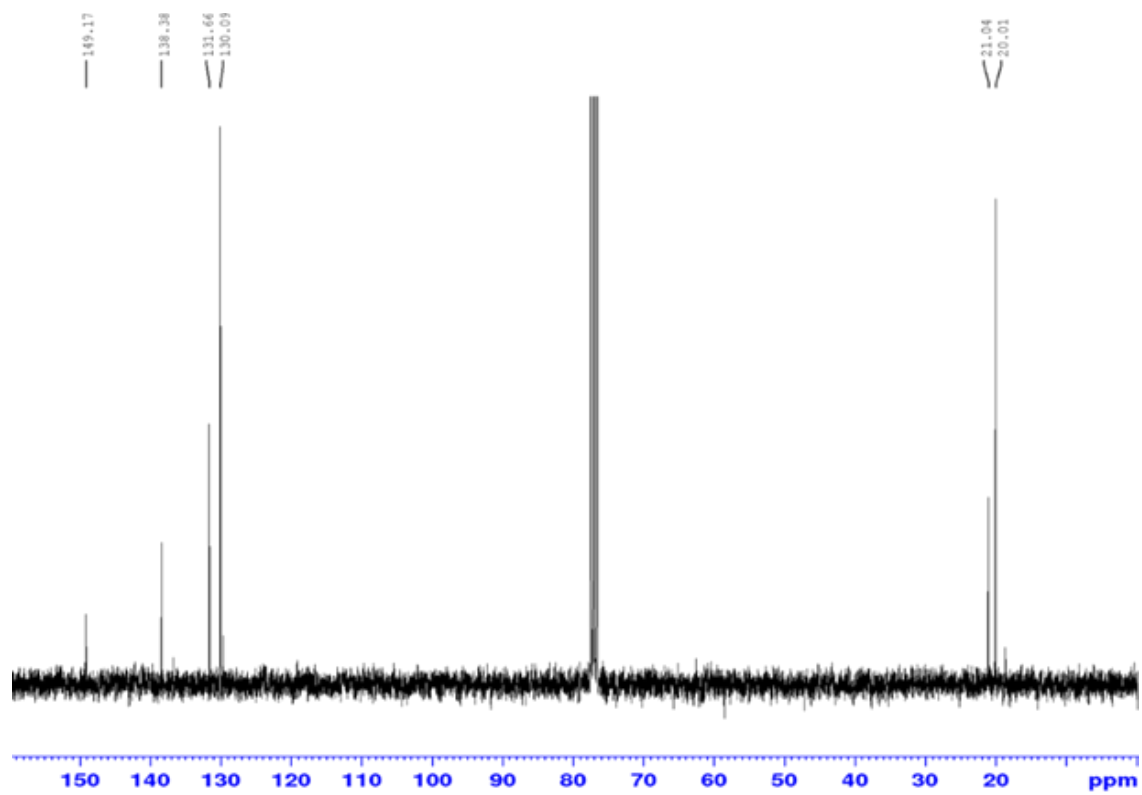


Figure A.16: ^{13}C NMR spectra of product 2.4 in CDCl_3 with solvent peak at 77.16 ppm.

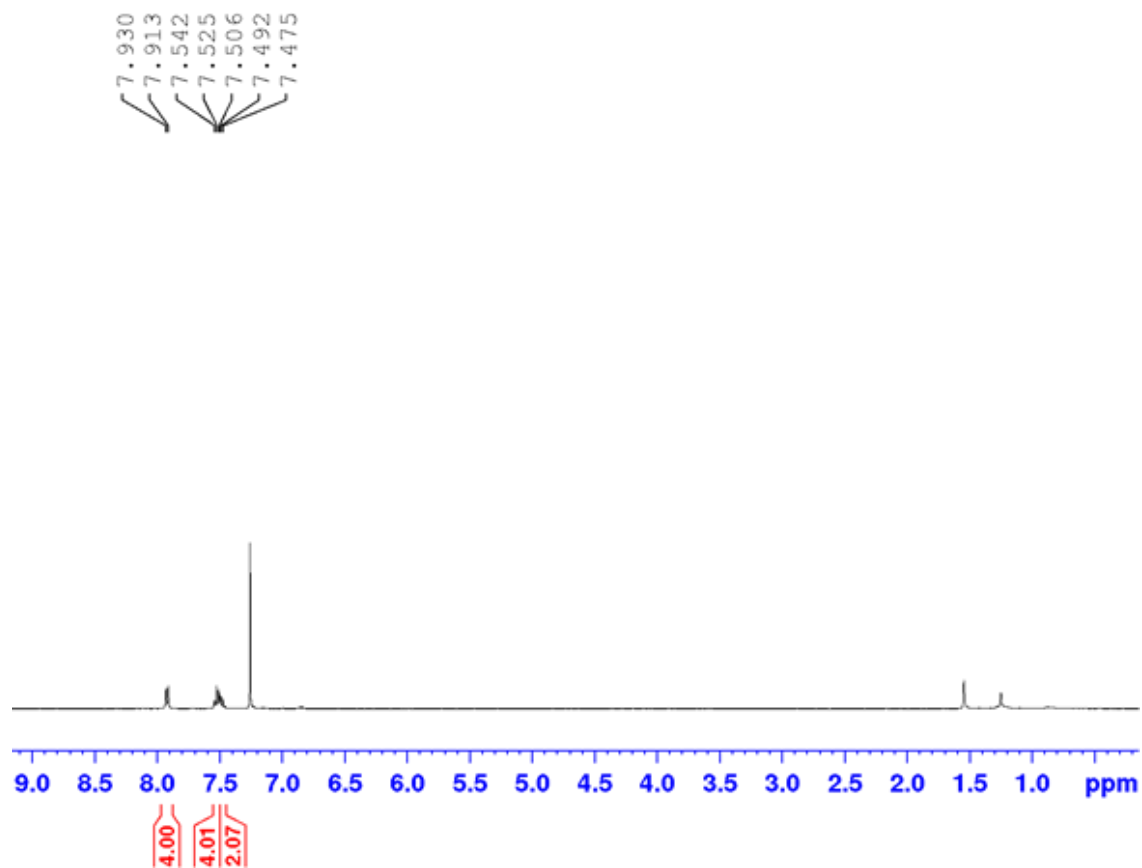


Figure A.17: ^1H NMR spectra of product 2.5.

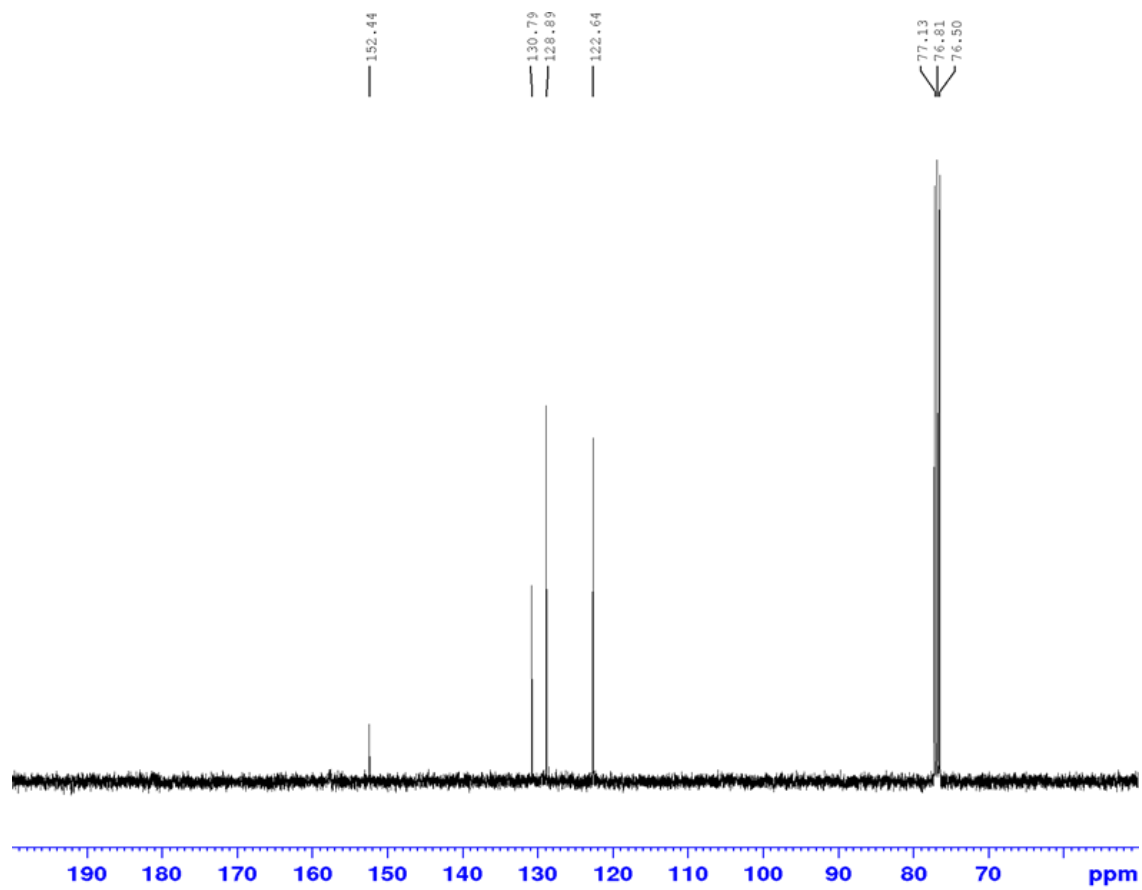


Figure A.18: ^{13}C NMR spectra of product 2.5.

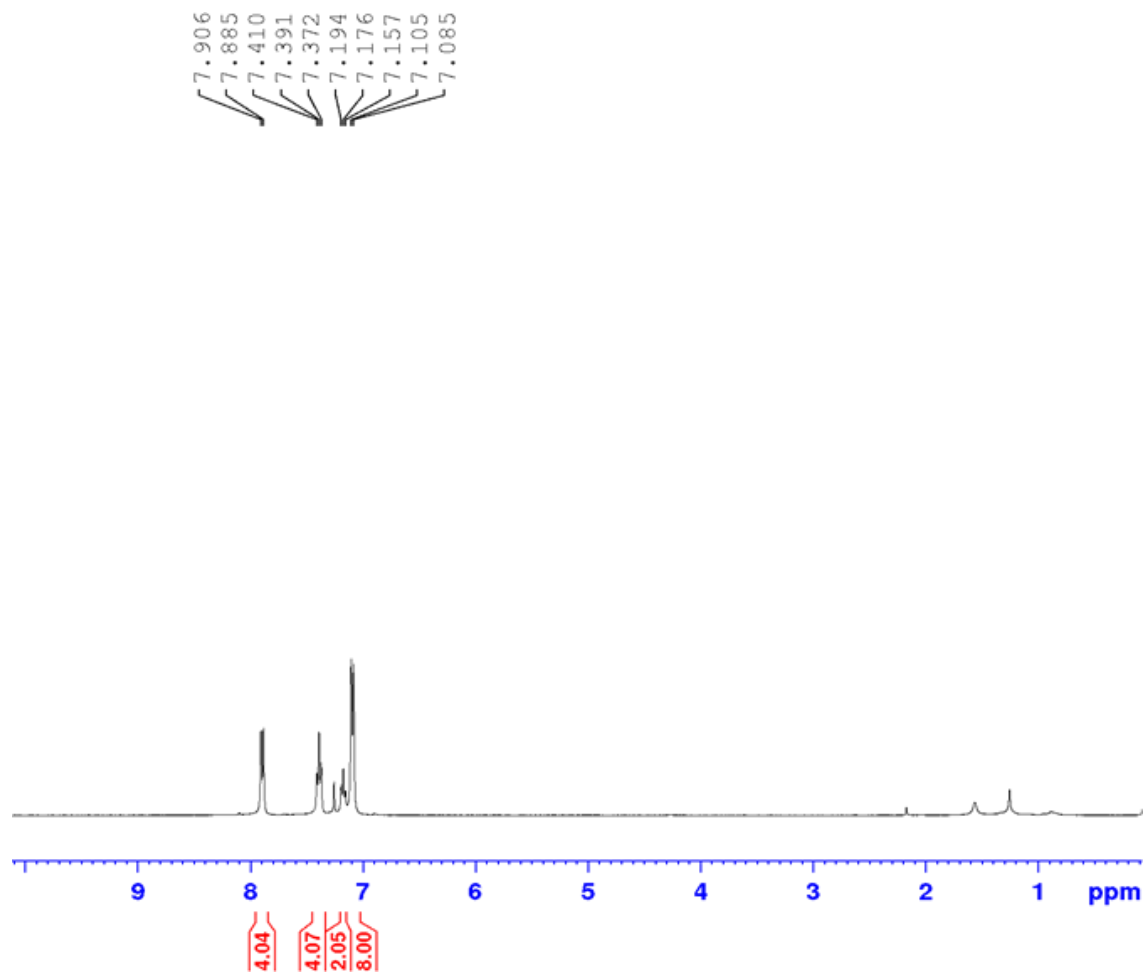


Figure A.19: ^1H NMR of product 2.6.

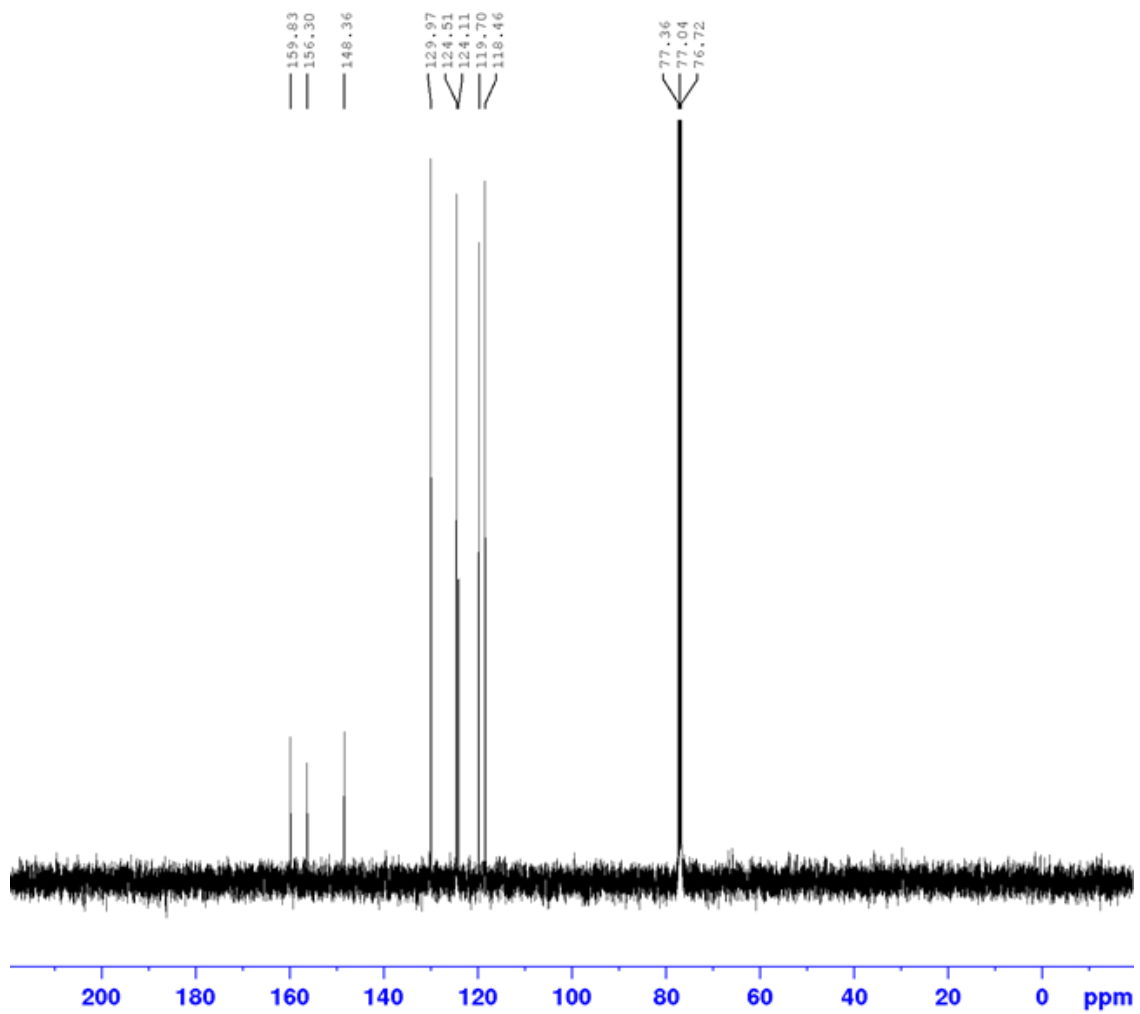


Figure A.20: ^{13}C NMR of product 2.6.

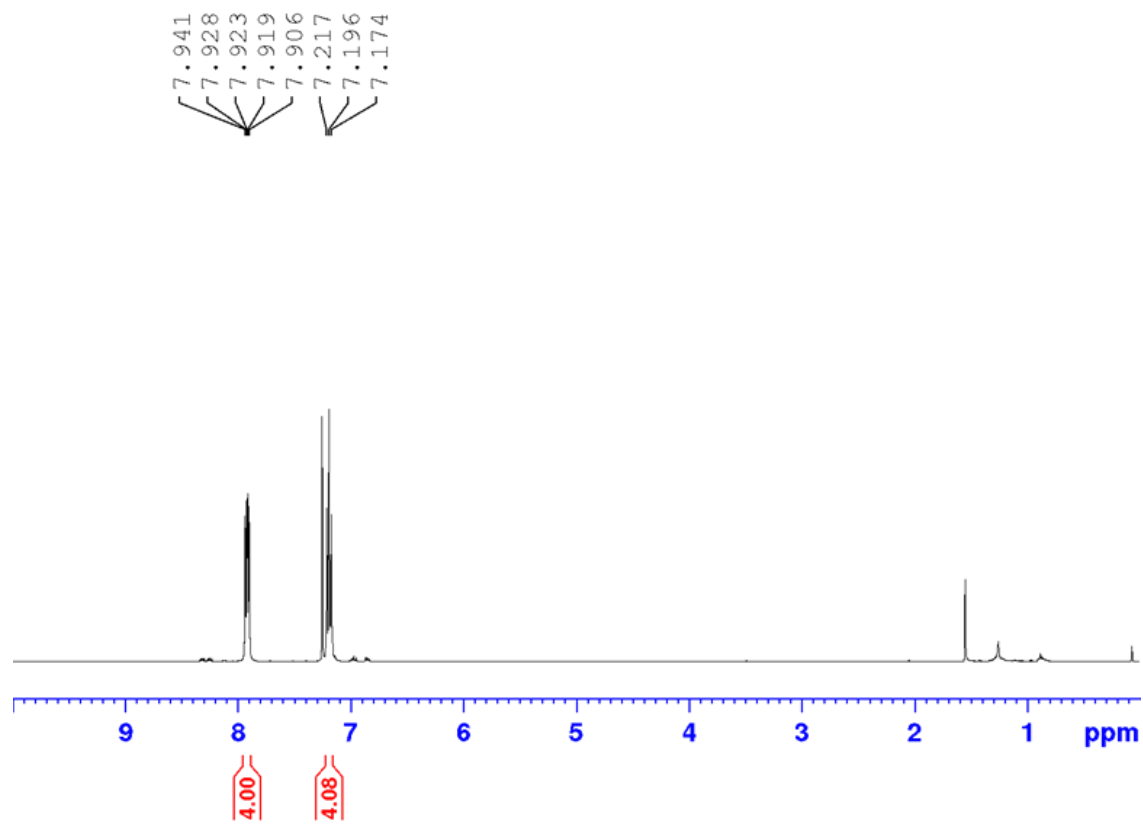


Figure A.21: ^1H NMR spectra of product 2.7.

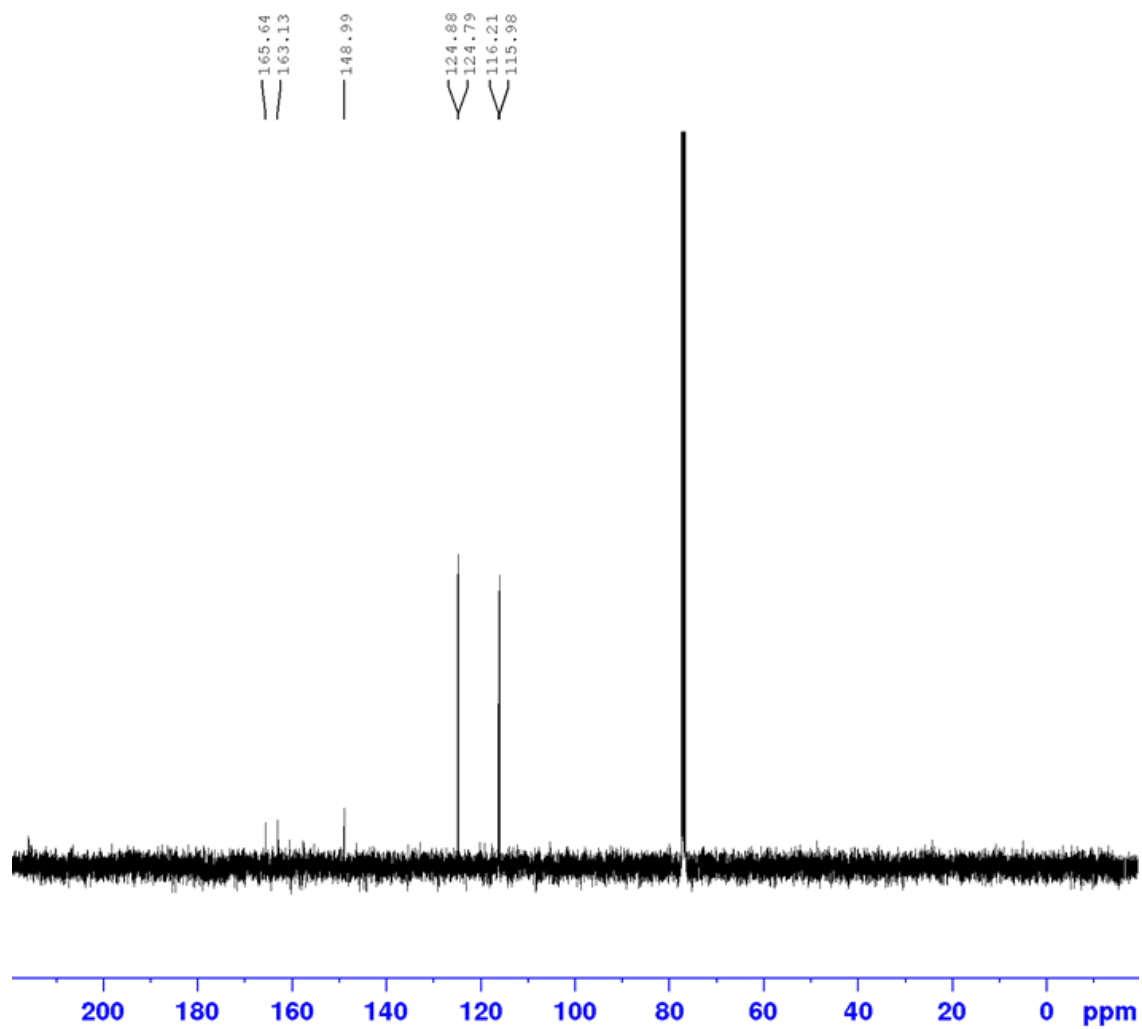


Figure A.22: ^{13}C NMR spectra of product 2.7.

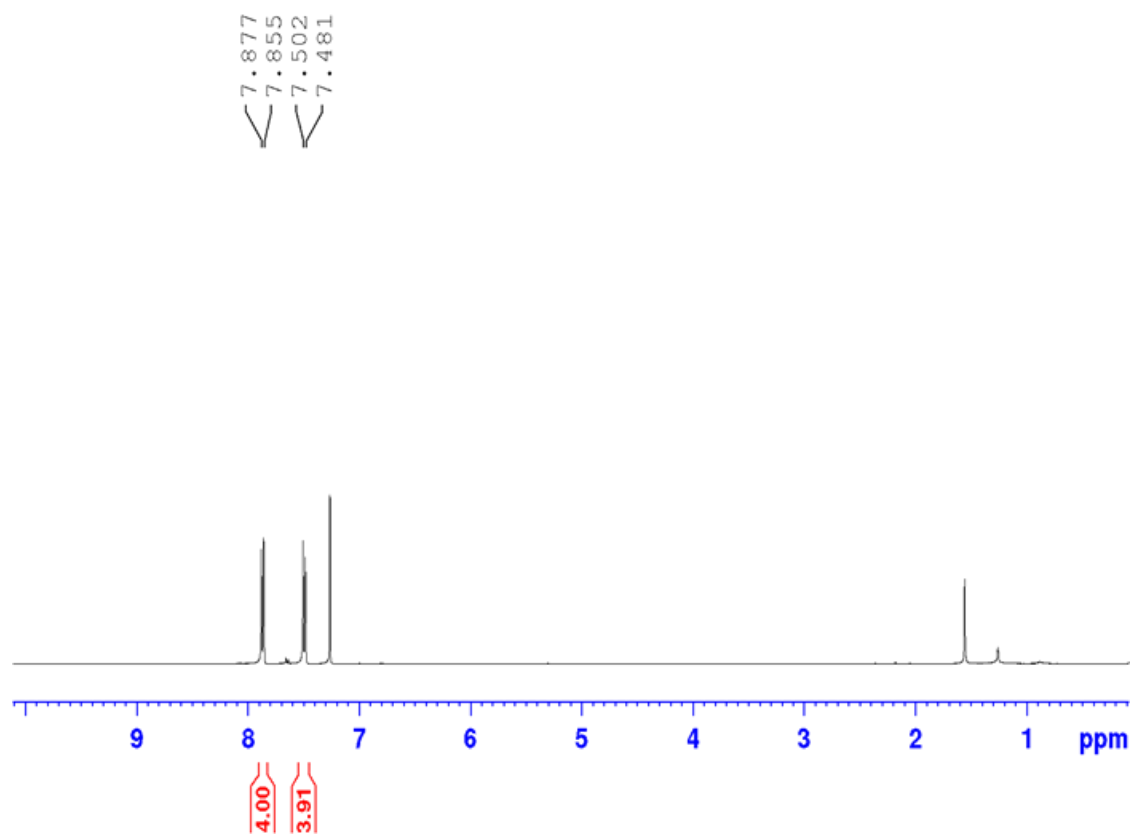


Figure A.23: ^1H NMR spectra of product 2.8.

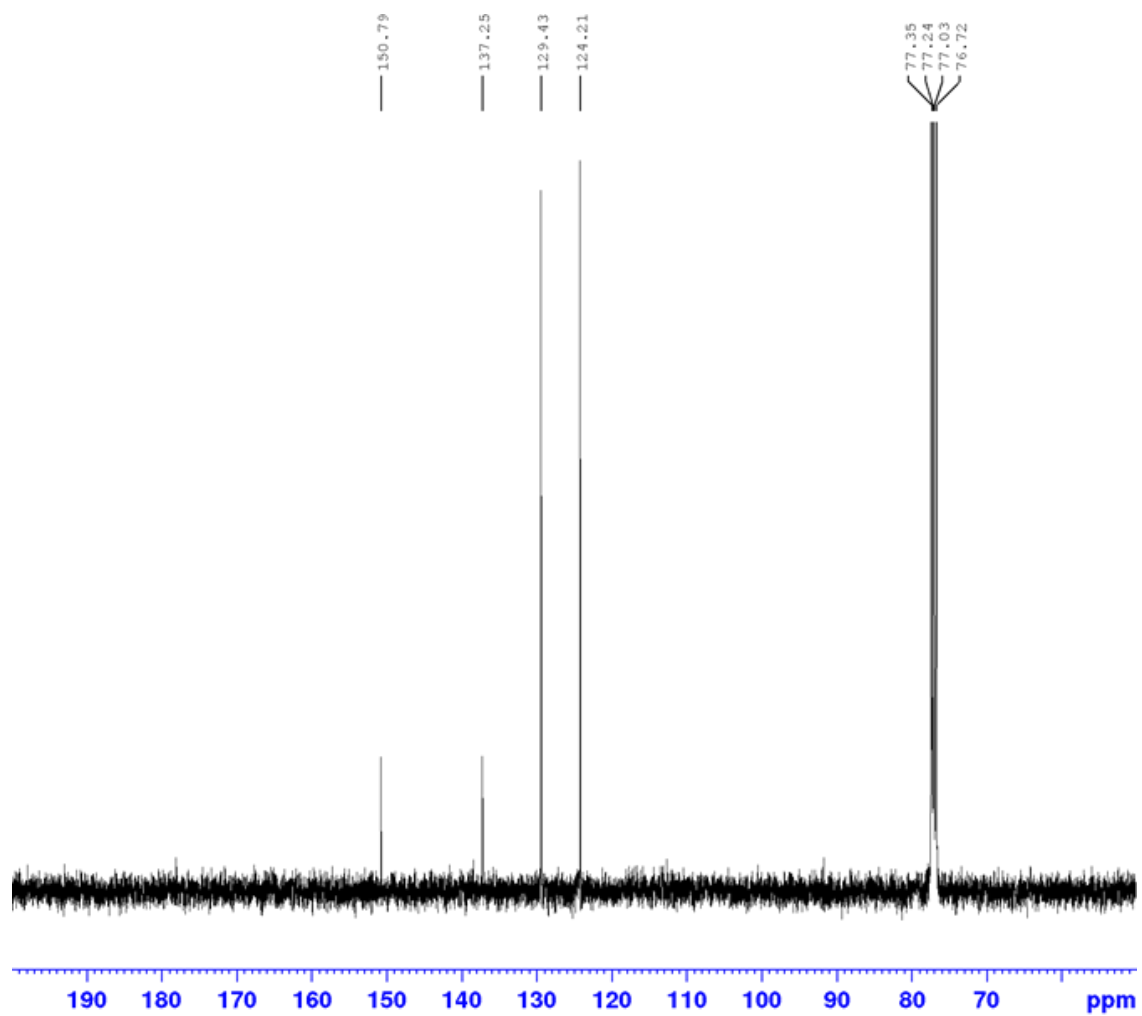


Figure A.24: ^{13}C NMR spectra of product 2.8.

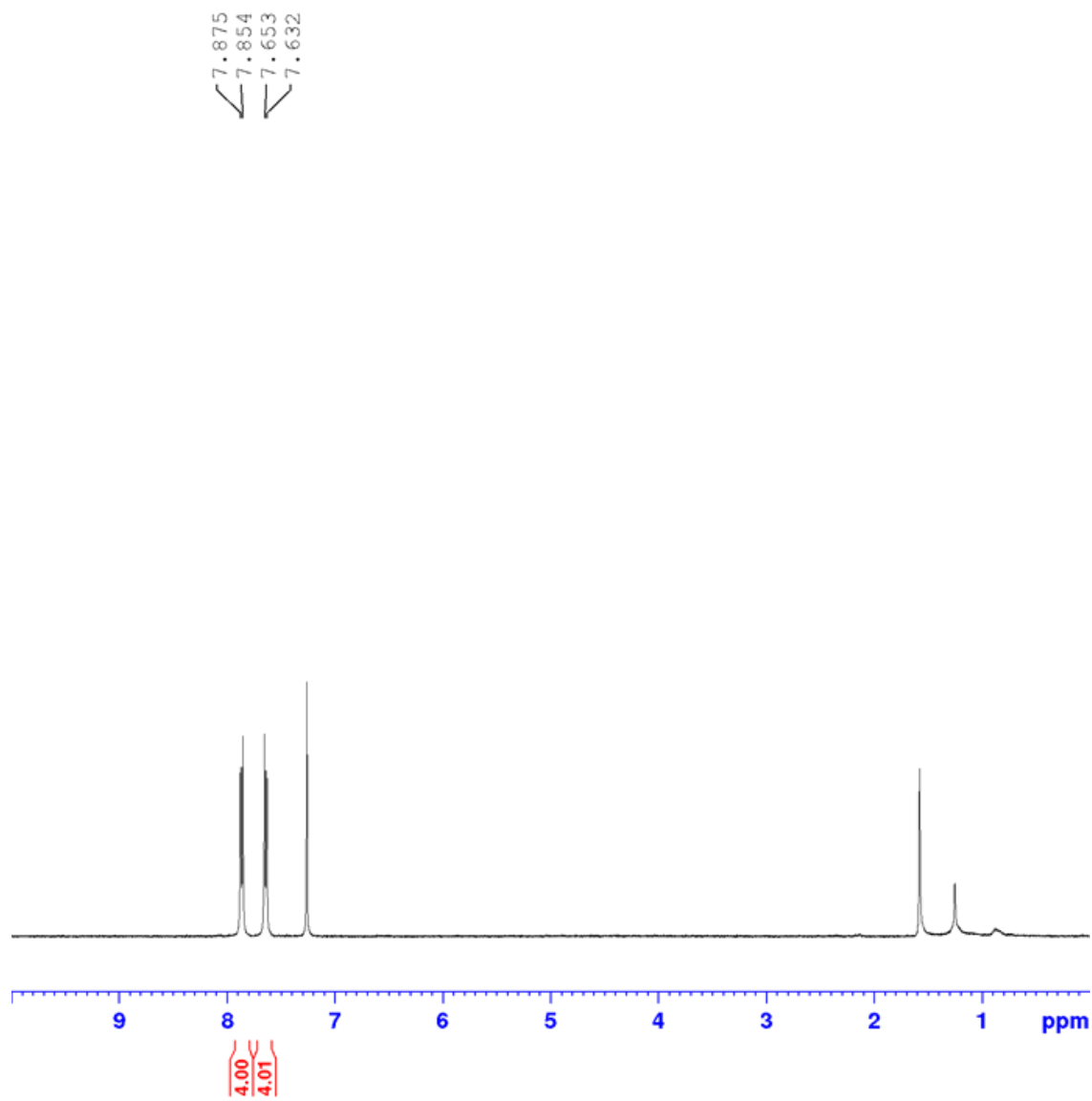


Figure A.25: ^1H NMR spectra of product 2.9.

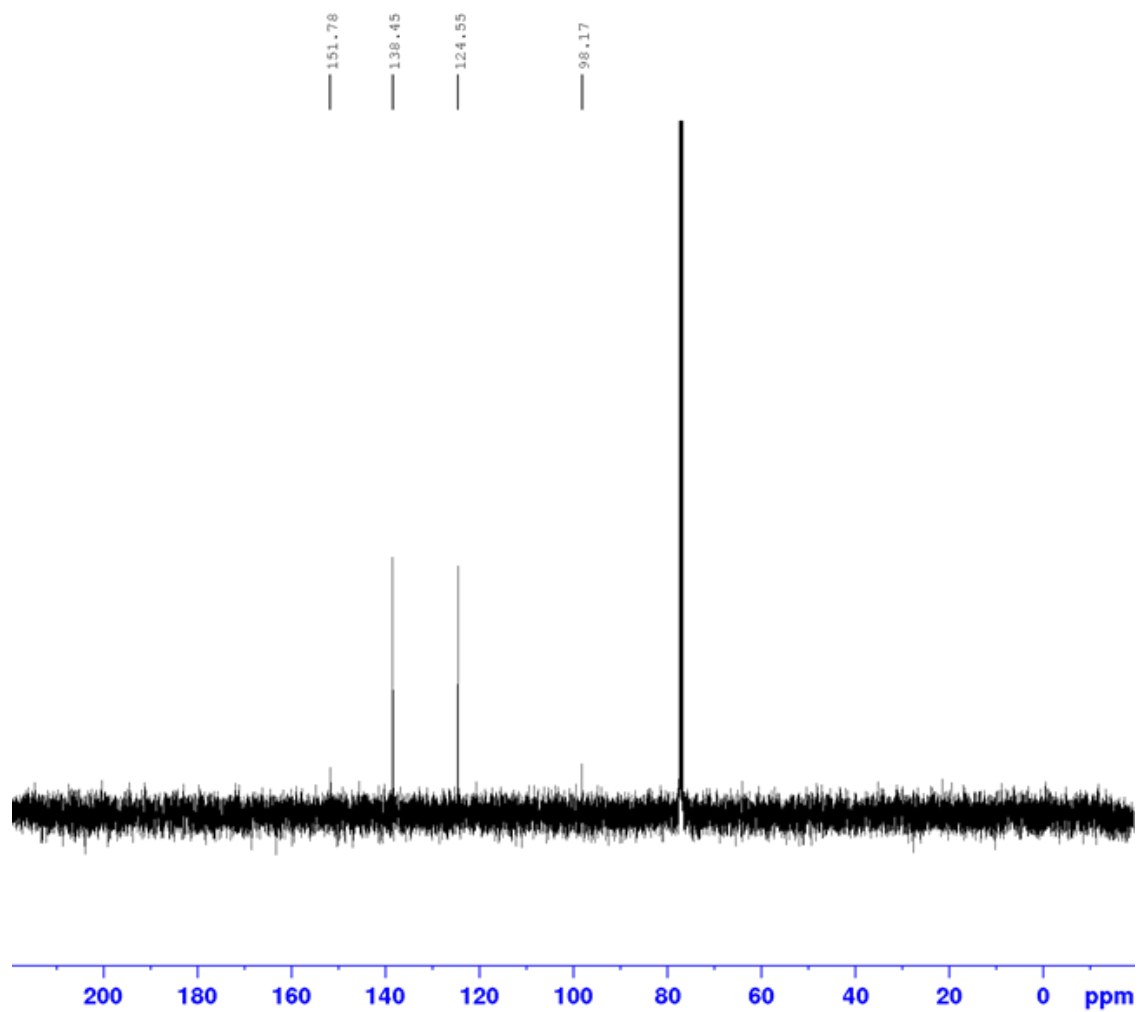


Figure A.26: ^{13}C NMR spectra of product 2.9.

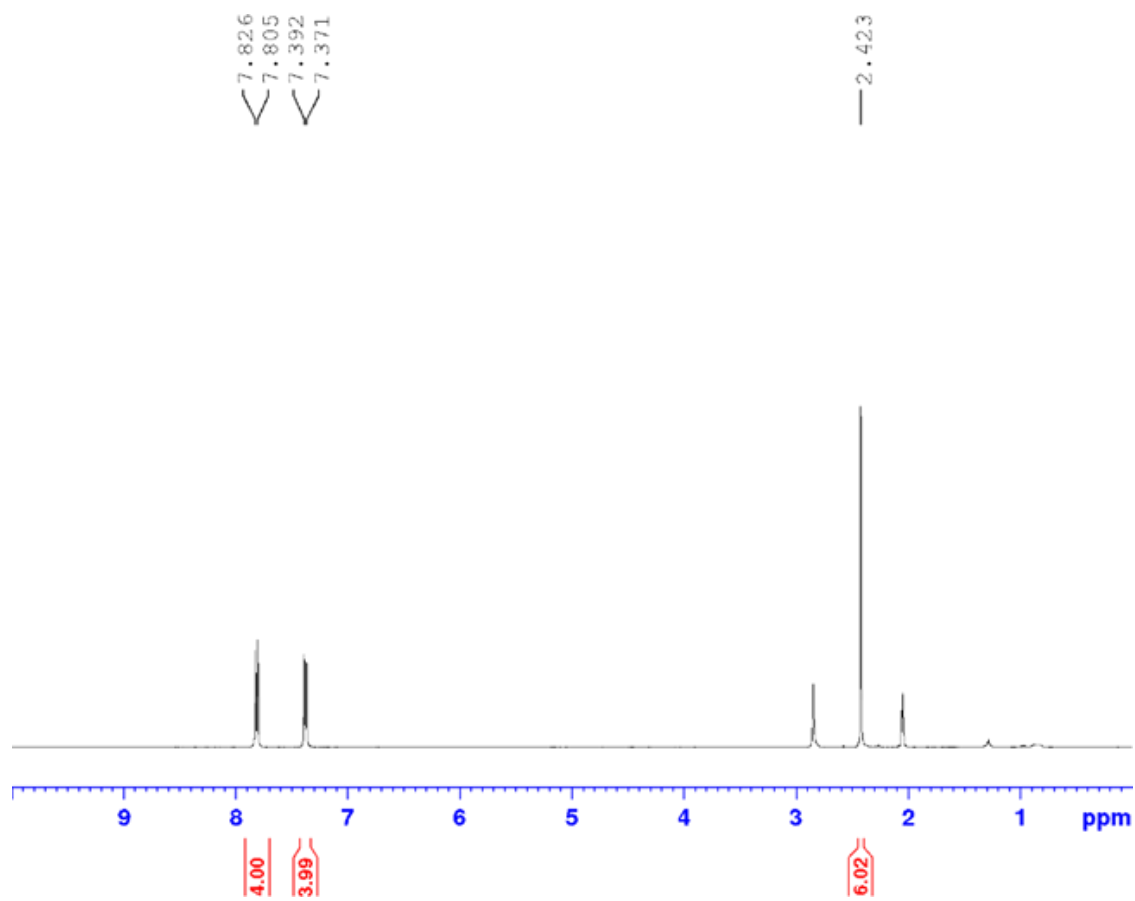


Figure A.27: ^1H NMR spectra of product 2.10.

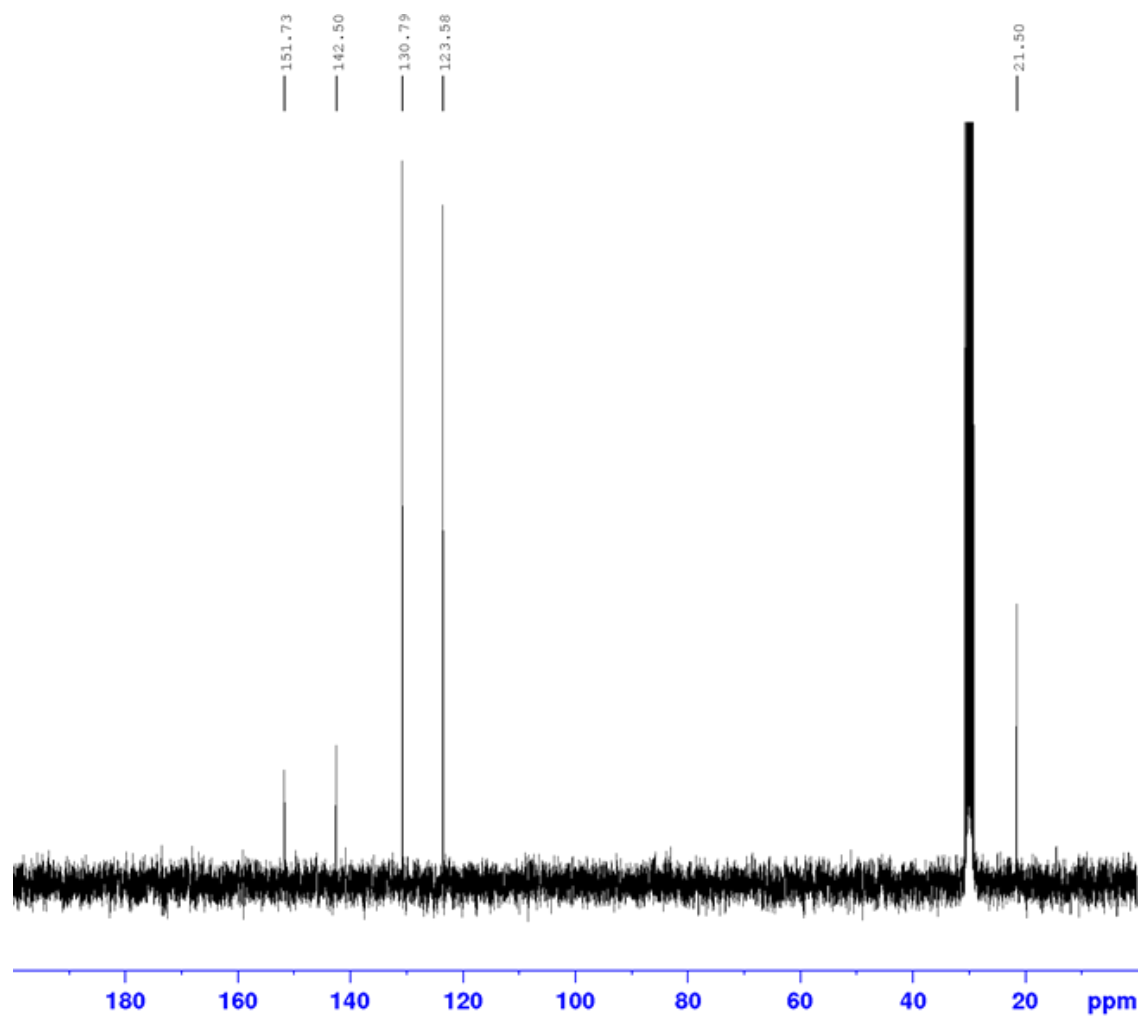


Figure A.28: ^{13}C NMR spectra of product 2.10.

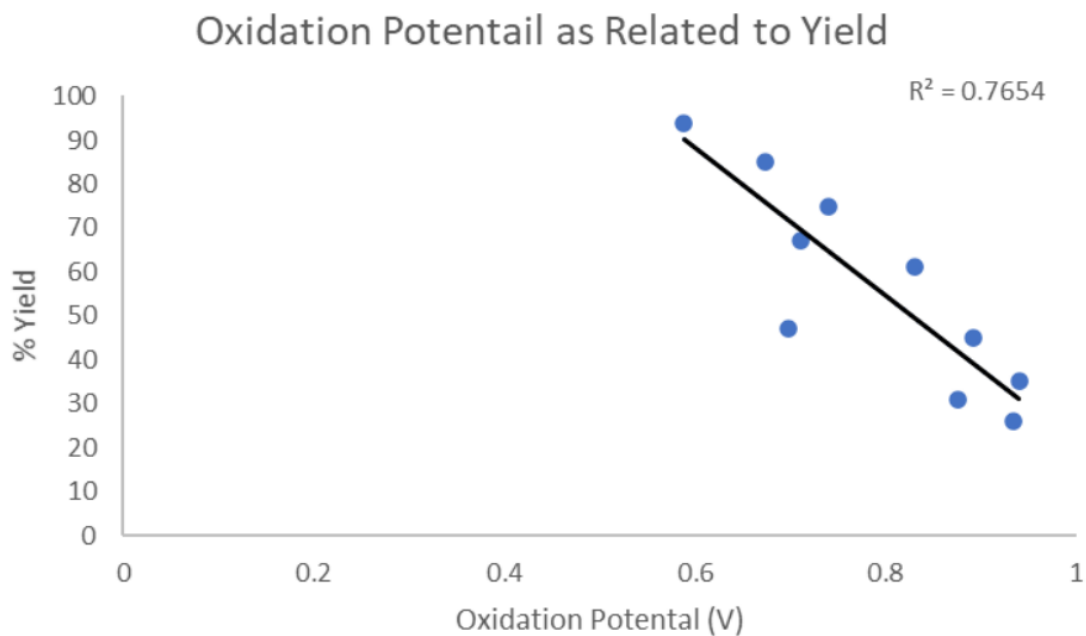


Figure A.29: Plot of determined oxidation potential (V) as compared to product % yield after 4 hours under optimized reaction conditions: 25 mM substrate, 75 mM K_3PO_4 , 5 mol% Ir PC, acetonitrile solution, O_2 bubbled into solution for 15 minutes.

APPENDIX B: SUPPORTING INFORMATION FOR CHAPTER 3

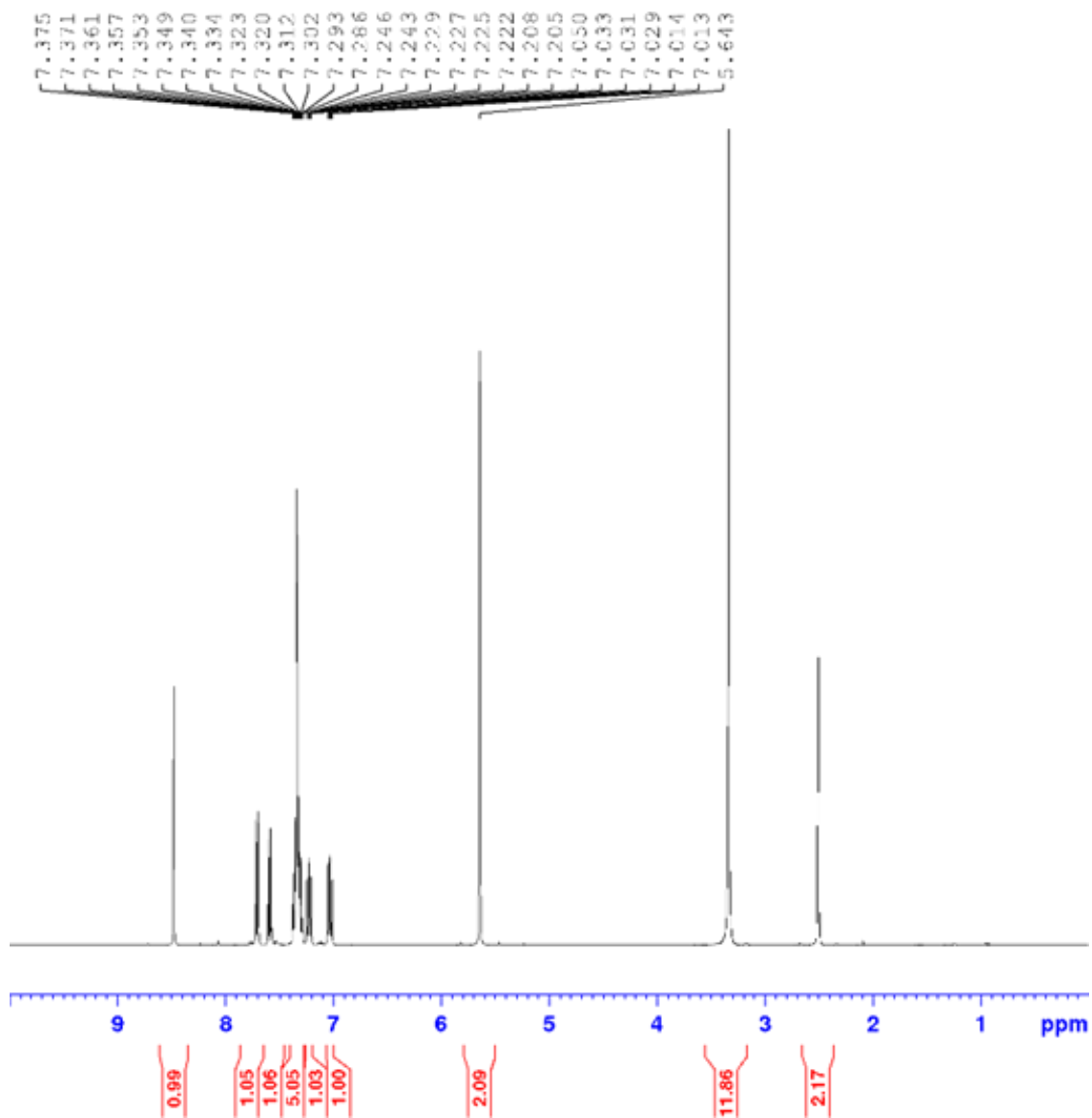


Figure B.1: ^1H NMR spectra of product 3.1.

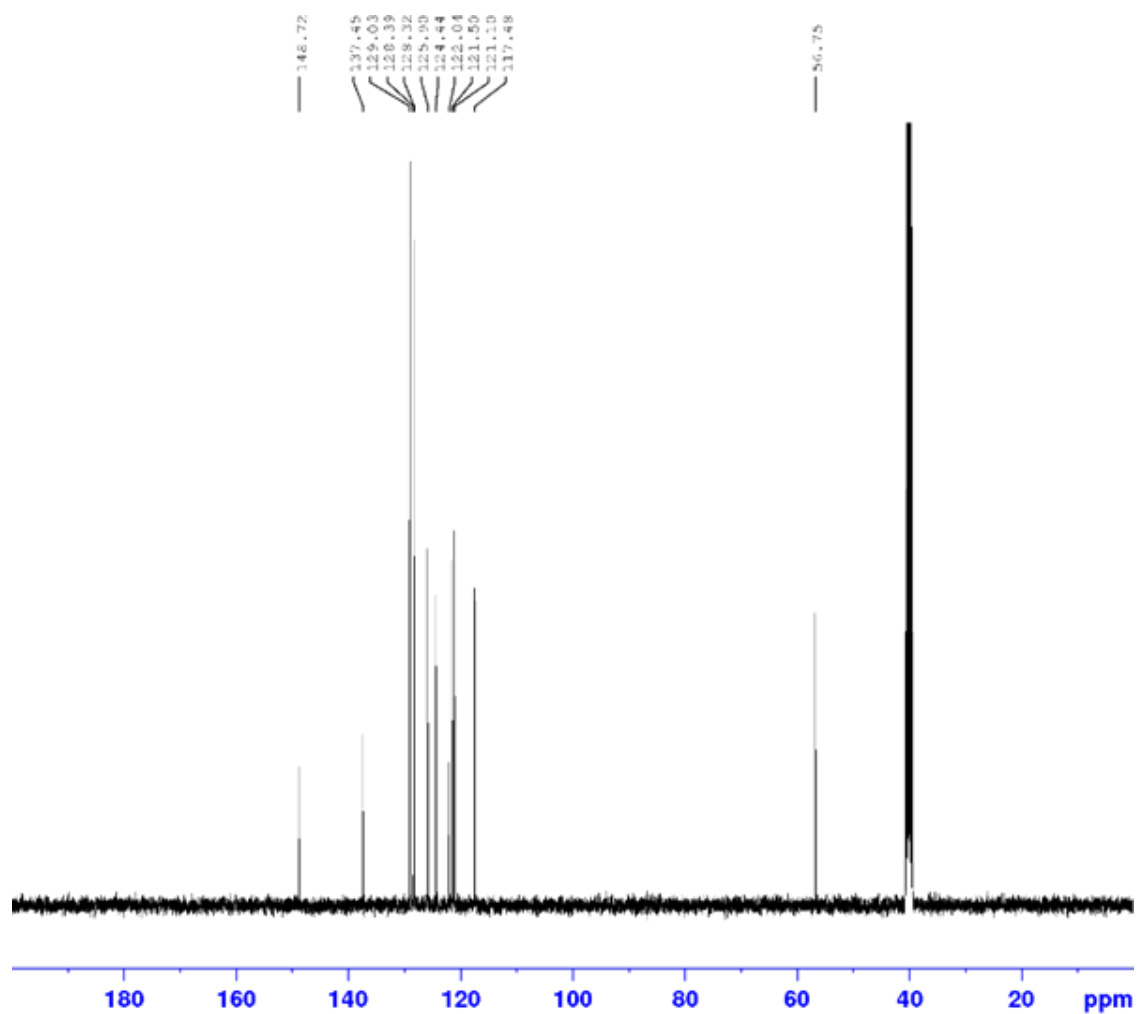


Figure B.2: ^{13}C NMR spectra of product 3.1.

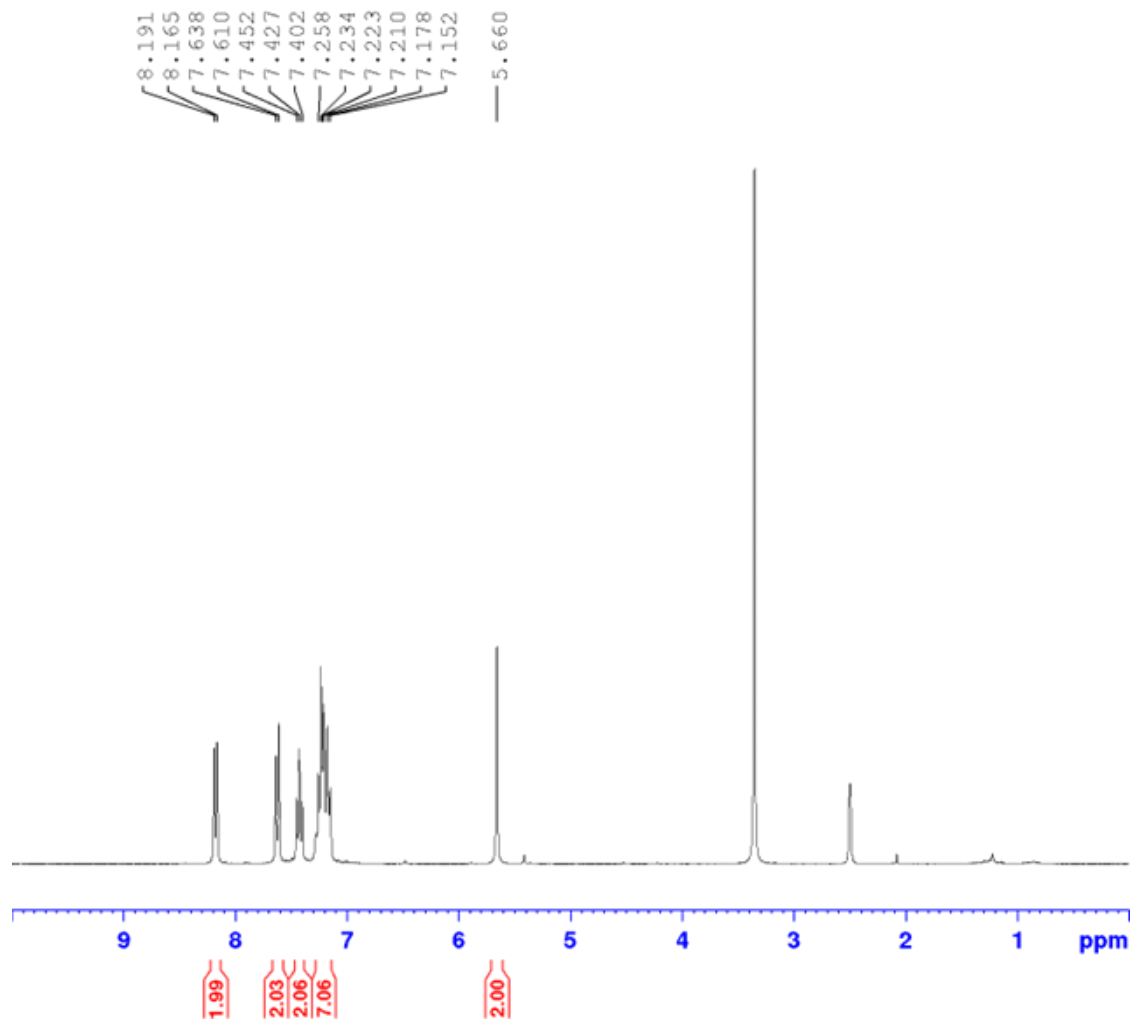


Figure B.3: ^1H NMR spectra of product 3.2.

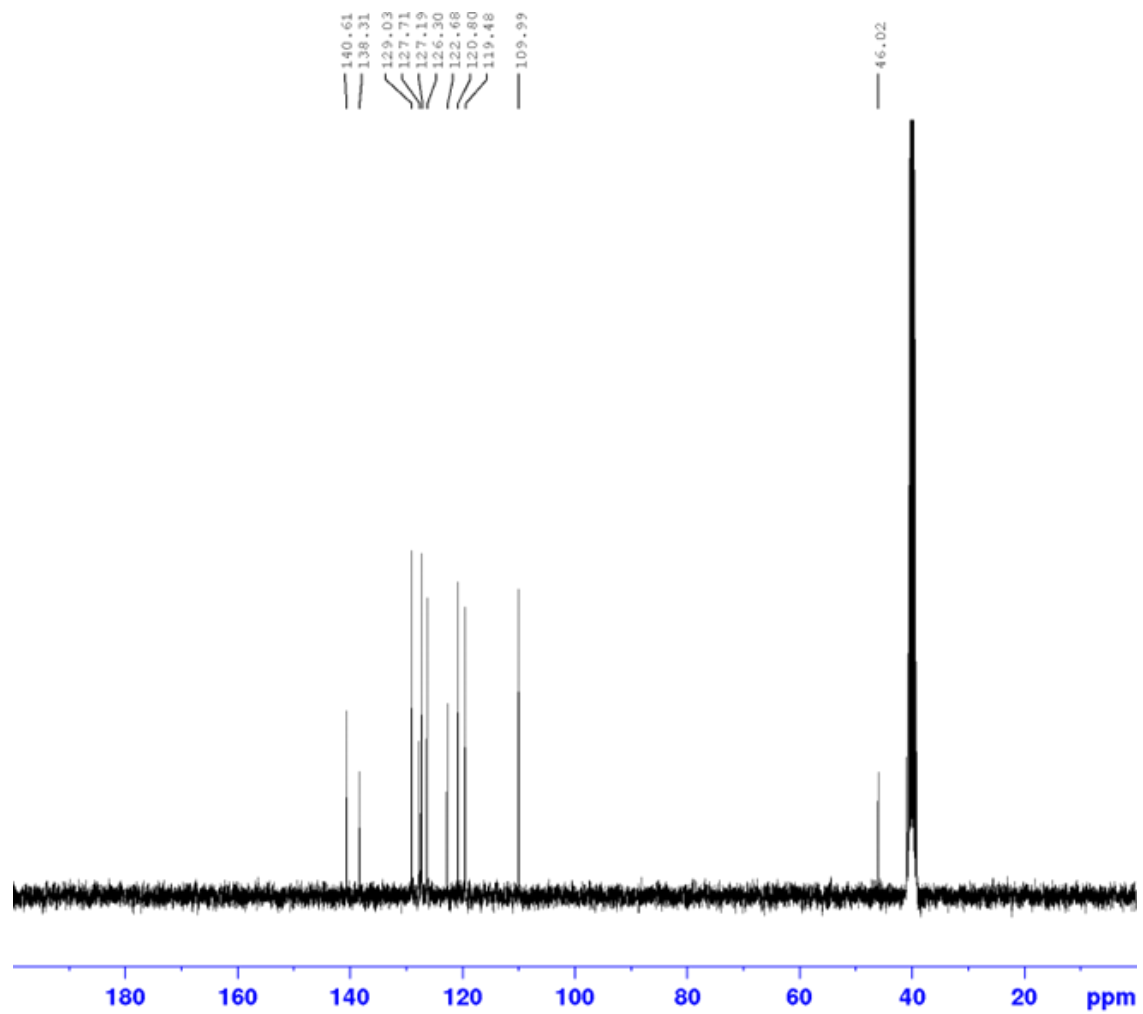


Figure B.4: ^{13}C NMR spectra of product 3.2.

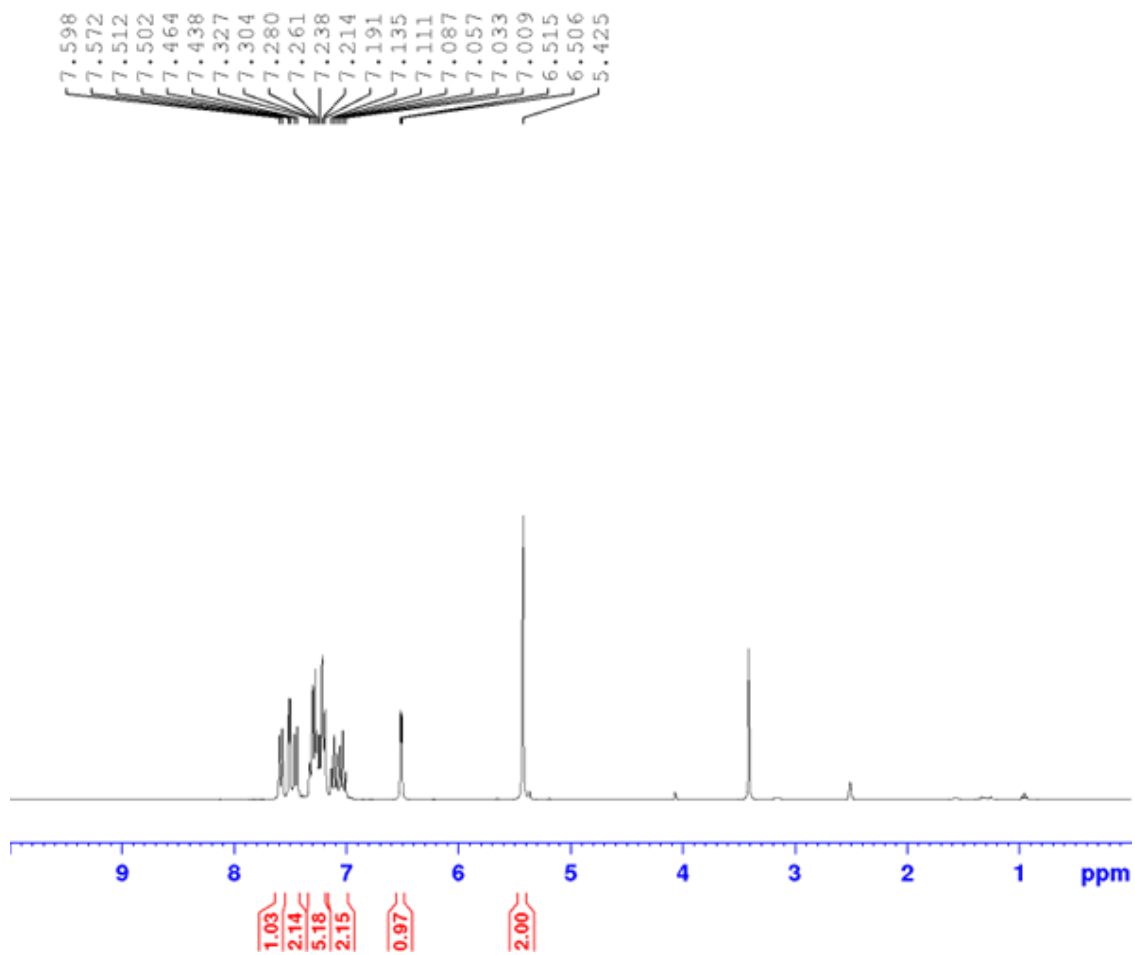


Figure B.5: ^1H NMR spectra of product 3.3.

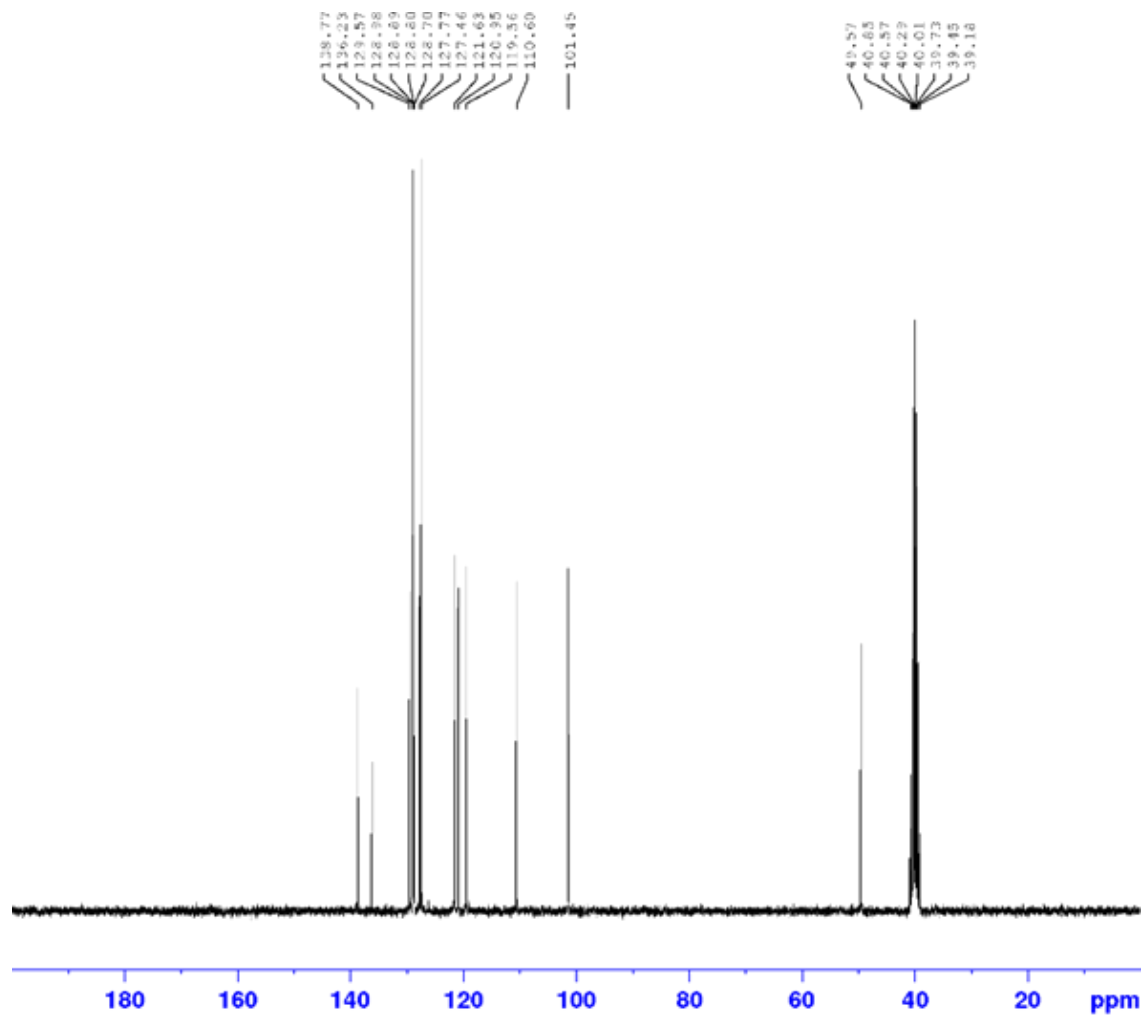


Figure B.6: ^{13}C NMR spectra of product 3.3.

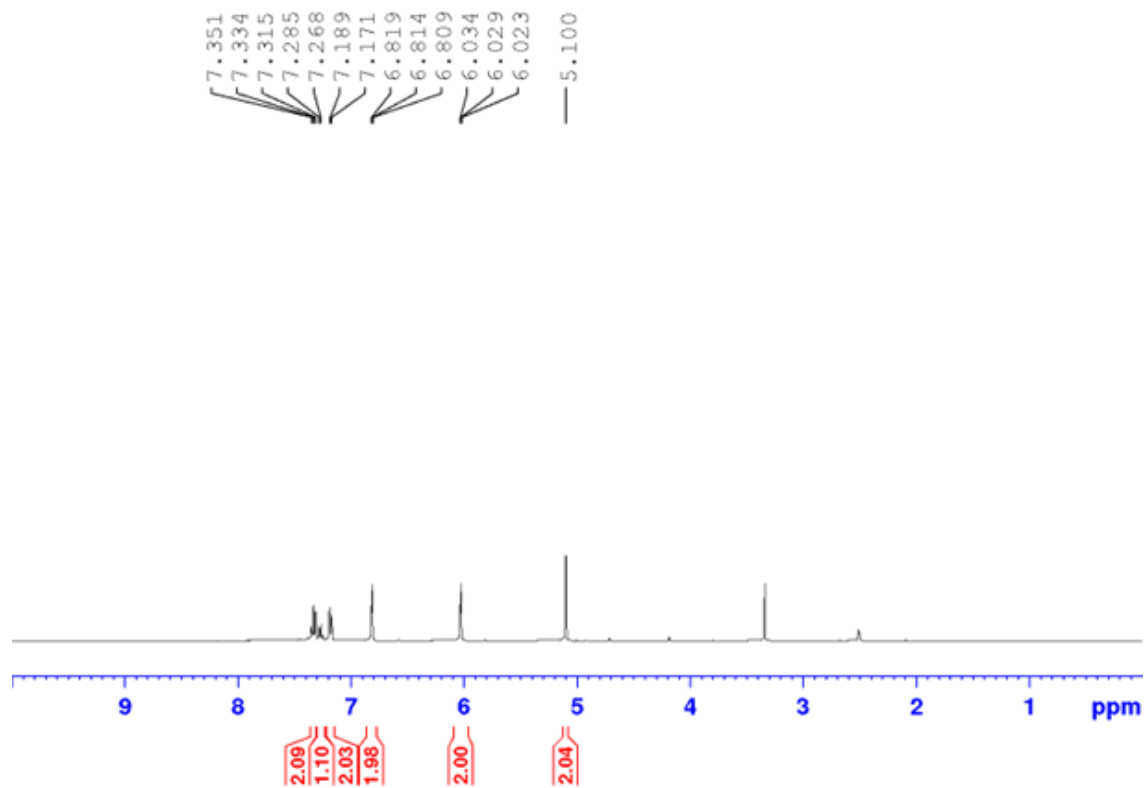


Figure B.7: ^1H NMR spectra of product 3.4.

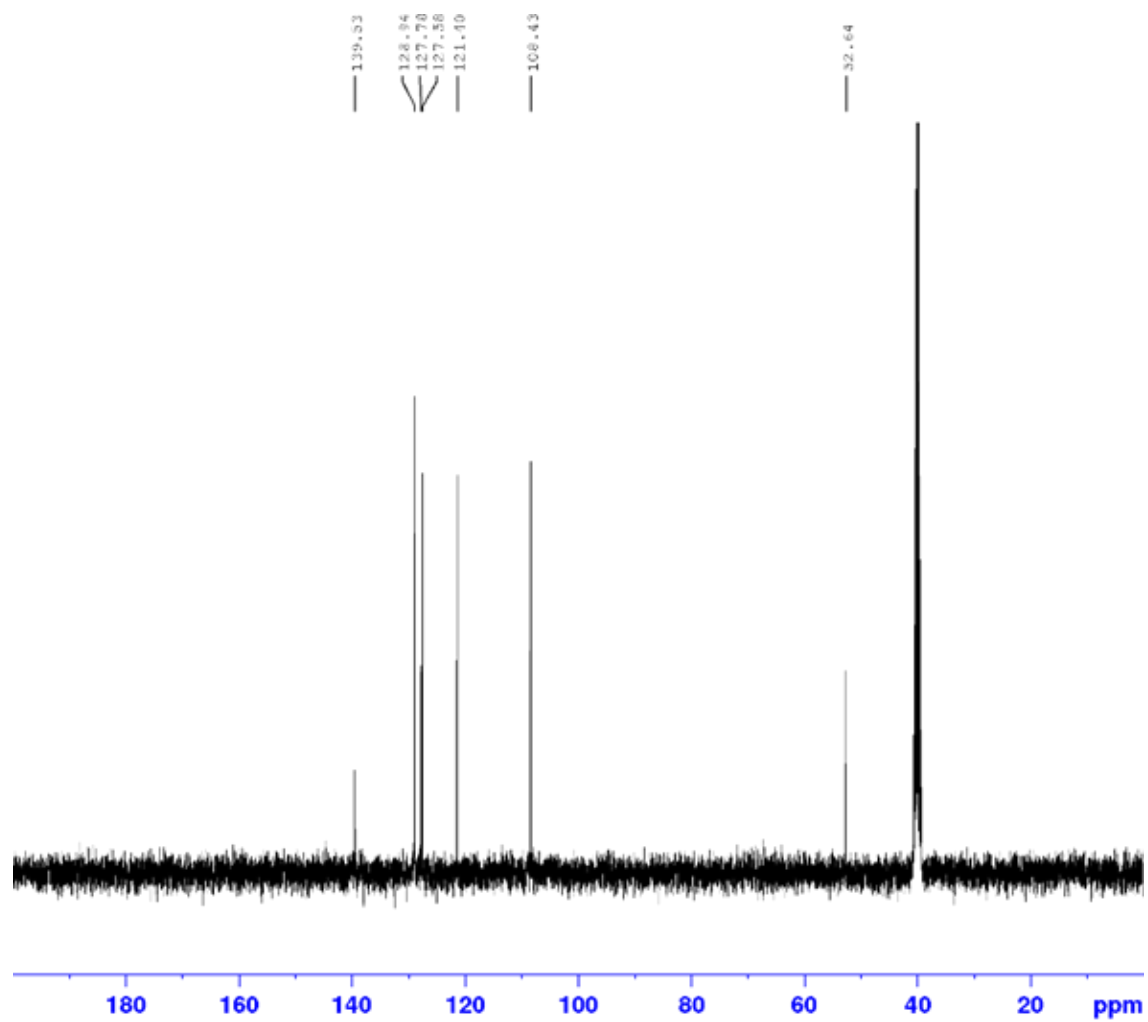


Figure B.8: ^{13}C NMR spectra of product 3.4.

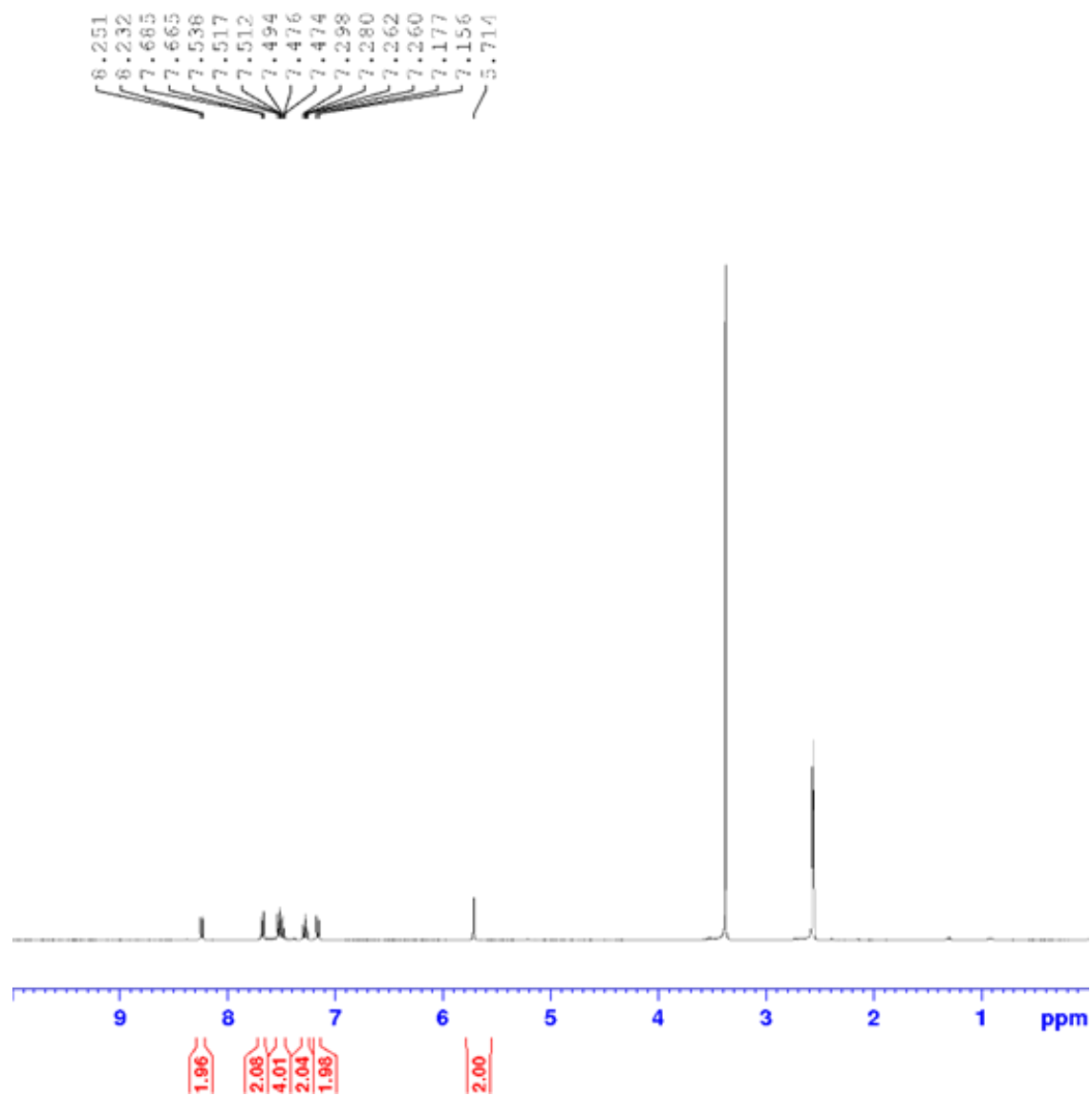


Figure B.9: ^1H NMR spectra of product 3.5.

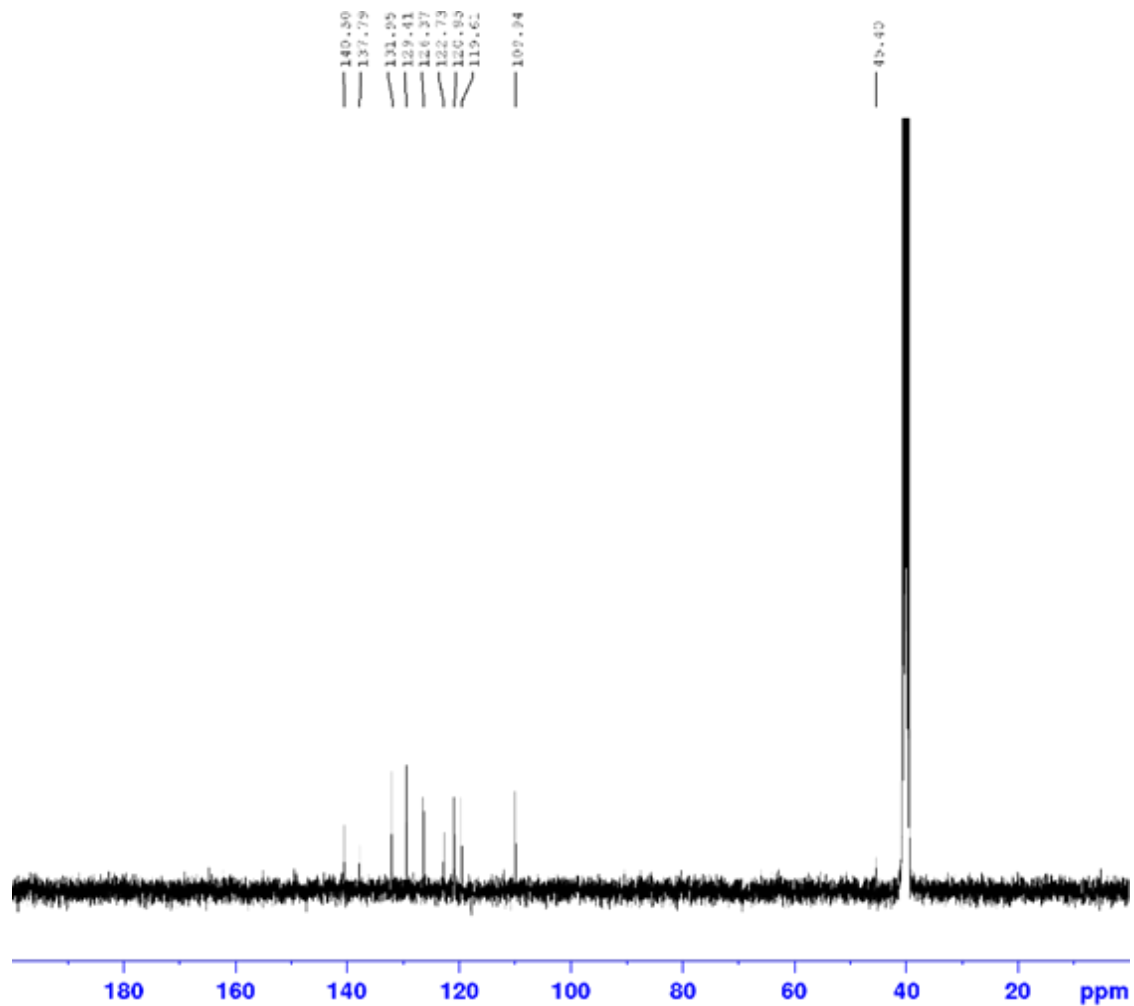


Figure B.10: ^{13}C NMR spectra of product 3.5.

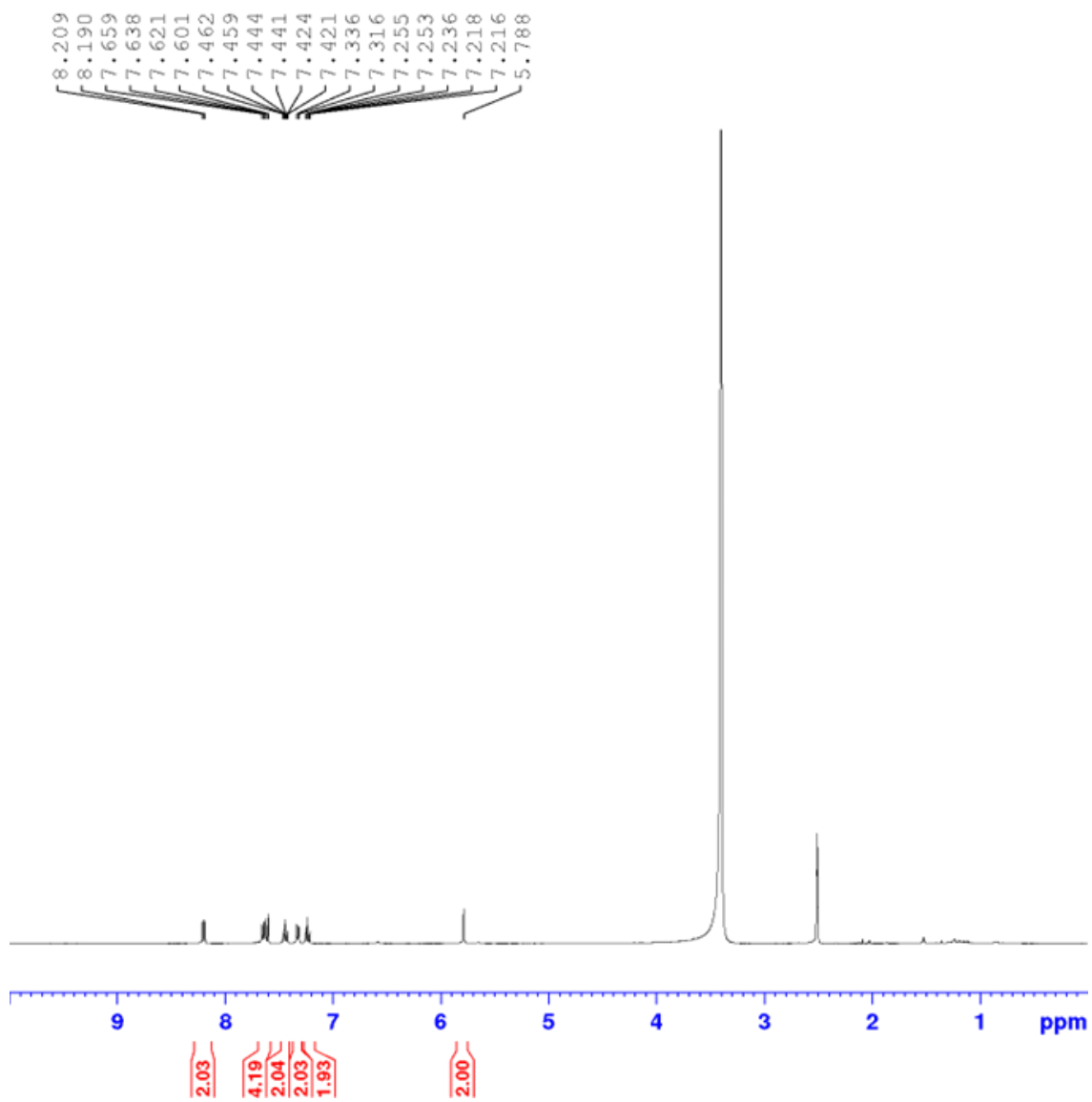


Figure B.11: ^1H NMR spectra of product 3.6.

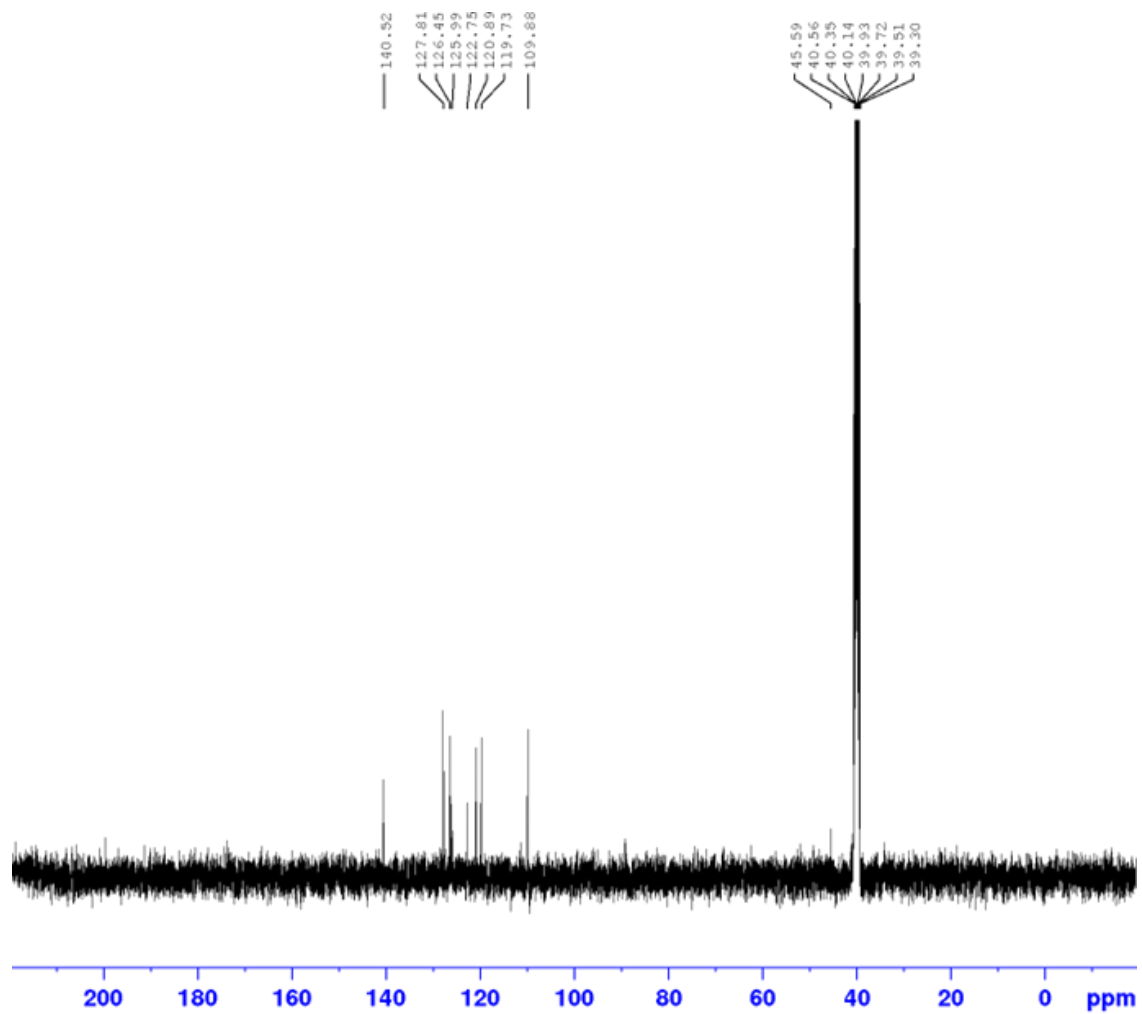


Figure B.12: ^{13}C NMR spectra of product 3.6.

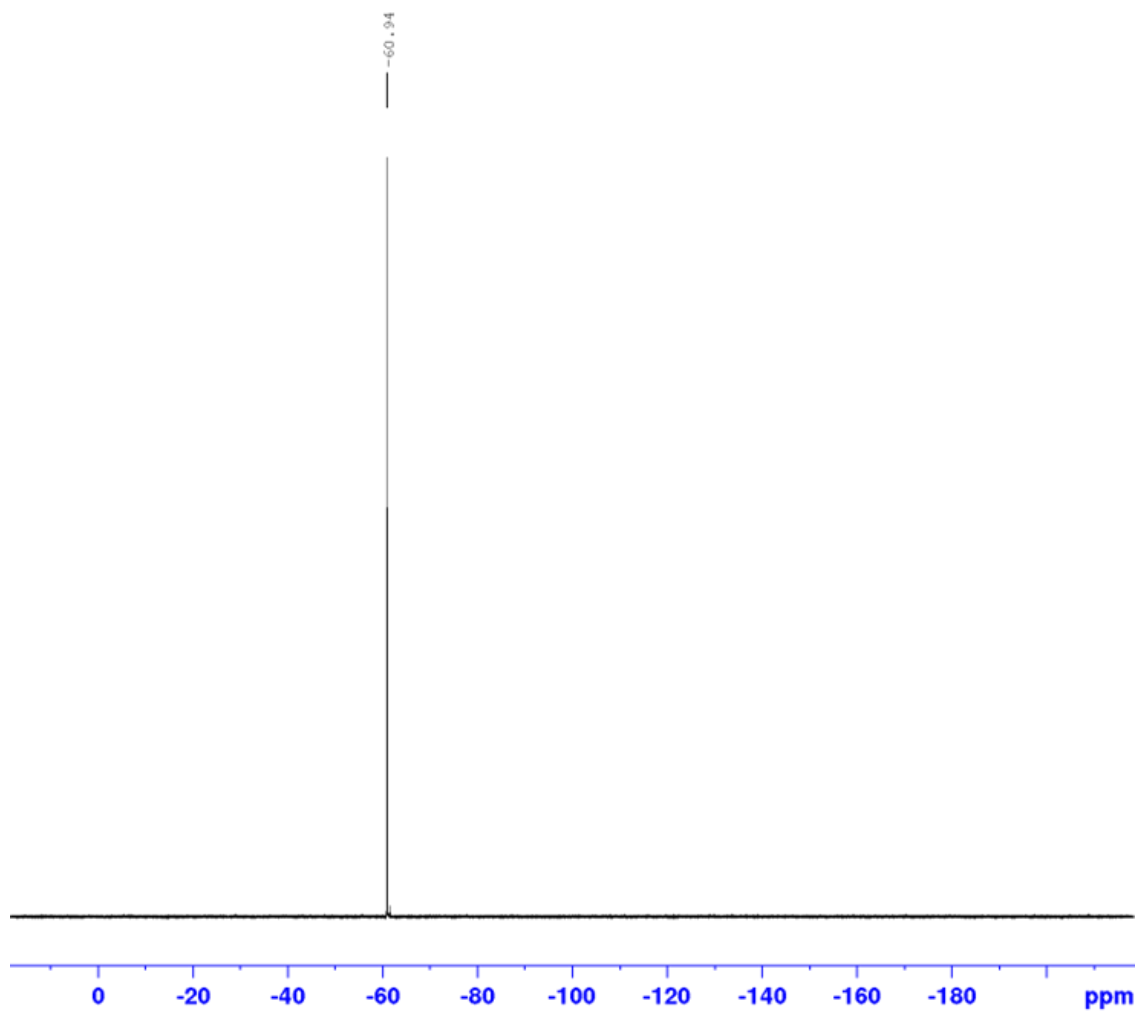


Figure B.13: ^{19}F NMR spectra of product 3.6.

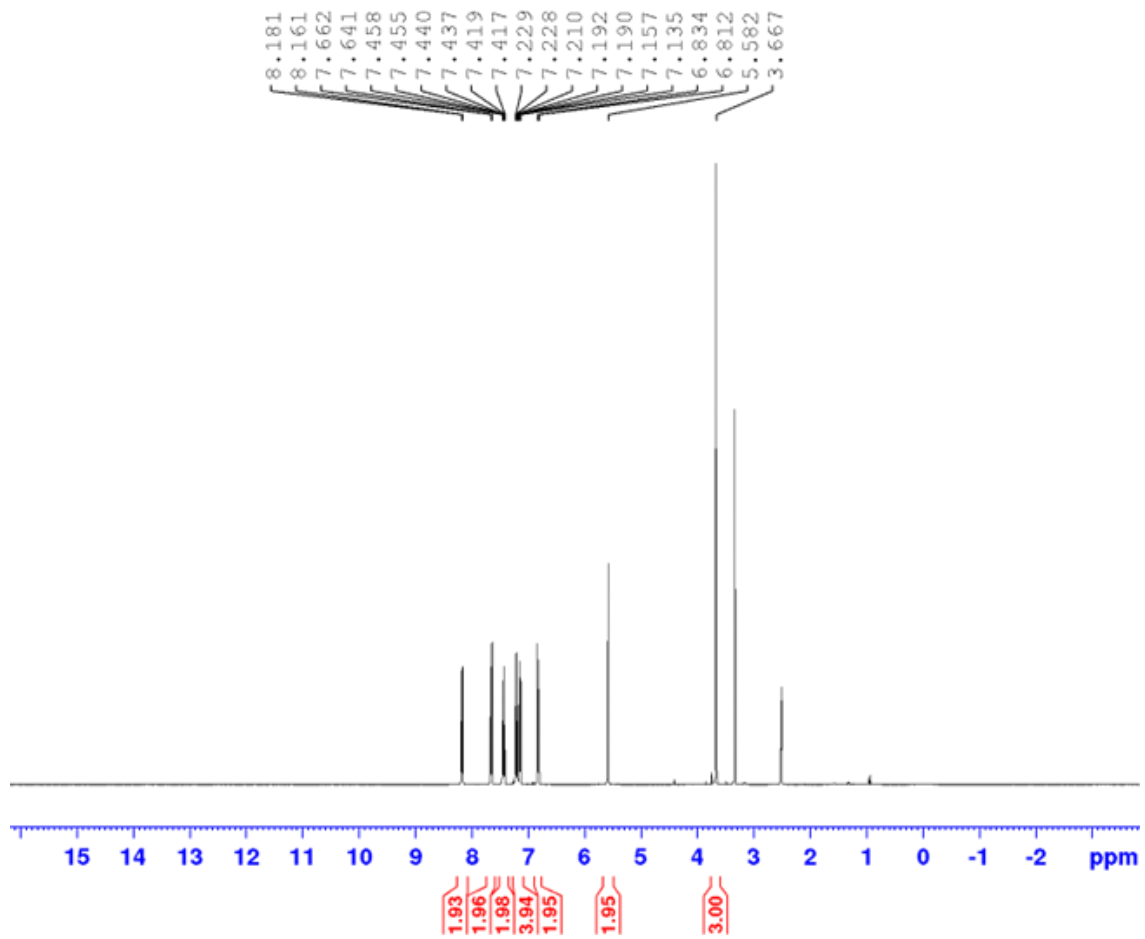


Figure B.14: ^1H NMR spectra of product 3.7.

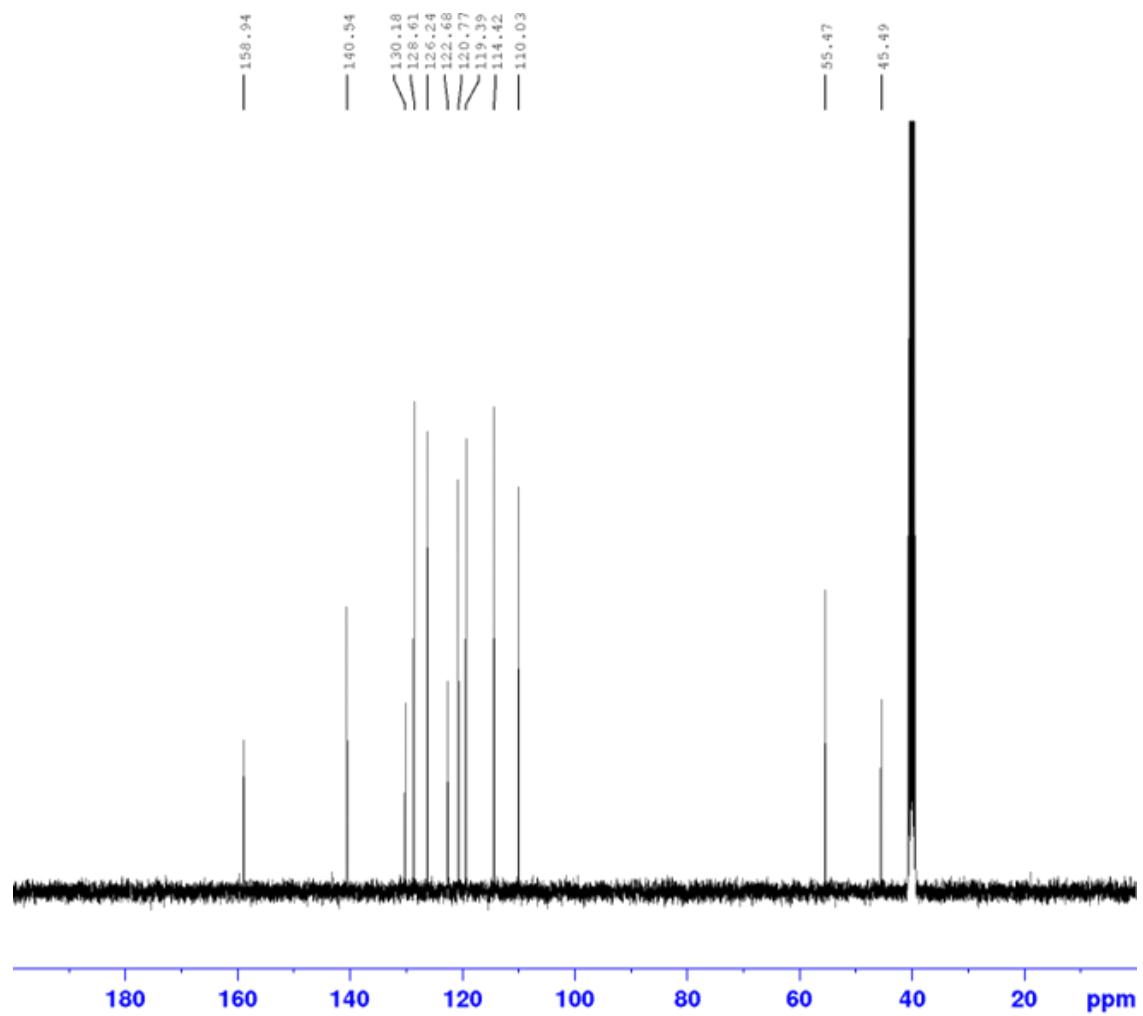


Figure B.15: ^{13}C NMR spectra of product 3.7.

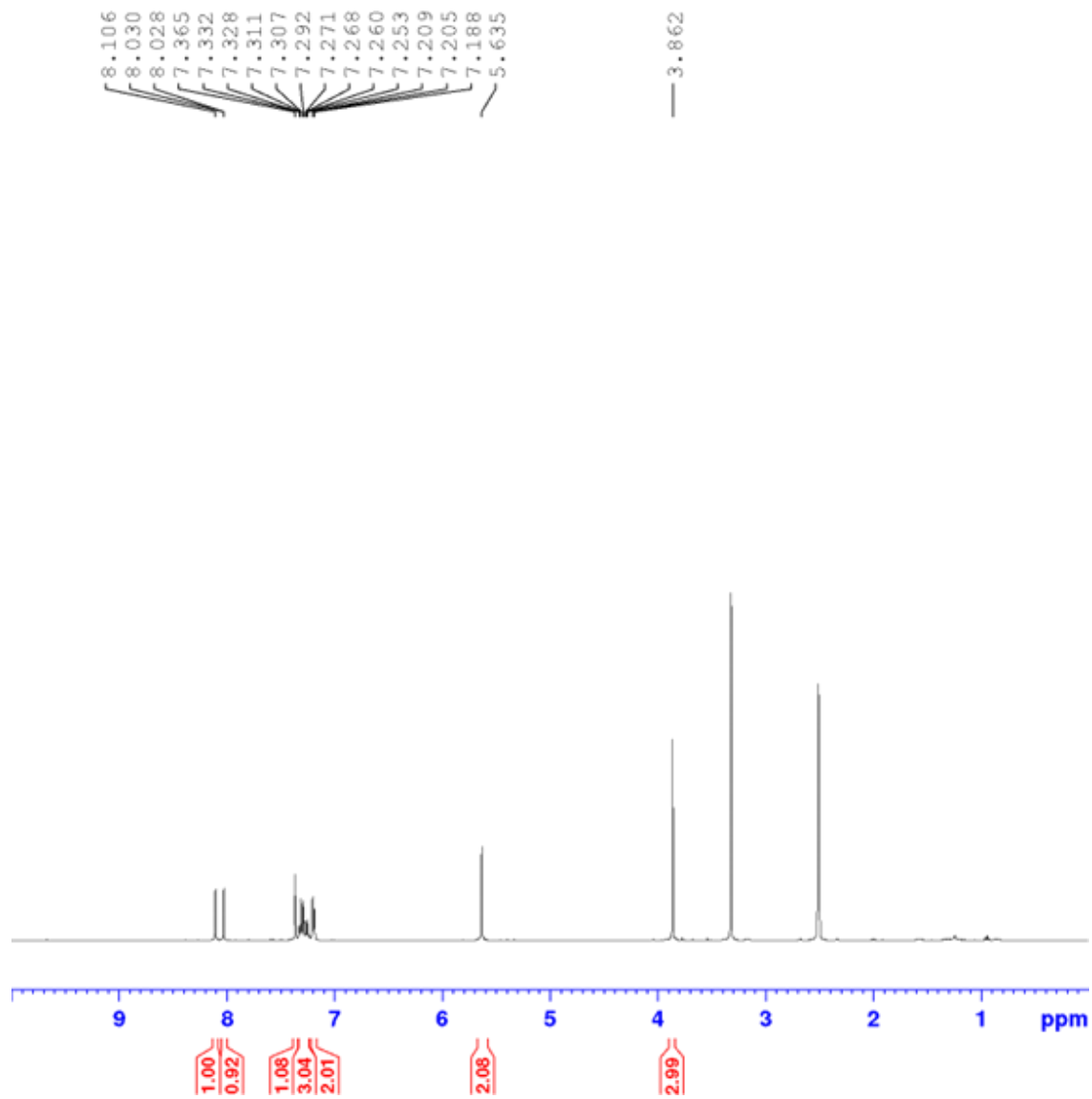


Figure B.16: ^1H NMR spectra of product 3.8.

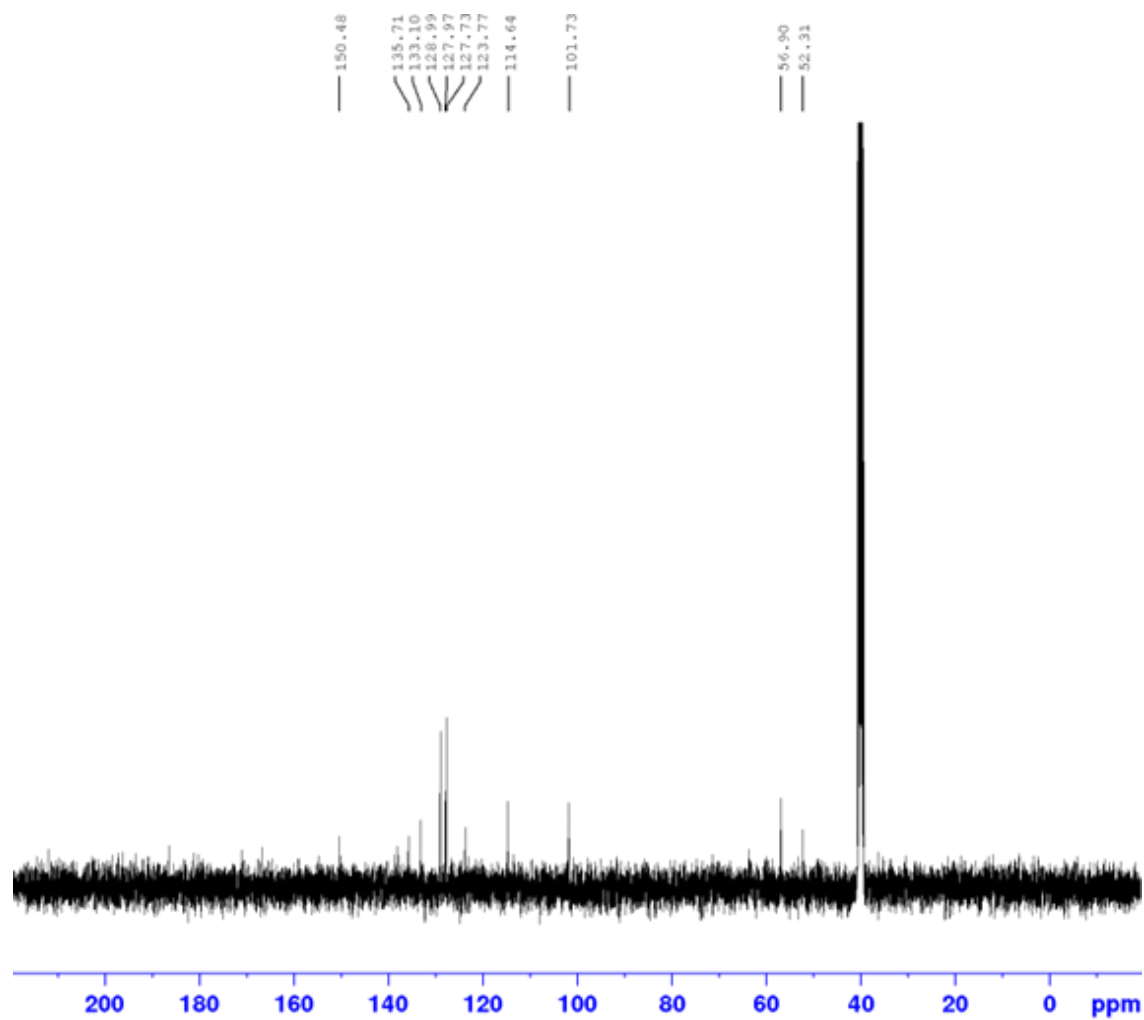


Figure B.17: ^{13}C NMR spectra of product 3.8.



Figure B.18: Illustration of anion pool method in an H-Cell performed with a 0.1 M solution of tetrabutylammonium hexafluorophosphate (Bu_4NPF_6) containing 0.375 mmol of carbazole in acetonitrile in the cathode side and 0.75 mmol of ferrocene on anode side. Benzyl bromide (excess) was added after 1.625 hrs and current was reduced to 0.5 mA. Reticulate Vitreous Carbon electrodes were employed as cathode and anode.

APPENDIX C: SUPPORTING INFORMATION FOR CHAPTER 4

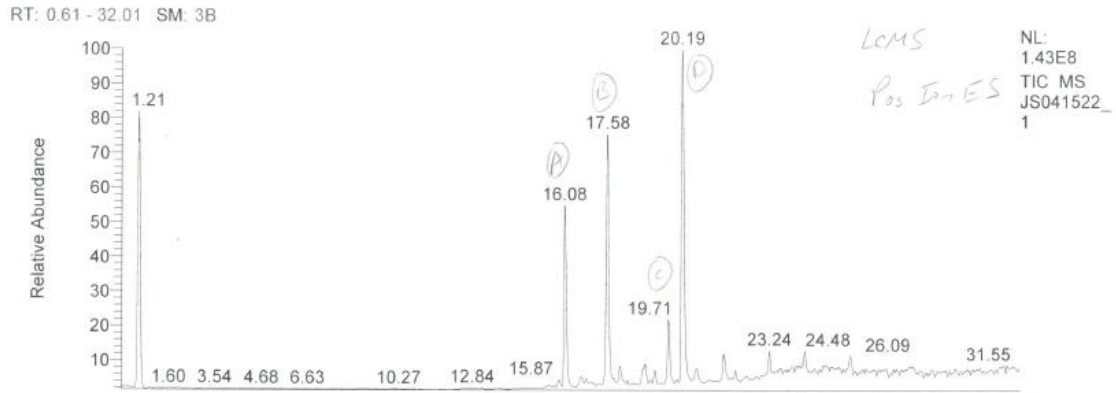


Figure C.1: LC-MS showing retention times of 2,2'-dichlorobenzidine rearrangement.

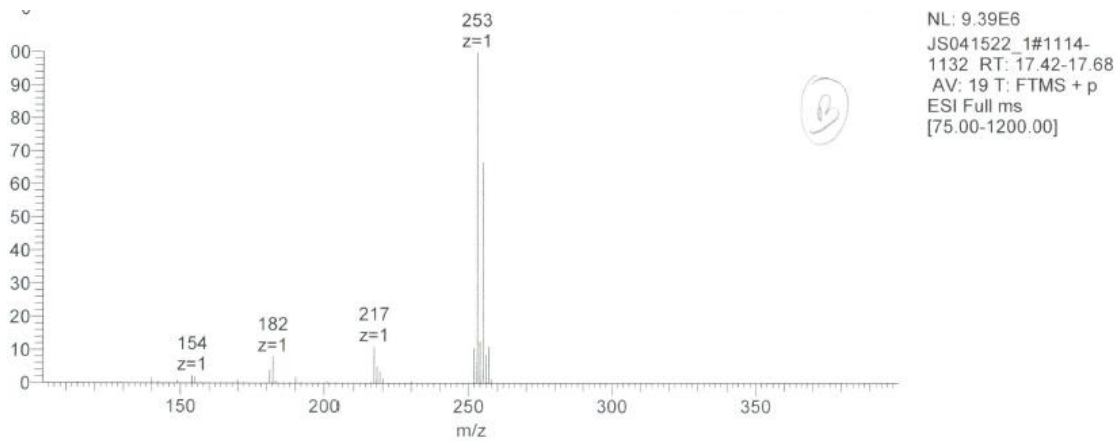


Figure C.2: Mass Spectra of peak B of Figure C.1 showing mass fragmentation of 2,2'-dichlorobenzidine product.

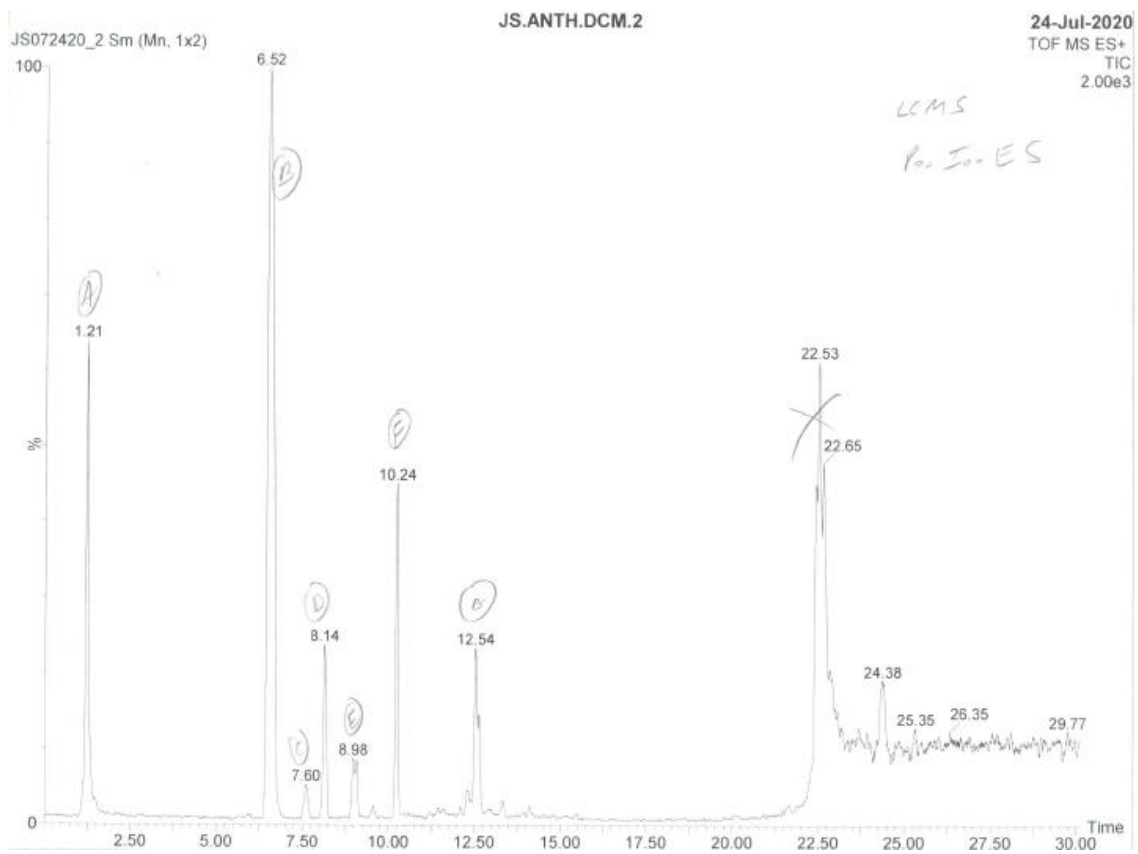


Figure C.3: LC-MS showing retention times of 4,4'-diamino-[1,1'-biphenyl]-3,3'-dicarboxylic acid rearrangement.

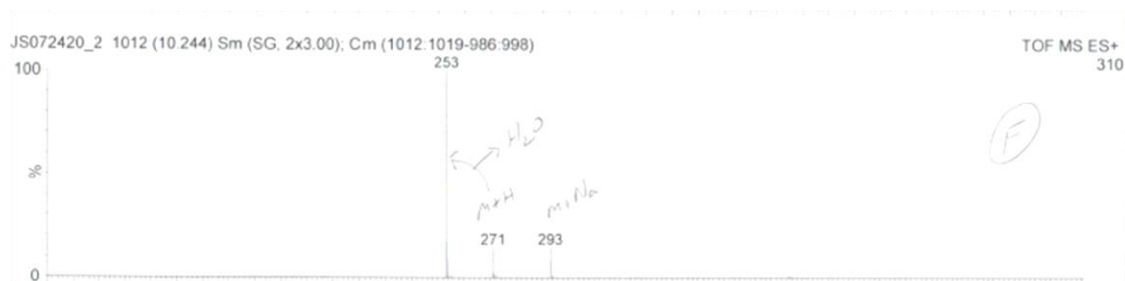


Figure C.4: Mass Spectra of peak F of Figure C.3 showing mass fragmentation of 4,4'-diamino-[1,1'-biphenyl]-3,3'-dicarboxylic acid product.

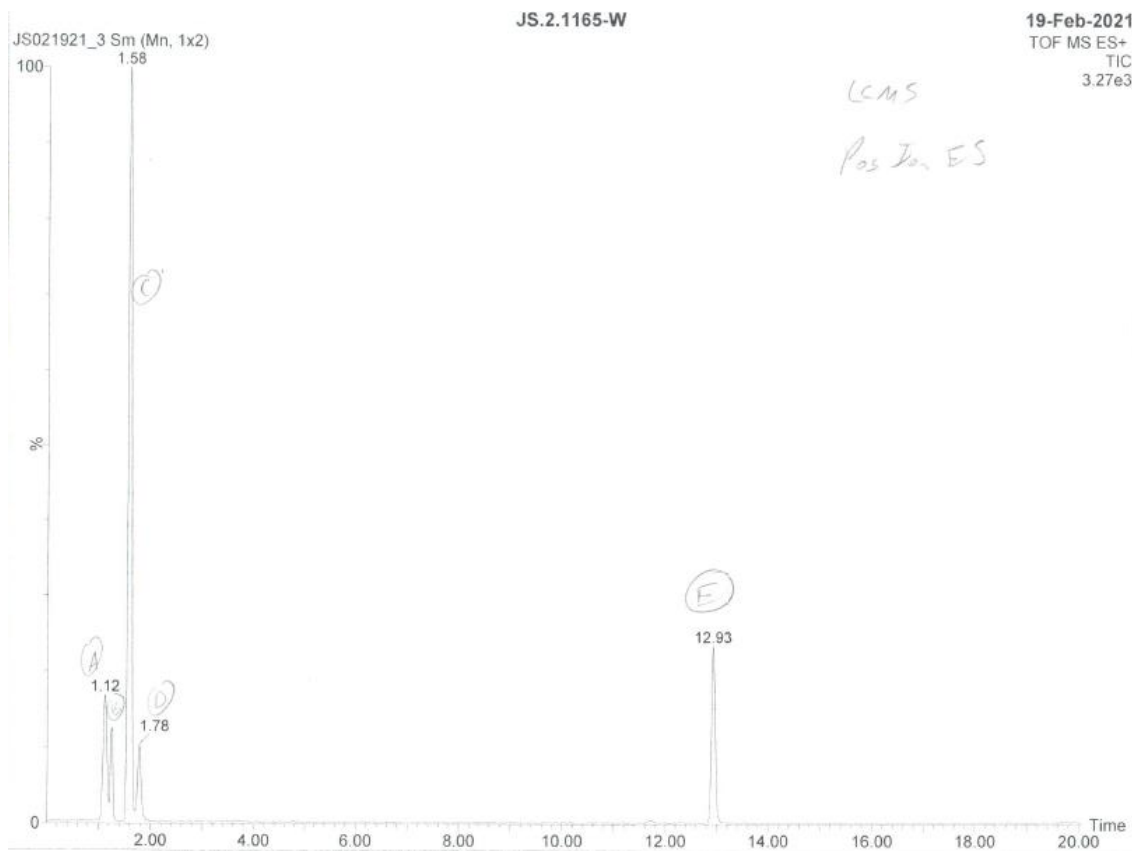


Figure C.5: LC-MS showing retention times of 2,2'-dimethyl-3H,3'H-5,5'-bibenzo[d]imidazole rearrangement.



Figure C.6: Mass Spectra of peak C of Figure C.5 showing mass fragmentation of 2,2'-dimethyl-3H,3'H-5,5'-bibenzo[d]imidazole product.

RT: 0.00 - 29.98 SM: 3B

LCMS

Pos Ion ES

NL:
1.49E8
TIC MS
JS092421_
5

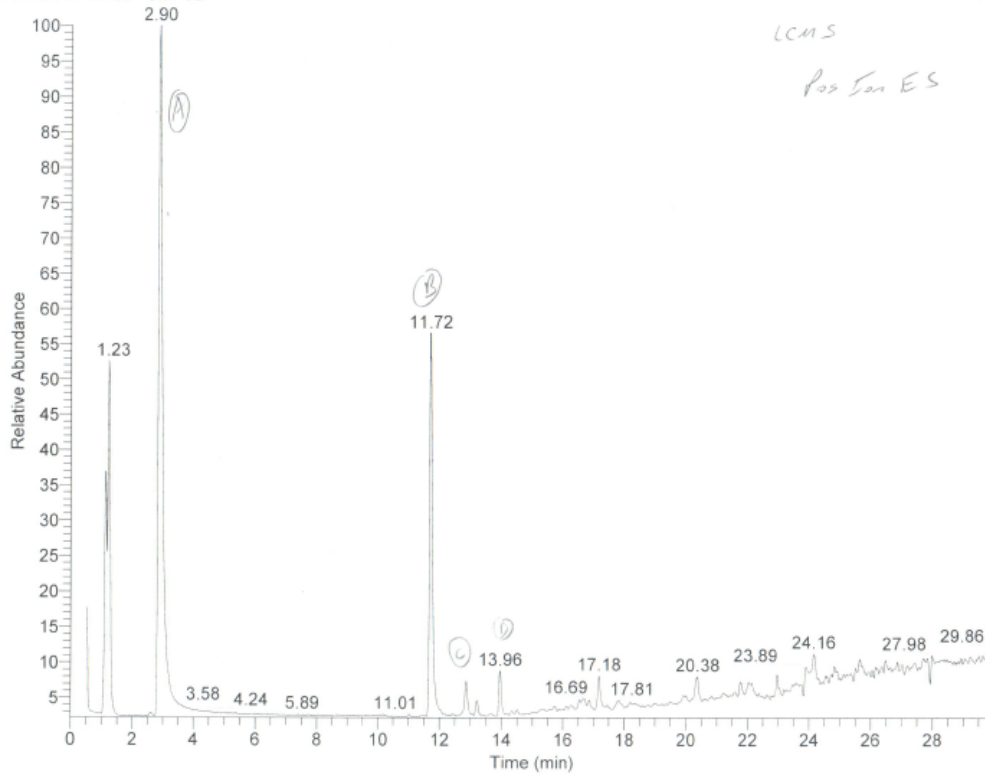


Figure C.7: LC-MS showing retention times of benzidine rearrangement.



Figure C.8: Mass Spectra of peak A of Figure C.7 showing mass fragmentation of benzidine product.